29 October 2020

Dear Christian Beer,

We thank you for considering our replies to the reviewer comments and for inviting us to submit a revised version of our article entitled „Effects of multi-scale heterogeneity on the simulated evolution of ice-rich permafrost lowlands under a warming climate". Please find below the point-by-point responses to the two reviews and an marked-up version with highlighted changes compared to the initially submitted version. In order to address all points of critique of the two reviewers, we made thorough revisions concerning all sections of our article. Please note that the automatically generated marked-up version might thus have misclassified some text as „new" or „deleted" which has actually only been moved to another part of the manuscript. Please note that we decided to omit the Outlook section from the initial manuscript, in order to shorten the article.

We are confident that the revision in which we followed many of the reviewers' suggestions has substantially improved our research article and we hope that the revised version is acceptable for publication in The Cryosphere.

Kind regards,
Jan Nitzbon (on behalf of all authors)

We thank the reviewer for the detailed review of our manuscript and the constructive feedback on our work. We provide answers to the comments below.

Reviewer comments are in *blue italics*.

Author replies are in normal font.

Extracts from the manuscript are in **bold**, and modifications in the revised manuscript are <mark>**highlighted yellow**</mark>.

Anonymous Referee #1

Received and published: 27 June 2020

Artic permafrost is considered one of the key tipping elements of the Earth system. However, researchers face the problem that modelling studies and observations show that the dynamics in permafrost affected regions often depend on abrupt, non-linear processes that are locally very confined, while quantifying the resulting impacts on the global climate requires using low resolution models which do not account for these small scale processes.

Here, Nitzbon et al. propose a tiling approach that allows representing surface heterogeneities – namely the polygonal structures typical for many permafrost regions and low gradient slopes with a length scale of ~100m – in the CryoGrid model. They use the model to investigate the effects of 21st-century warming (RCP8.5) and demonstrate that their approach is capable of capturing subrgid-scale variations in the resulting degradation of permafrost. Thus, the proposed approach could potentially facilitate the understanding of high-latitude processes and improve their representation in Earth System models.

In general, the study presents highly relevant work in an important field and, overall, the manuscript is well written. Especially the introduction-, discussion, -conclusion and outlook sections help the reader place the study in the context of previous and future research on permafrost-affected regions.

However, while I think that the proposed tiling approach could present an important step in improving coarse-resolution models as well as our understanding of high latitude landscapes, the authors do not demonstrate this in their work. As it stands, the manuscript only shows that the approach adds to the model's complexity, but fails to provide compelling evidence that this results in an actual improvement of the simulations. Here, the paper requires major revisions before it can be considered for publication.

We appreciate that the reviewer acknowledges the relevance of our study and identifies the potential significance of our work with respect to an improved understanding of permafrost landscape dynamics as well as the improvement of coarse-resolution models. We understand that the major point of criticism of the reviewer is that we do not demonstrate that our model

developments result in an actual improvement of projections of 21st-century permafrost degradation. We can understand the concerns of the reviewer, but we are confident that our model developments and numerical simulations constitute a substantial advancement compared to previous works. With the explicit representation of micro- and meso-scale landscape heterogeneity, our model facilitates simulation of permafrost landscape dynamics and feedbacks on permafrost degradation in an unprecedented way. We think that a clarification and reformulation of the scope and objectives of our study as well as an extended discussion of the model's advantages over more simple models will rule out this major criticism.

We further agree with the reviewer in that our simulations demonstrate the potential of the multi-scale tiling approach to improve coarse-resolution models. It was, however, not our main objective to prove this in the present study. Instead, our major goal was to show that our approach is capable of representing a wide range of different landscape evolution and permafrost degradation pathways which are known to occur in ice-rich permafrost lowlands. In particular, we investigated which effect the incorporation of micro- and meso-scale heterogeneities has on the simulated landscape evolution and permafrost degradation. Importantly, we do not claim that the most complex model configuration necessarily provides the most accurate projections. However, we do want to convey the insight that potentially important feedback mechanisms can only be represented by those model configurations which take into account micro- and/or meso-scale heterogeneities.

In the revised version of the article, we reworked the introduction section to point out that we do not primarily aim at improving coarse-resolution model projections, but that our study should be considered an explorative modelling exercise of potential feedbacks due to landscape heterogeneity on different spatial scales. We revised the text in different places, for example our objectives are now stated more clearly:

The overall scope of this study is to investigate the effect of micro- and meso-scale heterogeneities on the transient evolution of ice-rich permafrost lowlands under a warming climate. Specifically, we addressed the following objectives:

1. To identify degradation pathways and feedback processes associated with lateral fluxes on the micro- and meso-scale.

2. To quantify permafrost degradation in terms of thaw-depth increase and ground subsidence in dependence of the representation of micro- and meso-scale heterogeneities.

We further clarified these objectives by the following explanations:

Overall, our goal is to provide a scalable framework for exploring the evolution of permafrost landscapes in response to a warming climate, which could potentially be incorporated into LSMs to allow more robust projections of permafrost loss in response to climate change. The presented simulations should thus be considered as numerical experiments to identify important scales and controls of permafrost degradation.

With these modifications we hope to have clarified the scope of our study. In addition, we revised the Discussion section of our article such that it more clearly states the potentials and advantages of our approach compared to more simple models.

The detailed comments of the reviewer are addressed in a point-by-point fashion below.

General comments

1) As stated above, my main concern with the manuscript is that the authors do not compare any aspect of their simulations to observations or to simulations with any other point-scale model that has been validated in the past. Here, the authors claim that they investigate a site on Samoylov and even state that there is a large amount of observational data available for the island that can be used to validate numerical models. However, they make no use of this data making it impossible for the reader to judge whether the tiling approach leads to results that are closer to reality.

We agree that we do not present any comparison of our simulations with observational data from the field site in the present manuscript. However, in a preceding study (Nitzbon et al. 2019), it has been shown that the micro-scale tiling approach which was also used in this study, is capable of reflecting the heterogeneity of thermal, hydrological, and snow characteristics associated with polygonal tundra micro-topography. That study involved a comprehensive evaluation of the model using field observations.
The main reason for not presenting further model evaluation in the present study is that it was not the aim of the study to prove that the presented tiling framework necessarily enables a more accurate reproduction of measurements. Instead, our study primarily aims at identifying qualitative effects of subgrid-heterogeneity on the projections of landscape evolution and permafrost degradation. A second reason is that the available data (soil temperatures, thaw depths, etc.) from the field site on Samoylov Island only capture the micro-scale heterogeneity associated with ice-wedge polygons, while no long-term data are available which document the meso-scale variability of these parameters (Boike et al. 2019).
In the revised version of the manuscript, we clarified that it is not the goal of our study to provide quantitatively accurate simulations, but rather to explore which pathways of landscape evolution can be retraced by different model configurations (see reply above). We would further like to stress that the simulated landscape evolution in the model qualitatively corresponds well with established knowledge on thermokarst landscape dynamics and observations from across the Arctic (e.g. Kokelj et al. 2013, Liljedahl et al. 2016). A qualitative evaluation of our modelling is provided in Sections 4.1 and 4.3 of the revised manuscript.

2) It may be difficult to evaluate the model's performance even with the data that is available on Samoylov. However, in this case the results need to be described in a manner that allows the reader to understand how the newly implemented processes change the model's behaviour. In this way, the reader has at least the chance to judge whether the behaviour of the model is plausible. In the results section, the authors merely present the landscape evolution for

different setups without providing any details on the underlying mechanisms or explanations as to what causes the differences in the simulations. This is not only true for the more complex cases that involve subgrid-scale heterogeneities and later exchanges between the tiles, but even for the very basic one-tile setups. For example, while reading, I was always wondering why the permafrost degradation was so much faster in the poorly-drained than in the well-drained setup? Is it because of higher heat conductivity of water? Or is it an albedo effect due to wetter soils and due to the formation of surface water bodies? Admittedly, some details are provided in the discussion section, but this is nowhere near enough to understand what the model actually does.

We thank the reviewer for acknowledging the difficulties to evaluate the performance of the presented model framework with the scarce data available at Arctic field sites. We appreciate the suggestion to overcome this shortcoming by putting more effort into explaining the model dynamics such that it becomes possible for the reader to retrace the model behaviour and to judge its plausibility. We would like to note, however, that some of these explanations have been provided already in previous studies using the CryoGrid 3 model (Westermann et al. 2016, Langer et al. 2016, Nitzbon et al. 2019, Nitzbon et al. 2020), and that we wanted to avoid presenting these as novel findings.

For the revised version of the manuscript, we thoroughly extended the results section by explanations of the model dynamics and feedbacks and provided explanations which were previously contained in the Discussion section. We also restructured the Results section which is now sorted according to the different model setups, which increase in complexity. By this, it is easier for the reader to discern the feedback processes which are relevant to the different model configurations (i.e., the representation of heterogeneities).

3) If it is partly the aim of the paper to present the approach to large-scale modellers as a way of improving their parametrizations, it requires a better verbal description of the scheme's benefits. To exaggerate a bit: One could look at figure 3 and 4 and decide that actually the simple homogenous, well-drained setup does surprisingly well when compared to the complex polygon-landscape setup. In 2100, I find subsidence of roughly 1m, an active layer depth of about 1m and largely unchanged ground below, which is very close to what I get when I aggregate the three tiles of the complex setup. Admittedly, the simple scheme misses the water bodies (especially between 2025 – 2050), but they also seem to be quite small. The same is true when I compare 5a and b as well as 5c and d. There is very little in the paper that convinces the reader that the (overall) landscape evolution can't be simulated well with a single-tile setup with an appropriate set of soil parameters. I do believe that the scheme presents an important improvement, but that point needs to be made more clearly in the manuscript.

As we have stated above, our goal was to demonstrate that the model is capable of capturing pathways and feedbacks of permafrost landscape evolution which are not possible to reflect in simple single-tile setup. While we agree with the reviewer, that it might be possible to simulate a similar total amount of permafrost degradation (by 2100) in the most complex setup to that in an appropriate single-tile setup, the multi-tile setup shows a different transient

landscape evolution and captures subgrid-scale processes which are potentially relevant in other realms like biogeochemistry. For example, we stress the potential relevance of subgrid-scale heterogeneities for carbon decomposition, to which also small-scale landscape features can contribute substantially (e.g., Abnizova et al. 2012, Langer et al. 2015).

In the revised version of the manuscript, we discuss the benefits of the tiling method more extensively in the discussion Section 4.2 and put our modeling work in the context of approaches from the LSM/ESM community. Overall, our study is intended to inform coarse-scale modelers about the effects of including heterogeneities at different scales, and thus to enable them to decide whether and how these could be implemented in their model frameworks.

Specific comments

P.4, L.87 ff: Study area – To my understanding the study is more a demonstration of technical possibilities of your developments rather than an investigation that relies on the specific setup of Samoylov or on data from the island. Therefore I would suggest to leave out the entire description (subsection 2.2) of the study area, because it is a bit misleading in two ways:

A) Expectations – With such a detailed description of the site, one expects to find a comparison to observations from Samoylov at a later part of the manuscript.

B) Technical capabilities of the tiling approach – The tiling approach is not really capable of representing specific (complex) heterogeneous landscapes. With no real information of the actual spatial distribution of the tiles within the encompassing grid box, any tiling approach only ever represents a well mixed setting which is not really the case for the island.

I think it is sufficient to state that the initial soil conditions, forcing data and areal fractions were chosen based on Samoylov and that stratigraphy represents a generic profile based on previous studies of the island, without giving more information on the site. However, the ideal way would be to use any of the available observations from Samoylov to validate your model – then the information you provide would be very welcome.

We agree with the reviewer in this point and hence removed the extensive description of the study area from the main text. Instead, we provide a shortened version of the study area description as appendix A. We decided to keep the former Figure 1 in the appendix (now Figure A1) as we think that it gives a good impression of the abundance and scales of heterogeneities and landforms common to real-world permafrost lowlands. In the main text, we added an schematic figure (new Figure 1) which illustrates ice-rich permafrost lowlands with the micro- and meso-scale heterogeneities addressed in this study. We think that this new Figure 1 underlines the conceptual character of our modelling study instead of raising expectations which cannot be met.

P.6, L.117 ff: You provide the units for density and specific heat but not for heat capacity and conductivity. Other parameters are also introduced without unit later in the text. In my opinion it wouldn't be a problem to leave out the units altogether, however if you are nice enough to provide them, this should be done consistently.

We consistently provide the units of all physical quantities in the revised version of the manuscript.

P.6, L.123: What does the "effectively" refer to?

The change of the snow density can only change due to infiltration and refreezing, but not due to internal processes in the snowpack. We deleted the word „effectively" as it is admittedly confusing and did not contain additional information.

P.6, L.125 ff: How does the model deal with the surface water? Is there a (water) depth dependant runoff-formulation and does the water evaporate? Or does it simply pool until it can infiltrate?

The hydrology scheme allows for evaporation of surface water and it can run off laterally, either to an adjacent tile, or into an „external reservoir", if the tile is connected to one (see Figure 2). We clarified this point in the revised manuscript:

Excess water is allowed to pond above the surface, leading to the formation of a surface water body. Surface water is modulated by evaporation as well as lateral fluxes to adjacent tiles or into an external reservoir (see *Lateral fluxes* below).

P.6, L.127: Is the field capacity the same for the organic and mineral soil?

Yes, the field capacity parameter is identical for all soil layers. A sensitivity study in a previous study revealed that the overall model dynamics are not sensitive to this parameter (see Supplementary Information to Nitzbon et al. (2020)).

P.6, L.145: Why this formulation for the effective h. conductivity?

The lateral fluxes into the external reservoir are calculated based on a Darcy approach as described in Nitzbon et al. (2019). The „effective" hydraulic conductivity incorporates the distance (D) and contact length (L) between the respective tile and the reservoir. For a tile which can drain in all directions, the effective hydraulic conductivity is obtained as follows: $K_{eff}=K*P/D=K*2\pi*D/D=2\pi K$. This is further explained in the SI of Nitzbon et al. (2020).

P.7, L.164: is > are

Thanks. Corrected in the revised version.

P.7, L.171: I think the information that you are not treating meso-scale lateral heat fluxes should be a bit more prominent – e.g. in the abstract you say that your model captures lateral heat fluxes at the scales not captured by ESMs which implies that also the meso-scale heat fluxes are represented.

We agree with this concern and added a sentence in the model description to justify this simplification:

<mark>We did not consider lateral fluxes of heat, snow and sediment at the meso-scale, as these were assumed to be negligible on the time scale of interest (heat, sediment), or too uncertain (snow).</mark>

We also revised the formulation in the abstract. We mention the potential effect of meso-scale lateral heat fluxes in the Discussion (Section 4.1):

<mark>Previous modeling studies have also demonstrated that the stability and the thermal regime of permafrost in the vicinity of thaw lakes is affected by meso-scale lateral heat fluxes from taliks forming underneath the lakes (Rowland et al., 2011; Langer et al., 2016). These effects have not been considered in this study.</mark>

P.8, Figure 2: A very nice figure that gives a very intuitive overview over your setups. Maybe you could separate the vertical subplots more distinctly from the connection/network diagrams to make it clearer that these are two different aspects and that the vertical setups in a and b are also applicable in subplot c and d. Also the information with respect to dx and the ice content is slightly confusing because it is only shown in subfigure a – I think it could be left out from the plot.

We thank the reviewer for appreciating the added value of this figure. It is correct that the vertical cross-sections for the setups a and b are also applicable to the setups c and d, respectively. We revised this figure according to the suggestions of the reviewer. To clarify the different setups, we also revised the names assigned to the different setups in a way which we hope is more intuitive to understand.

P.9, L.181: What happens to the vegetation layer in the case that surfaces are inundated for longer periods?

The organic-rich vegetation layer does not change when the surface is inundated for longer periods. While the vegetation type would probably adapt to the aquatic conditions in reality, we assume that the thermal properties of this layer would not change substantially.

P.9, Table2: Has the column "Water" been mentioned before?

The column refers to the initial water/ice content. The water content in the unfrozen part of the ground is, however, modified by the hydrology scheme. We adopted the label of the column to clarify this.

P.10 Table3: The legend states that the average of the polygonal setup is equal to the single tile setup, however this does not seem to be the case for the Reservoir elevation (poorly drained).

The statement in the legend was indeed confusing. True is, that the depth of the excess ice layer and the excess ice content of the homogeneous tile correspond to the area-weighted mean of the three polygon tiles. In addition, the reservoir elevation of the poorly-drained setup was set 0.1m below the mean initial elevation of the surface. To clarify this point, we revised Table 3 and added a new Table 4 which gives an overview of the parameter variations.

P.11, L.219: What is a "repeatedly appended base climatological period" ?

The anomalies from the CCSM4 projections for the period after 2014 were applied to a fifteen-year „climatological base period" (2000-2014). The formulation has been clarified in the revised manuscript.

P.11, L.224: Why only the two extreme cases for the single-tile setup? I think it could also be helpful to see the behaviour for a medium-drainage constellation?

The idea behind considering only the two extreme cases for the hydrological boundary conditions was to create a direct link to the preceding study by Nitzbon et al. (2020), in which these boundary conditions were treated as confining extreme cases. We agree that, as a stand-alone independent work, the present study provides more insights, if simulations under intermediate hydrological conditions were considered as well. Thus, we conducted simulations for two additional intermediate levels of the external reservoir (e_{res}=-0.5m and

e_{res}=-1.0m) for both the single-tile and the polygon setups. The additional simulation results are described and discussed in the revised manuscript, in which the Results section is now structured more clearly according to the different model setups.

The degradation rate is primarily controlled by the thaw depth which is in turn affected by the hydrological regime of the active layer. On the one hand, thawed saturated soil has a higher thermal conductivity than drained soil, which allows higher ground heat fluxes and hence deeper thaw. On the other hand, ice-rich soil layers need more heat to thaw than ice-poor soil layers due to the higher latent heat content. These and other counteracting effects establish a non-trivial relationship between the hydrological regime of the active layer, and the annual (maximum) thaw depth (e.g., Atchley et al., 2016). Simulations with CryoGrid 3 typically show that wetter conditions cause deeper thaw depths and hence faster degradation (e.g., Nitzbon et al., 2019, Martin et al., 2019). This is particularly the case when surface water bodies form, since these alter the surface energy balance (e.g., lower albedo) and have a high heat capacity, which delays the refreezing and can favour the development of taliks.

In the revised manuscript, the dependency of degradation rate on the drainage conditions is further elaborated on through presentation of further simulations for intermediate drainage conditions and more extensive explanations in the main text. For example, we added the following paragraphs in section 3.1:

Overall, the simulation results indicate that permafrost degradation is strongest as soon as a limitation of water drainage results in the formation of a surface water body. The presence of surface water changes the energy transfer at the surface in different ways. First, it reduces the surface albedo, resulting in a higher portion of incoming shortwave radiation. Second, water bodies have a high heat capacity which slows down their freeze-back compared to soil. As a last point to mention, the thawed saturated deposits beneath the surface water body have a higher thermal conductivity compared to unsaturated deposits, which allows heat to be transported more efficiently from the surface into deeper soil layers. These findings are consistent with previous CryoGrid 3 simulations for ice-wedge polygons (Nitzbon et al., 2019) and peat plateaus (Martin et al., 2019).

During the initial phase of excess ice melt which occurs between 2050 and 2075, our simulations suggest a non-monotonous dependence of permafrost degradation on the drainage conditions. [...] This can likely be attributed to contrasting effects of the hydrological regime on thaw depths. When the near-surface ground is unsaturated [...], the highly-porous organic-rich surface layers have an insulating effect on the ground below due their low thermal conductivity. On the other hand, less heat is required to melt the ice contained in the mineral soil layers whose ice content corresponds to the field capacity, than if their pore space was saturated with ice. In the intermediate case

with e_{res}=-0.5m, the combination of dry, insulating near-surface layers and ice-saturated mineral layers beneath leads to the lowest thaw depths and hence the slowest initial permafrost degradation. However, as soon as a surface water body forms in that simulation (between 2075 and 2100), the positive feedback on thaw described above takes over, resulting in stronger degradation by 2100 compared to the well-drained settings (e_{res}=-1.0m and e_{res}=-10.0m) for which no surface water body forms during the simulation period.

P12, L.250 ff: Could you explain the cause of the diverging behaviour in the tiles, it appears to be similar to the differences between the well- and poorly drained single tile setups. Also why is the outer tile behaving very differently while the inner and intermediate tiles behave similarly? The figure seems to indicate that the same dynamics could be obtained with a two-tile setup (inner tile / outer tile).

The diverging behaviour of the outer tile from the inner ones can be explained by the fact that it is connected to a low-lying reservoir and hence well-drained, while the inner two tiles can only be drained via the outer tile. As the slope has a very low gradient (0.1%), this drainage is not very efficient and causes water to impound in the inner tiles, which in turn accelerates degradation due to the feedbacks discussed for the single-tile setup. In the revised version of the manuscript, we added the following explanations in section 3.3:

Irrespective of the slope gradient, the simulated evolution of the outer tiles is very similar to that of the well-drained single-tile simulations throughout the entire simulation period [...] The similarity to the well-drained single-tile simulations can be explained by the fact that the outer tile is very efficiently drained, such that the lateral water input from the intermediate tile is directly routed further into the external reservoir. Hence, the "upstream" influence on the outer tile becomes negligible.

It is furthermore correct, that a two-tile setup would likely result in a similar pattern. However, we decided to use a three-tile setup for several reasons:

- It was not clear a priori that the inner tiles would develop so similar, since the intermediate tile is closer to the drainage point of the slope. At the same time it is affected by water input from the inner tile which lies upstream. Hence it was of interest to us to see which of these effects would dominate.

- The variability of ice-wedge polygon types along transects on Samoylov Island (Figure A1 in the revised manuscript) suggested that degradation along the slope could be stronger than in the innermost part lying upstream.

- For consisency, we wanted to use the same number of tiles to represent heterogeneities on the micro- and meso-scale.

In fact, there are slight but significant differences between the "intermediate" and "inner" tiles which are explained in the revised manuscript (Section 3.3).

To present a broader picture of possible degradation pathways along low-gradient slopes, we conducted additional simulations for the two slope setups (homogeneous and polygon), where we set the slope gradient to 1.0%. These simulations reveal further insights which are presented, explained, and discussed in the revised version of the manuscript (Sections 3.3 and 3.4)

P.16, L.302 ff. | P.17, L.310 ff: It seems as if around the year 2060-2080 the rate of active-layer deepening (rate of ground subsidence) increases in all setups, which you also note on page 17 l. 312 . What is the reason for this non-linear behaviour? Is this related to the forcing? If so could you maybe provide a timeseries of the forcing – e.g. 2m temperatures?

The nonlinear increase in the degradation rate after 2060 or so is an important observation. The effect is noticeable irrespective of the specific model setup and has similarly been reported in previous studies using the same forcing data (Westermann et al., 2016, Langer et al., 2016, Nitzbon et al., 2020). We think that this effect can be explained by multiple factors: first, the meteorological forcing results in exceptionally high thaw depths during the 2060s, which initiates positive feedbacks to the excess ice melt (snow accumulation, water impoundment). Second, around that time the soil has warmed to a level, where residual liquid water critically slows down the back-freezing. In combination these effects cause a nonlinear shift in the degradation rate for most settings around the 2060s. While this effect can likely be generalized, the timing is strongly related to the forcing and hence the location of the study area. In the revised manuscript, we mention and discuss this effect in section 3.2:

[...] We explain the acceleration of permafrost degradation at the beginning of the second half of the simulation period (Figures 7 b and 8 b, purple lines) by a combination of additional warming from the meteorological forcing, and positive feedbacks due to the surface water body (as explained for the single-tile simulation in Section 3.1).

We decided to not include a time series of the forcing data, as we attribute the effect mainly to a non-linearity in the ground thermal dynamics. The temperature forcing does not show a non-linear increase during that period.

P.16, L.303: Which sub-grid scale interactions result in the active layer being deeper in the landscape simulation – at least until the year 2090? Based on the soil properties one would expect it to be a combination of the well- and poorly drained single tile setup?

This is an important observation which deserves further explanation. In the poorly-drained single-tile simulations, water can drain from the system as soon as the water table is above

-0.1m relative to the surface. Therefore, the drainage is still more efficient than for the two inner tiles of the three-tile slope setup, where drainage is very inefficient. For these tiles, surface water formation occurs much earlier than in the single-tile simulations and hence higher thaw depths are observed earlier (see answer and modifications mentioned above). In other words, the „poorly-drained" setting does not really reflect the most extreme case which would be a water-logged setting where runoff is precluded. This, however, would result in physically unrealistic situations where surface water would accumulate over multiple years, since evaporation is consistently lower than precipitation.

P.18, L.358 ff: Maybe these explanations – at least between lines 358 and 364 – fit better in the results section.

We agree and moved these explanations to the results section where we now provide further detailed explanations of the model dynamics.

P.18, L.371 ff: What does "become more involved" mean in this context?

We wanted to express that the dynamics become more complicated. We changed the wording in the revised manuscript.

P.19, L.382 ff: Again, this information may be better suited for the result section. As an afterthought on sections 4.1 and 4.2: maybe it is possible to disentangle the process description and the interpretation to how this relates to other studies? Because the descriptive parts would fit extremely well into the results section?

We agree with the reviewer and followed this suggestion in the revised manuscript.

P.19 L.401: Here, one could argue that your results actually show the opposite: When including both meso and micro-scale processes, the results are actually fairly close to the single tile (well drained) set-up. Thus, setting the soil parameters adequately may already be enough for projections with large-scale models.

Here, we wanted to express that the inclusion of micro- and/or meso-scale heterogeneities can result in permafrost degradation rates which are not reflected by single-tile simulations. For example, the polygon simulations consistently showed an earlier onset and stronger rate of permafrost degradation than the respective single-tile simulations. We agree, however, that this statement was imprecise and could be misinterpreted, such that we revised our formulation.

P21, Figure 6: A very nice overview figure. It would be nice though if you could explain the abbreviations in the caption.

The caption has been extended accordingly for the revised version. In addition, the distinction between high-centred polygons with inundated and drained troughs has been refined and is also indicated in Figures 5-8.

P.21, .L447: from > form

Thanks. Typo has been corrected.

P.22, L.453: I wouldn't say that this is specific to northeast Siberia but rather a simple test case.

We agree and changed the formulation accordingly.

P.22, L.462 ff: I am not convinced that you demonstrated that in this study: There is no comparison to observations or a detailed description of the subgrid-scale processes. Thus you present a new (and I do believe more suitable) approach, but you do not show how this helps reduce uncertainties.

We agree that claiming a reduction of uncertainty is not necessarily supported by the data we show in the study. However, we have shown that our approach allows us to simulate degradation pathways which correspond to observations from across the Arctic. Thus, they bear the potential for more realistic site-level assessments. We modified our conclusions for the revised manuscript.

P22, L.472 ff: Here, I do not agree with the authors' conclusion. On one hand they merely show that their approach increases complexity but not that this complexity improves the quality of the results and provides further constraints on projections of future permafrost degradation. On the other hand they do not show that their approach is suitable for the ESMs, i.e. that the approach can be scaled to the respective resolutions. With respect to permafrost-affected regions, one important issue would be that the dependencies in the model are sufficiently linear, allowing subgrid-scale heterogeneity to be represented by one (or a few) parameter set(s) that represent an average over large areas. Personally, I do believe that the scheme presents an important improvement, but that point needs to be made much more clearly in the manuscript.

As stated in previous points, we see the major contribution of our work in the possibility to simulate pathways and feedbacks of permafrost landscape evolution in an unprecedentedly realistic way. The tiling method allows to do this without the need to increase the grid resolution and hence computational costs drastically. Here, we do not suggest that our approach could be adopted 1:1 in coarse-scale LSM/ESM frameworks, but only state that our works contributes to the development of such model frameworks. For example, Aas et al. 2019 have demonstrated the applicability of the coupled tiles to represent polygonal tundra and peat plateaus in the Noah-MP LSM.

We carefully revised our conclusions in the revised manuscript, thereby also taking into account the additional simulations that we conducted. With respect to the implications of our study for coarse-scale modellers, we extended the Discussion in Section 4.2 and rephrased the criticized conclusion.

P.22, L.477 ff: I think it would greatly increase the quality of the study if the authors could provide some validation or evaluation of the model. There is neither a detailed description of the processes that lead to the results, nor have any aspects of the simulation been compared to observations or to simulations with any other point-scale model.

We agree with the reviewer that the validation and evaluation of the model is an important issue. Site-level studies which apply the presented model framework to different sites and compare the simulations to observational data, are thus highly desirable as future steps. However, suitable long-term datasets, particularly of ground subsidence, constitute a strong limitation to such endeavours. In addition, we would like to point out that the CryoGrid 3 model has already been applied in different contexts and other study areas, and those studies put a stronger focus on quantitative evaluations (Martin et al., 2019, Nitzbon et al., 2019, Schneider von Deimling et al., 2020, Zweigel et al., 2020). The need for suitable field data for model evaluation has been stressed in the revised Outlook section.

References (not contained in the original manuscript)

Abnizova, A., Siemens, J., Langer, M., & Boike, J. (2012). Small ponds with major impact: The relevance of ponds and lakes in permafrost landscapes to carbon dioxide emissions. Global Biogeochemical Cycles, 26(2). https://doi.org/10.1029/2011GB004237

Atchley, A. L., Coon, E. T., Painter, S. L., Harp, D. R., & Wilson, C. J. (2016). Influences and interactions of inundation, peat, and snow on active layer thickness: Influence of Environmental Conditions on ALT. Geophysical Research Letters, 43(10), 5116–5123. https://doi.org/10.1002/2016GL068550

Langer, M., Westermann, S., Walter Anthony, K., Wischnewski, K., & Boike, J. (2015). Frozen ponds: Production and storage of methane during the Arctic winter in a lowland tundra landscape in northern Siberia, Lena River delta. Biogeosciences, 12(4), 977–990. https://doi.org/10.5194/bg-12-977-2015

Schneider von Deimling, T., Lee, H., Ingeman-Nielsen, T., Westermann, S., Romanovsky, V., Lamoureux, S., Walker, D. A., Chadburn, S., Cai, L., Trochim, E., Nitzbon, J., Jacobi, S., & Langer, M. (2020). Consequences of permafrost degradation for Arctic infrastructure – bridging the model gap between regional and engineering scales. The Cryosphere Discussions, 1–31. https://doi.org/10.5194/tc-2020-192

We thank the reviewer for evaluating our manuscript, and for the numerous comments which help to improve it. We provide answers to the comments below.

Reviewer comments are in *blue italics*.

Author replies are in normal font.

Extracts from the manuscript are in **bold**, and modifications in the revised manuscript are <mark>**highlighted yellow**</mark>.

Anonymous Referee #2

Received and published: 24 August 2020

Authors implement micro- and meso-scale spatial grid resolution in the 1D CryoGrid model to illustrate the spatial effect of microtopographic feature on the rate of permafrost thaw. Authors found that implementing higher spatial resolution in the model leads to "more realistic possibilities (L13)". Now sure what type of possibilities they have in mind? Improving spatial representation of the polygonal tundra in the ESM type models is important. However, the current version of the manuscript lacks clarity. I found it hard to follow and the central Figure 2 looks like an electrical circuit diagram. If the take-home message is that very ESM needs to have micro-, meso-scale permafrost tundra representation, then it needs to be clearly stated. Maybe including recommendations on how authors think that can be done easily, in their opinion, using the current approach.

Overall, this is a timely and important work that needs to be published. However, the description, terminology, and flow require more work. I have a hard time reading and understanding the concept laid in the paper. I understand that much of the tiling concept was introduced in previous work (Aas et al.). However, the recap could be extremely helpful in setting up the stage in this study. Also, talking about uncertainties between different tiling approaches might be useful too. For example, if we average the overall effect from individual polygons, it could have the same carbon footprint as representing the polygonal tundra heterogeneity in one tile. When could that be or not be true? The comments below illustrate the lack of my knowledge of the presented scaling method. I hope the authors would not be discouraged by my comments and try to help me better understand their work in the revised version of the manuscript.

We appreciate that the reviewer acknowledges the importance and timeliness of our work. From the comments we understand that the main criticism of the reviewer is, that the description of our methodological approach lacks clarity and that the implications of our work with respect to large-scale models are not sufficiently explained. We think that these issues could be related to the fact that we presupposed that readers would be familiar with preceding works in which the concept of laterally coupled tiles was applied in a permafrost context (Langer et al., 2016, Aas et al.,2019, Nitzbon et al., 2019, and Nitzbon et al., 2020). In these

papers, the concept is introduced and applied to investigate different subgrid-scale processes in permafrost ecosystems. In particular, Nitzbon et al. (2019) introduced a three-tile setup for ice-wedge polygonal tundra and evaluated it using field observations from Samoylov Island in the Lena River delta. In the present study, we use that setup to represent micro-scale heterogeneity of ice-rich lowlands, and extended it by a representation of meso-scale heterogeneity. We show that the combined representation of micro- and meso-scale heterogeneities gives rise to pathways and feedbacks of landscape evolution which qualitatively agree with observations, but which have not been simulated with a numerical model before.

In order to underline the original and novel contributions of the present study, we carefully revised the manuscript and took care that it stands for its own. In particular, we revised the objectives, extended the description of the tiling approach, reworked the figures, conducted additional simulations, restructured and extended the results sections, and extended the discussion with respect to large-scale modelling. Hereafter, we address the specific comments of the reviewer in a point-by-point style.

Abstract Can be shortened and cleaned. There are too many we found. . ., also found. . ., for example. . ., our results suggest. . . It was really hard to wrap my head around what exactly was found and how that helps science, stakeholders, economy, etc.

We agree that the abstract contained a lot of detailed information. We revised and shortened it for the revised manuscript.

L50. What is tile-based modeling approach? Need to define.

We added a paragraph in the Introduction which introduces the „tiling approach" and summarizes previous work:

Many of the above-referenced modelling studies employed a so-called "tiling approach" to account for subgrid-scale heterogeneities of permafrost terrain. Instead of discretizing extensive landscape domains on a high-resolution mesh, the landscape is partitioned into a low number of characteristic landscape units, each of which is associated with a representative "tile" in the model. Thereby, geometrical characteristics (e.g., areas, distances, perimeters) are used to parameterize lateral fluxes among the landscape units. For example, Langer et al. (2016) used a two-tile model setup to investigate the effect of lateral heat fluxes in a lake-rich permafrost landscape, and Nitzbon et al. (2019) suggested a three-tile model setup to represent the micro-scale heterogeneity associated with ice-wedge polygon tundra. Schneider von Deimling et al. (2020) applied a five-tile setup to represent the interaction of linear infrastructure such as roads with underlying and surrounding permafrost. To date, the tiling method has not been applied to simultaneously represent permafrost landscape heterogeneities and their interactions across multiple spatial scales.

Moreover, we extended the description of the tiling scheme in the Methods section so that the methodology is now understandable without being familiar with the tiling concept in advance:

We used the concept of laterally coupled tiles to represent subgrid-scale spatial heterogeneities of permafrost terrain (Langer et al., 2016; Aas et al., 2019; Nitzbon et al., 2019). In general, the tiling concept involves the partitioning of real-world landscapes into a certain number of characteristic units, which are associated with the major surface and subsurface heterogeneities found in the landscape. Each of these units is then represented by a single ``tile'' in a permafrost model, and multiple tiles can interact through lateral exchange processes. The tiling approach thus allows to simulate subgrid-scale heterogeneities and lateral fluxes in macro-scale models like LSMs/ESMs, without discretizing extensive landscape domains on a high-resolution mesh, thereby keeping computational costs at a reasonable level.

In addition to these modifications in the main text, we think that the new Figure 1 as well as the revised Figure 2 facilitate a more intuitive understanding of our modelling approach.

L77. "To quantify the sensitivity". I am not sure how the sensitivity was addressed?

We understand that this formulation is imprecise. We wanted to express that our objective was to investigate how the projected permafrost degradation is affected by different representations of subgrid-heterogeneities. We rephrased the objectives which now read as follows:

Specifically, we address the following objectives:

1. To investigate the transient evolution of ice-rich permafrost landscapes in response to climate warming using different representations of micro- and meso-scale heterogeneity, thereby identifying degradation pathways and feedback processes associated with lateral fluxes on these different spatial scales.

2. To quantify the sensitivity of projected permafrost thaw and ground subsidence to different representations of micro- and meso-scale heterogeneity.

L79. What type of sources of uncertainty? See my main comments. By making super refined models, we can introduce many small uncertainties which will superposition at the end. The question is, where is the golden ratio?

We understand that this formulation is imprecise. In a preceding study, Nitzbon et al. (2020) found that different hydrological boundary conditions can lead to large deviations in the projections of ice-rich permafrost thaw under the RCP8.5 warming scenario. Here, we wanted to investigate whether these deviations are reduced, when heterogeneities on the meso-scale

are represented in the model. We removed this sentence from the manuscript as might be misleading, and modified the respective paragraph which now reads:

Overall, our goal is to provide a scalable framework for exploring the evolution of permafrost landscapes in response to a warming climate, which could potentially be incorporated into LSMs to allow more robust projections of permafrost loss in response to climate change. The presented simulations should thus be considered as numerical experiments to identify important scales and controls of permafrost degradation, instead of providing accurate site-specific projections.

Table 1. should it be m2? Are we talking about the gridcell resolution?

The table is only intended to introduce the terminology with respect to spatial scales. The length scales are given in the unit [m] and the numbers reflect the order of magnitude of landscape features on the respective length scale. The numbers do not correspond to a grid cell resolution of the employed model. We hope that this becomes more clear with the extended description of the tiling approach.

Figure 1. Are you simulating the transect or an entire area? If you model an entire area, then how that area is going to look under different resolutions? In an ideal case, we should be able to take any area and then apply a deferent resolution to it (zooming in and out). The different surface features will be more/less pronounced based on spatial resolution. Then we can model future changes under different resolutions and the difference between modeling results should tell us how fine we should go. This way sounds more straight forward to me...

The figure is primarily intended to give an impression of the various types and scales of landscape heterogeneities in permafrost lowlands. The transects are intended to give an impression of the variability of the ice-wedge polygons along low-gradient slopes. In light of the critique of reviewer #1 regarding this figure (and the entire section on the study area), we understand that the figure might raise wrong expectations regarding the scope of our modelling work. In fact we do not intend to simulate the landscape evolution for Samoylov Island, but rather consider generic test cases in which we vary the representation of micro- and meso-scale heterogeneities. For this, we use the tile-based modelling approach which involves some assumptions on the geometry of the modelled landscape. To clarify the scope of our study, we replaced Figure 1 with a schematic illustration of a generic ice-rich lowland landscape. In this new figure, we also indicated how the different tiles represent different parts of the overall landscape. The revised Figure 1 (in addition with the revised Figure 2), should make the scope of the study and the modelling approach more intuitive to understand. We moved the Figure of Samoylov Island to the Appendix (Figure A1), as it provides a real-world example for the simulated permafrost lowlands.

L127 what is field capacity?

Field capacity refers to the capacity of the soil to „hold" water after drainage of excess water. In CryoGrid3, there is a parameter which specifies the volumetric water content which the soil takes upon infiltration. We modified the respective formulation:

Infiltrating water is instantaneously routed downwards through unfrozen soil layers, whose water content is set equal to the field capacity parameter (i.e., the water holding capacity): [...]

If I understand it correctly, the θ_i is initialized? I suggest to rename Δp to Δd_ice. Typically, p represent pressure. So, ice thickness is initialized too? Does the model start from the initialized ice thickness or there is a steady-state run? So, the second term in equation 2 should be less than or equal to 1? Otherwise subsidence could be greater than the ice thickness. Can that be the case? I did not understand the denominator. What is $1-phi\_\{nat\}$ mean?

The volumetric ice contents θ_i are initialized as presented in Table 2. The excess ice content and the depth of the excess ice bearing layers can vary between different tiles (e.g. between polygon centres, rims and troughs). We did not conduct steady-state runs for the excess ice distribution, as our numerical model is not capable of simulating the accumulation of excess ice in the subsurface (see Discussion section 4.3). Instead, we based the cryostratigraphy on available measurements from the study area and previous modelling studies.

We renamed the variable Δp to Δd. Note, however, that it corresponds to the thickness of a soil cell which contains excess ice which is not to be confused with the thickness of the excess ice fraction. To clarify this point, and also to derive equation (2), we added a section in the Appendix (B), where we derive the formula and illustrate the composition of soil cells which contain excess ice (Figure B1). With these additional derivations it should be clear why the $1-\varphi_{nat}$ term is necessary, and that the θ_x is indeed bounded between 0 and 1, so that the subsidence cannot be larger than the ice thickness.

L149. Need a reference after "... hierarchical approach".

This terminology was introduced in our article to refer to the novel approach to apply the tiling concept on multiple scales (micro- and meso-scale) at the same time. In the revised manuscript we dropped the adjective „hierarchical" as it might be misleading. Instead, we only speak of „multi-scale tiling". As far as we know, the concept has not been applied in this form to permafrost environments so that we do not have additional references to provide.

N^μ is that somewhat standard notation? I had a hard time following that notation and remembering what it means. Is there a way to change it or use some other more intuitive notation? For example, use 1m2 or 1km2 notations. What is the total area modeled? Is this modeling represent a transect or a 2d area?

N^μ and N^m refer to the number of tiles which have been used to represent the heterogeneities on the micro- and meso-scale, respectively. In our simulations, these are either set to 1 or 3, as mentioned in the listing of the model setups in Section 2.2.1 as well as in Figure 2. These variables do not directly relate to an area or a grid resolution. The tiling concept which we employed in this study does not use an explicit 2D or 3D mesh, but rather a combination of multiple (coupled) 1D „submodels", each of which is representative for a different landscape unit.

The questions of the reviewer indicate that the tile-based modelling approach was not sufficiently explained in the original article. We hence entirely revised the description of the tiling approach and added a schematic (Figure 1), which illustrates the concept in combination with the revised Figure 2.

Does homogeneous means that one tile represents the entire transect. If so, then it would be easier to say that 1 tile approach.

We renamed all model configurations for the revised manuscript and adopted the reviewer's suggestion to call the most simple setup „single-tile".

What is the external reservoir? Is that water table depth?

The external reservoir can be thought of as a constant water table exterior to the model domain. If a tile which is connected to such a reservoir has a water table which exceeds that of the external reservoir, excess water can run off into the reservoir (without changing the level of the reservoir).

Figure 2, I had a hard time to understand and follow.

We revised the Figure based on suggestions of reviewer #1 who otherwise found the Figure very helpful as it provides an overview of all setups. We are confident that the revised Figure layout, together with the extended description of the tile-based modelling approach, facilitate a more intuitive understanding of our methodology.

L204 How many topological characteristics were used? Are these characteristics represent only magnitude of the lateral fluxes or something else too?

We used the following geometrical relations to characterize the tiles: area of a tile, elevation of a tile, distance between adjacent tiles, contact length between adjacent tiles. These relations have been used to calculate the magnitude of lateral fluxes as explained in the preceding studies Nitzbon et al. (2019) and Nitzbon et al. (2020). In addition, the areal proportions of the tiles have been used to calculate the area-weighted mean thaw depth and accumulated subsidence which is displayed in Figures 7 and 8.

Table 3 what is 'not a null' over 'big sigma' columns represent?

The column shows the area-weighted mean or the sum of the different characteristics of the micro-scale tiles. For the revised manuscript, we split up the column into two and labeled it with text instead of symbols.

I like the results section and was able to make more sense of it. I think that discussing the geomorphological processes as well as figure 6 diversify the message: "the importance of the tile-approach adoption by the ESM type models." I guess, it is important to focus on that message instead of diving into the concepts and pathways of the polygonal tundra geomorphological evolution.
For this type of paper, I would like to see a more in-depth mathematical analysis of the difference between different spatial resolutions as well as discussion of the corresponding uncertainties. I understand that this might lead to way too much work and may not be feasible in this paper. Then I suggest to exclude the ESM modeling discussion from the article and give it a different angle from the beginning.

We are happy that the reviewer could follow the results section despite the lack of clarity in our method description. We agree with the reviewer that the adoption of our tile-based model-setup in coarse-scale model frameworks would deserve a more in-depth mathematical analysis and framing, which is, however, beyond the scope of our study. We still see several important implications of our work for the LSM/ESM community which we discuss in Section 4.2 of the revised manuscript.
In addition to this, we think that it is an important contribution of our work, that manifold pathways of landscape evolution can be simulated and that these involve various feedback processes which influence permafrost degradation in response to a warming climate. In the revised manuscript, we explain these (geomorphological) processes and feedbacks directly along with the results (following the suggestion of reviewer #1), and discuss them in Section 4.1. The extended discussion of the geomorphological evolution of ice-wedge polygons and thaw lakes in Section 4.3 is intended to highlight links between our modelling work and the efforts of field researchers to develop conceptual models of these processes and landforms.

Consider bringing Figure 6 into the methods or introduction. Then it will setup the stage for the follow-up story.

We thank the reviewer for the suggestion. However, we decided to keep this figure in the discussion section, as it illustrates not only the capacities of our modeling scheme but also its limitations.

References (not contained in the original manuscript)

Schneider von Deimling, T., Lee, H., Ingeman-Nielsen, T., Westermann, S., Romanovsky, V., Lamoureux, S., Walker, D. A., Chadburn, S., Cai, L., Trochim, E., Nitzbon, J., Jacobi, S., & Langer, M. (2020). Consequences of permafrost degradation for Arctic infrastructure – bridging the model gap between regional and engineering scales. The Cryosphere Discussions, 1–31. https://doi.org/10.5194/tc-2020-192

Effects of multi-scale heterogeneity on the simulated evolution of ice-rich permafrost lowlands under a warming climate

Jan Nitzbon[1,2,3], Moritz Langer[1,2], Léo C. P. Martin[3], Sebastian Westermann[3], Thomas Schneider von Deimling[1,2], and Julia Boike[1,2]

[1]Permafrost Research, Alfred Wegener Institute Helmholtz Centre for Polar and Marine Research, Potsdam, Germany
[2]Geography Department, Humboldt-Universität zu Berlin, Berlin, Germany
[3]Department of Geosciences, University of Oslo, Oslo, Norway

Correspondence: Jan Nitzbon (jan.nitzbon@awi.de)

Abstract.

~~Thawing~~ In continuous permafrost lowlands, thawing of ice-rich ~~permafrost deposits can cause the formation of thermokarst terrain, thereby involving ground subsidence and feedbacks to the thermal and hydrological regimes~~ deposits and melting of massive ground ice leads to abrupt landscape changes called thermokarst, which have widespread consequences on the thermal, hydrological and biogeochemical state of the subsurface. ~~Thermokarst activity can entail manifold pathways of landscape evolution and cause rapid permafrost thaw in response to a warming climate. Numerical models that realistically capture these degradation pathways and represent the involved feedback processes at different spatial scales, are required to assess the threats and risks that thermokarst processes pose to the functioning of ecosystems and human infrastructure in the Arctic~~ However, macro-scale land surface models (LSMs) do not resolve such localized subgrid-scale processes and could hence miss key feedback mechanisms and complexities which affect permafrost degradation and the potential liberation of soil organic carbon in high latitudes. ~~In this study, we therefore introduce a multi-scale tiling scheme to~~ Here, we extend the CryoGrid 3 permafrost model ~~which allows to represent~~ with a multi-scale tiling scheme which represents the spatial heterogeneities of surface and subsurface conditions ~~, together with lateral fluxes of heat, water, snow, and sediment, at spatial scales not resolved in Earth system models (ESMs). We applied the model setup to a lowland tundra landscape in northeast Siberia characterized by ice-wedge polygons at various degradation stages. We present numerical simulations under a climate-warming scenario and investigate the sensitivity of projected permafrost thaw to different terrain heterogeneities, on both a~~ in ice-rich permafrost lowlands. We conducted numerical simulations using stylized model setups to assess how different representations of micro- and meso-scale heterogeneities affect landscape evolution pathways and the amount of permafrost degradation in response to climate warming. At the micro-scale~~(, the terrain was assumed to be either homogeneous or composed of~~ ice-wedge polygons~~) and a~~, and at the meso-scale ~~(to be either homogeneous or resembling a~~ low-gradient ~~slopes)~~slope. We found that ~~accounting for both micro- and meso-scale heterogeneities yields the most realistic possibilities for simulating landscape evolution . Simulations that ignored one or the other of these scales of heterogeneity were unable to represent all of the possible spatio-temporal feedbacks in ice-rich terrain. For example, we show that the~~ by using different model setups and parameter sets, a multitude of landscape evolution pathways could be simulated which correspond well to observed thermokarst landscape dynamics across the Arctic. These pathways include the formation, growth, and gradual drainage of thaw lakes, the transition

from low-centred to high centred ice-wedge polygons, and the formation of landscape-wide drainage systems due to melting of ice wedges ~~in one part of the landscape can result in the drainage of other parts, where surface water has been impounded a number of decades earlier as a result of ice-wedge thermokarst . We also found that including subgrid-scale heterogeneities in the simulations resulted in a more gradual response in terms of ground subsidence and permafrost thaw, compared to the~~

30 ~~more abrupt changes in simple one-dimensional simulations.~~ Moreover, we identified several feedback mechanisms due to lateral transport processes which either stabilize or destabilize the thermokarst terrain. The amount of permafrost degradation in response to climate warming was found to depend primarily on the prevailing hydrological conditions which in turn are crucially affected by whether or not micro- and/or meso-scale heterogeneities were considered in the model setup. Our results suggest that ~~, under a warming climate, the investigated area is more likely to experience widespread drainage of polygonal~~

35 ~~wetlands than the formation of new thaw lakes, which is in general agreement with evidence from previous field studies. We also discuss how the presented model framework is able to capture a broad range of processes involved in the cycles of ice-wedge and thaw-lake evolution. The results of this study improve our~~ the multi-scale tiling scheme allows to simulate ice-rich permafrost landscape dynamics in a more realistic way than simplistic one-dimensional models, and thus facilitates more robust assessments of permafrost degradation pathways in response to climate warming. Our modelling work improves

40 the understanding of how micro- and meso-scale processes ~~control~~ affect the evolution of ice-rich permafrost landscapes~~.~~ ~~Furthermore, the methods that we have developed allow improved representation~~ , and it informs macro-scale modellers focusing on high-latitude land surface processes about the necessities and possibilities for the inclusion of subgrid-scale processes such as thermokarst ~~in ESMs~~ within their frameworks.

1 Introduction

Thawing of permafrost in response to climatic change ~~,~~ poses a threat to ecosystems, infrastructure, and indigenous communities in the Arctic (AMAP, 2017; Vincent et al., 2017; Schuur and Mack, 2018; Hjort et al., 2018). ~~Permafrost degradation involves a wide range of feedback process from local to global scales, including widespread changes in soil moisture (Andresen et al., 2020) and the~~ Pan-Arctic modelling studies have suggested substantial permafrost loss (Lawrence et al., 2012; Slater and Lawrence, 2013) and associated changes in the water and carbon balance of the permafrost region (Burke et al., 2017; Kleinen and Brovkin, 2018; Andresen et al. the course of the twenty-first century and beyond. The potential liberation of ~~greenhouse gases, posing~~ carbon dioxide and methane from thawing permafrost poses a positive feedback to global climate warming (Schuur et al., 2015; Schneider von Deimling et al., 2015) ~~. However, the large-scale~~ which is yet poorly constrained. Indeed, the macro-scale[1] models used to project the response of permafrost to climate warming ~~,~~ employ a simplistic representation of permafrost thaw dynamics, which only reflects gradual and spatially homogeneous top-down thawing of frozen ground ~~(Lawrence et al., 2012; Slater and Lawrence, 2013; An~~

In particular, such models lack representation of thaw processes in ice-rich permafrost deposits that cause localized and rapid landscape changes called thermokarst ~~(Kokelj and Jorgenson, 2013)~~ (Kokelj and Jorgenson, 2013; Olefeldt et al., 2016). Thermokarst activity is induced on small spatial scales that are ~~not resolved in large-scale Earth system models (ESMs~~ below the grid resolution of macro-scale land surface models (LSMs), but it can have widespread effects on the ground thermal and hydrological regimes (Fortier et al., 2007; Liljedahl et al., 2016), on soil erosion (Godin et al., 2014), and on carbon decomposition pathways ~~(Lara et al., 2015; Turetsky et al., 2020). In addition, thermokarst features~~ (Lara et al., 2015; Walter Anthony et al., 2018; Turetsk Thermokarst activity can induce positive feedback processes leading to accelerated permafrost degradation and landscape collapse ~~(Walter Anthony et al., 2018; Turetsky et al., 2019; Farquharson et al., 2019; Nitzbon et al., 2020)~~ (Turetsky et al., 2019; Farquharson but also stabilizing feedbacks have been observed ~~(Jorgenson et al., 2015; Kanevskiy et al., 2017), overall establishing thermokarst as~~ in ice-rich terrain (Jorgenson et al., 2015; Kanevskiy et al., 2017). Overall, thermokarst processes can be considered a key factor of uncertainty in ~~any~~ future projections of how ~~permafrost and hydrology~~ the energy, water, and carbon balances of permafrost environments will respond to Arctic climate change (Turetsky et al., 2019).

~~To address these issues, numerical models resolving heterogeneities at the spatial scales of thermokarst features and representing the vertical and lateral physical processes~~ Ice-rich permafrost landscapes prone to thermokarst activity are typically characterized by marked spatial heterogeneities that can be linked to the accumulation and melting of excess ice (Kokelj and Jorgenson, 2013). For example, polygonal-patterned tundra in the continuous permafrost zone is underlain by networks of massive ice wedges which give rise to a regular and periodic partitioning of both the surface and the subsurface at the micro-scale (Lachenbruch, 1962). At the meso-scale, past thermokarst activity has led to a high abundance of thaw lakes in ice-rich permafrost lowlands (Morgenstern et al., 2011). Excess ice melt on the micro-scale can lead to the emergence of thaw features and feedbacks on the meso-scale, such as the formation of drainage networks (Liljedahl et al., 2016), the lateral expansion of thaw lakes (Jones et al., 2011), or the development of thermo-erosional gullies (Godin et al., 2014). These features have the potential to interact with each other, thereby adding more complexity to the landscape evolution, for example, when a thaw lake drains upon

---

[1]See Section 2.1 and Table 1 for the terminology used in this manuscript to designate different spatial scales.

incision of the thermo-erosional gully (Morgenstern et al., 2013). Overall, there is emerging evidence from field observations (Jorgenson et al., 2006; Farquharson et al., 2019) and remote sensing (Liljedahl et al., 2016; Nitze et al., 2018, 2020) that these subgrid-scale processes crucially affect permafrost degradation pathways and hence also the potential liberation of frozen

80 carbon pools.

Numerical models which represent the *thermokarst-inducing processes* (Nitzbon et al., 2020) that give rise to the observed complex pathways of permafrost landscape evolution ~~observed in the real world are required (Rowland et al., 2010)~~are an important tool to improve our understanding of how subgrid-scale processes affect permafrost degradation in response to climate warming (Rowland et al., 2010; Turetsky et al., 2019). In recent years, substantial progress has been made in the de-

85 velopment of numerical models to study the thermal and hydrological dynamics of permafrost terrain on small sptial scales (Painter et al., 2016; Jafarov et al., 2018), and to identify important feedbacks associated with various thermokarst landforms such as ice-wedge polygons (Abolt et al., 2018; Nitzbon et al., 2019; Abolt et al., 2020) or peat plateaus (Martin et al., 2019). The development of numerical schemes simulating ground subsidence resulting from excess ice melt (Lee et al., 2014; Westermann et al., 2016) enabled the assessment of transient changes of thermokarst terrain using dedicated permafrost models

90 (Langer et al., 2016; Nitzbon et al., 2019), but also more broadly using ~~ESM framworks (Aas et al., 2019)~~the frameworks of LSMs (Lee et al., 2014; Aas et al., 2019).

~~Using a tile-based modelling approachto represent lowlands underlain by massive ice wedges, Nitzbon et al. (2020) recently suggested the potential for substantial permafrost degradation in northeast Siberia in response to a warming climate, which is not captured by large-scale models that ignore thermokarst-inducing processes. These projections revealed a considerable~~

95 ~~uncertainty range associated with different hydrological boundary conditions in the simulations, that gave rise to contrasting pathways of landscape evolution, ranging from the development of high-centred polygons (HCPs) to the formation of thaw lakes. This uncertainty can be attributed to the fact that while the numerical modelexplicitly incorporates the micro-scale heterogeneity of ice-wedge polygon terrain (i.e., meters to tens of meters), it did not explicitly reflect meso-scale (i.e., hundreds to thousands of meters) landscape dynamics (see Table 1 for the terminology used to refer to different spatial scales)~~Several

100 of these models employed a so-called "tiling approach" to account for subgrid-scale heterogeneities of permafrost terrain. Instead of discretizing extensive landscape domains on a high-resolution mesh, the landscape is partitioned into a low number of characteristic landscape units, each of which is associated with a representative "tile" in the model. Thereby, geometrical characteristics of the landscape units (e.g., size and shape, symmetries, adjacencies) are used to parametrize lateral fluxes among the tiles. For example, ~~kilometer-scale mapping of ice-wedge polygon types at different Arctic sites revealed, that~~

105 ~~polygons of the same degradational stage are located close to each other, but that there is a variability of different polygon types at the meso-scale (Kartoziia, 2019; Abolt and Young, 2020). These patterns could thus be linked to lateral surface and subsurface water fluxes which follow the terrain's topography and affect the degradation of ice wedges (Nitzbon et al., 2019). Moreover, excess ice melt on the micro-scale, can lead to~~ Langer et al. (2016) used a two-tile model setup to investigate the effect of lateral heat fluxes in a lake-rich permafrost landscape, Nitzbon et al. (2019) suggested a three-tile setup to represent the

110 ~~emergence of thaw features and feedbacks on the meso-scale, such as the formation of drainage networks (Liljedahl et al., 2016), laterally expanding thaw lakes, or thermo-erosional gullies. These features have the potential to interact with each other, thereby~~

~~adding more complexity to the landscape evolution, for example, when a thaw lake drains upon incision of the thermo-erosional gully. Hence, in order to constrain the most likely landscape evolution and permafrost degradation pathways further, landscape heterogeneity and lateral processes at the meso-scale need to be considered. Tiling schemes which proved successful in realistically reflecting~~ micro-scale ~~permafrost dynamics (Aas et al., 2019), constitute a promising approach to also capture meso-scale processes in order to constrain those uncertainties further while keeping computational costs low~~<u>heterogeneity associated with ice-wedge polygon tundra, and Schneider von Deimling et al. (2020) applied a five-tile setup to represent the interaction of linear infrastructure such as roads with underlying and surrounding permafrost. So far, the tiling approach has not been applied to simultaneously represent heterogeneities of permafrost landscapes and their interactions across multiple spatial scales.</u>

~~In this study , we employ a multi-scale hierarchical tiling approach~~ <u>The overall scope of the present study was</u> to investigate the ~~transient response~~ <u>effect of micro- and meso-scale heterogeneities on the transient evolution</u> of ice-rich permafrost lowlands ~~in northeast Siberia to projected twenty-first century climate warming~~ <u>under a warming climate</u>. Specifically, we ~~address~~ <u>addressed</u> the following objectives:

1. To ~~investigate the transient evolution of ice-rich permafrost landscapes in response to climate warming using different representations of micro- and meso-scale heterogeneity, thereby identifying~~ <u>identify</u> degradation pathways and feedback processes associated with lateral fluxes ~~on these different spatial scales~~<u>of mass and energy on the micro- and meso-scale</u>.

2. To quantify ~~the sensitivity of projected permafrost thaw~~ <u>permafrost degradation in terms of thaw-depth increase</u> and ground subsidence ~~to different representations~~ <u>in dependence of the representation</u> of micro- and meso-scale ~~heterogeneity~~<u>heterogene</u>

<u>For this, we introduced a multi-scale tiling scheme into the CryoGrid 3 permafrost model and conducted numerical simulations for a site in northeast Siberia under a strong twenty-first century climate warming scenario (Representative Concentration Pathway (RCP) 8.5). We considered different model setups reflecting either the micro-scale heterogeneity associated with ice-wedge polygons, the meso-scale heterogeneity associated with low-gradient slopes, or a combination of both. As a reference, we considered "single-tile" simulations which emulate the behaviour of macro-scale LSMs.</u> Overall, our ~~study intends~~ <u>goal was</u> to provide a ~~transferable and~~ scalable framework for ~~more robustly assessing ice-rich permafrost landscape evolution, and at the same time aims at reducing sources of uncertainty in the projections of ice-rich permafrost~~ <u>exploring the transient evolution of permafrost landscapes in</u> response to a warming climate ~~presented by Nitzbon et al. (2020). Instead of providing quantitative site-specific projections , the~~ <u>which could potentially be incorporated into LSMs to allow more robust projections of permafrost loss under climate change. The</u> presented simulations should thus be considered as numerical experiments to ~~explore important scalesand controls~~ <u>identify the spatial scales, environmental factors, and feedback mechanisms which affect the degradation</u> of ice-rich permafrost~~landscape dynamics in response to a warming climate~~.

2 Methods

2.1 Terminology for spatial scales

Throughout ~~the manuscript we use~~ this manuscript we used a consistent terminology to refer to different characteristic length
scales of landscape features and processes. This terminology is summarized in Table 1.

~~Terminology Superscript Length scale Example subgrid $-\lesssim 10^5$ m all mentioned below micro $\mu \simeq 10^0 - 10^1$ m Ice-wedge polygon micro-topography meso m $\simeq 10^2 - 10^3$ m Thermo-erosion catchments, thaw lakes macro $- \simeq 10^4 - 10^5$ m River delta, ESM grid cell Overview of the terminology used in this manuscript to refer to the spatial scale of permafrost landscape features and processes.~~

2.2 Model description

2.3 ~~Study area~~

2.2.1 Multi-scale tiling to represent spatial heterogeneity

~~While the the scientific objectives and the modelling concept pursued in this study are general and applicable to any ice-rich continuous permafrost terrain~~ We used the concept of laterally coupled tiles (Langer et al., 2016; Aas et al., 2019; Nitzbon et al., 2019) to
represent subgrid-scale spatial heterogeneities of permafrost terrain. In general, the tiling concept involves the partitioning of
real-world landscapes into a certain number of characteristic units, which are associated with the major surface (or subsurface)
heterogeneities found in the landscape. Each of these units is then represented by a single "tile" in a permafrost model,
and multiple tiles can interact through lateral exchange processes. The tiling approach thus allows to simulate subgrid-scale
heterogeneities and lateral fluxes in macro-scale models like LSMs without discretizing extensive landscape domains on a
high-resolution mesh, and hence keeping computational costs at a reasonable level.

For the present study, we applied the tiling concept at multiple scales to represent common spatial heterogeneities of ice-rich
continuous permafrost lowlands (see Figure 1). At the micro-scale, these landscapes are typically characterized by ice-wedge
polygons which give rise to a regular patterning of the landscape (see Appendix A for an example site from northeast Siberia).
Here, we adopted the three-tile approach by Nitzbon et al. (2019), which partitions polygonal tundra lowlands into polygon
centres, polygon rims and inter-polygonal troughs. At the meso-scale, tundra lowlands are characterized by gently-sloped
terrain and often feature abundant thaw lakes that formed in the past due to thermokarst activity (see Appendix A). Here,
we used three meso-scale tiles to represent a low-gradient slope which is efficiently drained at its lowest elevation ("drainage
point").

Figure 2 provides an overview of the four model setups which were investigated in this study. These setups differ with
respect to the number of micro-scale tiles (N^{μ}) and meso-scale tiles (N^{m}), the product of which amounts to the total number
of tiles ($N = N^{\mu} \cdot N^{\mathrm{m}}$):

a. *Single-tile* ($N^\mu = 1$, ~~we chose Samoylov Island in the Lena river delta in northeast Siberia as our focus study area (72.36972°N, 126.47500°E). The island is located in~~ $N^m = 1$, Figure 2 a): This is the most simple case which reflects homogeneous surface and subsurface conditions across all spatial scales via only one tile (H). Water can drain laterally into an external reservoir at a fixed elevation (e_{res}). This setup emulates the one-dimensional representation of permafrost in LSMs and corresponds to the setup used for the simulations conducted by Westermann et al. (2016).

b. *Polygon* ($N^\mu = 3$, $N^m = 1$, Figure 2 b): This setting reflects the micro-scale heterogeneity associated with ice-wedge polygons via three tiles: polygon centers (C), polygon rims (R) and inter-polygonal troughs (T). The heterogeneity of the surface topography is expressed in different initial elevations of the soil surface of the tiles. The subsurface stratigraphies of the tiles differ with respect to ~~the central southern part of the Lena River delta within the lowland tundra vegetation zone and features cold continuous permafrost~~ depth (d_x) and amount (θ_x) of excess ice, reflecting the subsurface ice-wedge network which is linked to the polygonal pattern at the surface. Lateral fluxes of heat, water, snow, and sediment are enabled among the tiles, and the trough tile is connected to an external water reservoir. This model setup has previously been used by Nitzbon et al. (2019) and Nitzbon et al. (2020).

c. *Low-gradient slope* ($N^\mu = 1$, $N^m = 3$, Figure 2 c): This setup reflects a meso-scale gradient of slope S^m, for which the outer (i.e., downstream) tile (H^o) is well-drained into an external reservoir. The intermediate (H^m) and inner (H^i) tiles represent the landscape upstream of the outer tile at constant distances (D^m). The setting assumes a translational symmetry perpendicular to the direction of the slope, i.e., each tile represents the same areal proportion at the meso-scale. Lateral surface and subsurface water fluxes are enabled among the meso-scale tiles, while lateral heat fluxes as treated by Langer et al. (2016) were not considered at this scale.

d. *Low-gradient polygon slope* (~~mean annual ground temperature of about −9°C (Boike et al., 2019))~~$N^\mu = 3$, ~~which has been warming rapidly in recent years (about 0.9°C per decade (Biskaborn et al., 2019)).~~

~~a: Aerial photography of Samoylov Island with elevation contour lines based on the ArcticDEM. The study area is covered with water bodies of different sizes and ice-wedge polygons of different geomorphological stages. b: Two (arbitrary) examples of transects across the island, reflecting the gently-sloped terrain with steep cliffs at the margins. The inlets are details (about 100 m in diameter) of the aerial photography, reflecting polygon clusters of similar stages along the transects. Arrows point towards the main drainage direction. Note that ice-wedge polygons show little signs of degradation in the highest-elevated parts and close to the margins of the island (first and last inlet of both Transects). Along Transect A, the abundance of thermokarst troughs increases in the downstream direction of the slope. Small water bodies are visible in the central part of Transect B.~~

~~Samoylov Island belongs to the first terrace of the Lena River delta which formed during the Holocene (Schwamborn et al., 2002). The fluvial deposits contain substantial amounts of excess ice, mainly in form of ice wedges up to 10 m deep, which can be of epigenetic and syngenetic type. The surface of the island is characterized by~~ $N^m = 3$, Figure 2 d): This setup reflects a meso-scale slope featuring ice-wedge ~~polygons and water bodies of different sizes, ranging from ponds in~~

205　~~polygon troughs and centers to thermokarst lakes several hundred meters in diameter (Figure A1 a). While the low-lying western part of Samoylov Island is regularly flooded in spring, the eastern part is more elevated but with an overall very flat topography (Fig. A1 a). Ice-wedge polygons show different features across different parts of the island, including mostly low-centered polygons with water-covered centers, but also water-filled troughs indicative of~~ polygons at the micro-scale. Each meso-scale tile includes three micro-scale tiles (C,R,T), corresponding to the *polygon* setup described
210　above. However, only the trough tile of the outer polygon (T$^\text{o}$) is connected to an external reservoir (well-drained), while the intermediate and inner trough tiles are hydrologically connected along the meso-scale slope.

In the initial configurations, the landscapes were assumed to be undegraded, i.e., the ice-wedge ~~degradation, and some high-centered polygons with drained troughs . Polygons of different geomorphological type tend to occur as grouped "clusters" in the same areas of the island (Kartoziia, 2019), and the pre-dominant types differ along gently-sloped (about 0.1%)transects across the~~
215　~~island (Fig.A1 b) .~~

~~Meteorological and ground conditions have been measured on Samoylov Island for almost two decades, establishing it as a key site for the long-term monitoring of permafrost and~~ polygons were low-centred (LCPs), and no thaw lakes (water bodies, WBs) were present along the meso-scale slope. However, the ~~validation of numerical models (Boike et al., 2013, 2019). Various field studies addressed the climatology, hydrology, and geomorphology of the Island on different scales (Boike et al., 2008; Langer et al., 20~~
220　~~allowing the calibration and evaluation of numerical models used to assess permafrost dynamics in northeast Siberia under recent (Gouttevin et al., 2018; Nitzbon et al., 2019) and future (Westermann et al., 2016; Langer et al., 2016; Nitzbon et al., 2020) climatic conditions~~model allowed thermokarst features like high-centred polygons (HCPs) and thaw lakes to develop dynamically as a consequence of excess ice melt at different scales.

2.3　~~Model description~~

225　**2.2.1　~~Process~~ Processes representations (CryoGrid 3~~Xice~~)**

~~For the numerical experiments in this study, we used~~ Each of the tiles described in section 2.2.1 was associated with a one-dimensional representation of the subsurface through the CryoGrid 3 ~~(Xice)~~permafrost model, which is a physical process-based land surface model tailored for applications in permafrost environments (Westermann et al., 2016). ~~CryoGrid 3 has a one-dimensional representation of the subsurface for which it~~

230　*Heat diffusion with phase change:* The numerical model computes the subsurface temperatures ($T(z,t)$ [~~°C~~°C]) by solving the heat diffusion equation, thereby taking into account the phase change of soil water (θ_w [-]) through an effective heat capacity $\div (C_\text{eff}(z,T))$:

$$C(z,T) + \rho_w L_\text{sl} \frac{\partial \theta_\text{w}}{\partial T} \underbrace{\left(C(z,T) + \rho_w L_\text{sl} \frac{\partial \theta_\text{w}}{\partial T} \right)}_{C_\text{eff}(z,T)} \frac{\partial T}{\partial t} = \frac{\partial}{\partial z}\left(k(z,T) \frac{\partial T}{\partial z} \right) \div \tag{1}$$

In ~~Equation~~ Eqn. (1) ~~,~~$k(z,T)$ [$\text{W}\,\text{K}^{-1}\,\text{m}^{-1}$] denotes the thermal conductivity and $C(z,T)$ ~~is~~[$\text{J}\,\text{K}^{-1}\,\text{m}^{-3}$] the volumetric heat
235　capacity of the soil, ~~$k(z,T)$ the thermal conductivity of the soil, both parameterized~~ both parametrized depending on the soil

8

constituents. ρ_{w} [kg m^{-3}] is the density of water, and L_{sl} [J kg^{-1} K^{-1}] the specific latent heat of fusion of water. The upper boundary condition to Eq. (1) is prescribed as a ground heat flux $(Q_{\mathrm{g}}$ [W m^{-2}]) which is obtained by solving the surface energy balance ~~(Westermann et al., 2016).~~ as described in Westermann et al. (2016). The lower boundary condition is given by a constant geothermal heat flux at the lower end of the model domain $(Q_{\mathrm{geo}} = 0.05\,\mathrm{W\,m}^{-2})$.

Snow scheme: CryoGrid 3 simulates the dynamic build-up and ablation of a snow pack above the surface, heat conduction through the snowpack, changes to the snowpack due to infiltration and refreezing of rain and meltwater, and changes in snow albedo due to ~~aging (Westermann et al., 2016)~~ageing. Snow is deposited at ~~a constant~~ an initial density $(\rho_{\mathrm{snow}} = 250\,\mathrm{kg\,m}^{-3})$ which can ~~effectively~~ increase due to infiltration and refreezing of water.

Hydrology scheme: The model further employs a simple vertical hydrology scheme to represent changes in the ground hydrological regime due to infiltration of rain or meltwater, and evapotranspiration (Martin et al., 2019; Nitzbon et al., 2019). Infiltrating water is instantaneously routed downwards through unfrozen soil layers, whose water content is set equal to the field capacity parameter (i.e., the water holding capacity): $\theta_{\mathrm{fc}} = 0.5$. Once a frozen soil layer is reached, excess water successively saturates the above-lying unfrozen soil layers upwards. Excess water is allowed to pond above the surface, ~~and heat~~ leading to the formation of a surface water body. Surface water is modulated by evaporation as well as lateral fluxes to adjacent tiles or into an external reservoir (see paragraph *Lateral fluxes* below). Heat transfer through unfrozen surface water bodies is ~~represented~~ realized by assuming complete mixing of the water column ~~throughout~~ during the ice-free period ~~(Westermann et al., 2016).The field capacity parameter was set to $\theta_{\mathrm{fc}} = 0.5$~~(i.e., the water column has a constant temperature profile with depth).

Excess ice scheme: CryoGrid 3 ~~represents a range of physical processes which enable~~ has an excess ice scheme ("Xice"), which enables it to simulate the ~~formation of thermokarst in ice-rich permafrost deposits Westermann et al. (2016); Langer et al. (2016); Ni~~ ~~layers~~ground subsidence as a result of excess ice melt (i.e., thermokarst), following the algorithm proposed by Lee et al. (2014): Subsurface grid cells which have an ice content (θ_{i}) ~~exceeding~~ that exceeds the natural porosity (ϕ_{nat}) of the soil constituents ~~,~~ $(\theta_{\mathrm{m}} + \theta_{\mathrm{o}})$ are treated as ~~excess ice layers. Once an excess ice layer~~ excess-ice-bearing cells; once such a cell thaws, the resulting excess water ~~$\theta_{\mathrm{i}} - \phi_{\mathrm{nat}}$~~ is routed upwards, while above-lying soil constituents are routed downwards ~~, following the scheme proposed by Lee et al. (2014). Thawing of an excess icelayer of thickness Δp thus~~ and fill the space previously occupied by the excess ice. According to this scheme, thawing of a excess-ice-bearing grid cell of thickness Δd results in a net ground subsidence (Δs) ~~of the ground surface:~~ which equals

$$\Delta s = \Delta \underline{d} \underbrace{\frac{\theta_{\mathrm{i}} - \phi_{\mathrm{nat}}}{1 - \phi_{\mathrm{nat}}}}_{\theta_{\mathrm{x}}}, \tag{2}$$

where θ_{x} denotes the excess ice ~~content~~ fraction of the ice-rich soil ~~layer~~cell (see Appendix B for a derivation). The excess water is then treated by the hydrology scheme, i.e., it can either pond at the surface or run off laterally.

Lateral fluxes: The thermal regime and thaw processes in ice-rich permafrost are ~~further controlled~~ affected by lateral fluxes of mass and energy at subgrid-scales. We used the concept of laterally coupled tiles ~~(Langer et al., 2016; Nitzbon et al., 2019) to represent subgrid heterogeneity~~ to represent subgrid-scale heterogeneities of permafrost terrain (see Section 2.2.1 for details). We followed Nitzbon et al. (2019) to represent lateral fluxes of heat, water, and snow between adjacent tiles at the micro-

scale. Furthermore, we included micro-scale advective sediment transport due to slumping, following the ~~scheme introduced by Nitzbon et al. (2020). For this study, we advanced the model capacities by taking into account lateral fluxes of water on the meso-scale~~ approach and using the same parameter values as Nitzbon et al. (2020). At the meso-scale, we only considered lateral water fluxes, for which we further ~~distinguished between surface fluxes~~ discriminated between surface and subsurface contributions. Both surface and subsurface water fluxes were calculated according to a gradient in water table elevations following Darcy's law, but the hydraulic conductivities differed considerably ($K^{\mathrm{subs}} = 10^{-5}\,\mathrm{m\,s^{-1}}$, $K^{\mathrm{surf}} = 10^{-2}\,\mathrm{m\,s^{-1}}$; see Appendix C for details). ~~Finally, our model allowed for lateral~~ We did not consider lateral fluxes of heat, snow, and sediment at the meso-scale, as these were assumed to be either negligible on the time scale of interest (heat, sediment), or of uncertain importance (snow). Finally, the model allows for drainage of water ~~, by assuming an external reservoir~~ into an "external reservoir" at a fixed elevation (e_{res}) and a constant ~~effective~~ hydraulic conductivity ($K_{\mathrm{res}} = 2\pi K_{\mathrm{subs}}$ ~~) as hydrological boundary condition for a tile.~~

2.2.2 ~~Multi-scale hierarchical tiling~~

; see Supplementary Information of Nitzbon et al. (2020) for details).

~~For the present study, we extended the concept of laterally coupled tiles (Langer et al., 2016; Nitzbon et al., 2019) to a multi-scale hierarchical approach that allows to represent the subgrid-scale heterogeneity of permafrost terrain in general, and of thermokarst processes in particular. The multi-scale tiling hierarchy can flexibly be adapted to represent heterogeneous permafrost landscapes and features across several spatial scales. Different numbers of micro-scale tiles (N^{μ}) and meso-scale tiles (N^{m}) are used to reflect heterogeneity at different subgrid-scales. Each of the tiles is associated with a one-dimensional representation of the subsurface.~~

2.3 Model settings and simulations

~~Overview of the the different tile-based model setups used to represent heterogeneity at micro- and meso-scales. The depth of excess ice (d_{x}) and the excess ice content (θ_{x}) determine the distribution of excess ground ice in each of the tiles. An external reservoir (blue triangle) at a fixed elevation (e_{res}) prescribes the hydrological boundary conditions. Note that d_{x} and θ_{x} for the simple tile are chosen such that they correspond to the area-weighted mean of the three tiles of the polygon setup.a: The homogeneous setup used only one tile (H) and does not reflect any subgrid-scale heterogeneity.b: The polygon setup reflects micro-scale heterogeneity of topography and ground ice distribution associated with ice-wedge polygons via three tiles: polygon centres (C), polygon rims (R) and inter-polygonal troughs (T). The parameters e_{R} and e_{T} indicate the (initial) elevation of rims and troughs relative to the center. The micro-scale tiles are interacting through lateral fluxes of heat, water, snow, and sediment.c: The homogeneous landscape setup reflects meso-scale heterogeneity of an ice-rich lowland via three tiles (H$^{\mathrm{o,m,i}}$) of which the outer one (H$^{\mathrm{o}}$) is connected to a draining reservoir. The intermediate (H$^{\mathrm{m}}$) and inner tiles (H^{i}) are located at distances D^{m} along a low-gradient slope S^{m}. The meso-scale tiles are interacting through lateral surface and subsurface water fluxes.d: The polygon landscape setup incorporates heterogeneities at both micro- and meso-scales via a total of nine tiles.~~

~~While the concept of the multi-scale tiling is very general, we applied it for the present study to create the subsequent four model setups (see Figure 2): *Homogeneous* ($N^\mu = 1$, $N^m = 1$, Figure 2 a): This is the most simple case which reflects homogeneous surface and subsurface conditions across all spatial scales via only one tile (H). Water can drain laterally into an external reservoir at a fixed elevation (e_{res}). This setup comes closest to the simplistic representation of permafrost in ESMs and corresponds to the set-up for the simulations presented in Westermann et al. (2016). *Polygon* ($N^\mu = 3$, $N^m = 1$, Figure 2 b): This setting reflects the micro-scale heterogeneity associated with ice-wedge polygons via three tiles: polygon centers (C), polygon rims (R) and inter-polygonal troughs (T). The heterogeneity of the surface topography is expressed in different initial elevations of the soil surface of the tiles. The subsurface stratigraphies of the tiles differ with respect to the depth (d_x) and amount (θ_x) of excess ice, reflecting the network of ice wedges linked to the polygonal surface pattern. Lateral fluxes of heat, water, snow, and sediment is enabled among the tiles, and the trough tile is connected to an external water reservoir. This configuration has been used by Nitzbon et al. (2019) and Nitzbon et al. (2020). The characteristics of the polygon setting are summarized in Table 3. *Homogeneous landscape* ($N^\mu = 1$, $N^m = 3$, Figure 2 c): This setup reflects a meso-scale gradient of slope S^m, for which the outer tile (H^o) is connected to a low-lying reservoir (well-drained).The intermediate (H^m) and inner (H^i) tiles represent the landscape upslope of the well-drained tile (drainage point) at constant distances (D^m). The setting assumes a translational symmetry perpendicular to the direction of the slope, i.e. each tile represents an equal total area at the meso-scale. Lateral surface and subsurface water fluxes are enabled among the meso-scale tiles, while lateral heat fluxes as treated by Langer et al. (2016) were not considered in this study . *Polygon landscape* ($N^\mu = 3$, $N^m = 3$, Figure 2 d): This setup reflects a meso-scale slope featuring~~ While the the scientific objectives and the modelling concept pursued in this study are general and in principle transferable to any ice-rich permafrost terrain, we chose Samoylov Island in the Lena River delta in northeast Siberia as our focus study area. The island lies in the continuous permafrost zone and is characterized by ice-wedge ~~polygons at the micro-scale. Each meso-scale tile is represented by three tiles (C,R,T) at the micro-scale, corresponding to the *polygon* setup described above. However, only the trough tile of the outer polygon (T^o) is connected to a low-lying reservoir (well-drained), and the intermediate and inner troughs are hydrologically connected along the meso-scale slope.~~

2.4   ~~Model settings and simulations~~

polygons and surface water bodies of different sizes. The model input data (soil stratigraphies, parameters, meteorological forcing, etc.) were specified based on available observations from this study site. Details on the study area are provided in Appendix A.

2.3.1   Soil stratigraphies and ground ice distribution

The subsurface composition of all tiles ~~is~~ was represented via a generic soil stratigraphy (Table 2). The stratigraphy ~~is~~ was based on previous studies ~~using~~ that applied CryoGrid 3 ~~for~~ to the same study area (Nitzbon et al., 2019, 2020). It consists of two highly porous layers of $0.1\,\text{m}$ thickness which reflect the surface vegetation and an organic-rich peat layer. Below ~~that~~

those, a mineral layer with silty texture follows. An excess ice layer of variable ~~total~~ ice content θ_i extends from a variable depth

335 d_x down to a depth of $10.0\,\mathrm{m}$. Between the variable excess ice layer and the mineral layer, we assumed an ice-rich intermediate layer of $0.2\,\mathrm{m}$ thickness ~~is placed~~and a total ice content of 0.65. Below the variable excess ice layer follow an ice-poor layer and bedrock down to the end of the model domain.

The default ice content assumed for the excess ice layer of homogeneous tiles (no micro-scale heterogeneity) was $\theta_i^H = 0.75$ and the default depth of this layer was $d_x = 0.9\,\mathrm{m}$. To reflect the heterogeneous excess ice distribution associated with ice-wedge

340 polygons, different ice contents were assumed for the excess ice layers of polygon centres ($\theta_i^C = 0.65$), rims ($\theta_i^R = 0.75$), and troughs ($\theta_i^T = 0.95$). However, the area-weighted mean ~~excess~~ ice content of ice-wedge polygon terrain is identical to the default value assumed for ~~simple~~ homogeneous tiles (Table 3).

~~Generic soil stratigraphy used to represent the subsurface of all tiles. An ice-rich layer of variable ice content (θ_i) is located~~

345 ~~at variable depth (d_x) from the surface. Note that the effective excess ice content (θ_x) is linked to the absolute ice content~~ ~~(θ_i) and the natural porosity (ϕ_{nat}) via the relation given in Equation (2). The soil texture is only used to parameterize the~~ ~~freezing-characteristic curve of the respective layer. Depth from mDepth to mMineral θ_m Organic θ_o Nat. por. ϕ_{nat} Soil texture~~ ~~Water θ_w^0 Comment0 0.1 0 0.15 0.85 sand 0.85 Vegetation layer 0.1 0.2 0.10 0.15 0.75 sand 0.75 Organic layer 0.2 $d_x - 0.2$~~ ~~0.25 0.10 0.65 silt 0.65 Mineral layer $d_x - 0.2$ d_x 0.20 0.15 0.55 sand 0.65 Intermediate layer d_x 10 $\frac{1.05-\theta_i}{2}$ $\frac{0.95-\theta_i}{2}$ 0.55 sand~~ ~~θ_i Variable excess ice layer 10 30 0.50 0.05 0.45 sand 0.45 Ice-poor layer (Taberit) 30 1000 0.90 0 0.10 sand 0.10 Bedrock~~

350 ### 2.3.2 Topography and geometrical relations among the tiles

~~For the~~ *Topography:* For the ~~homogeneous~~*single-tile* setup (Figure 2 a) the initial ~~altitude~~ elevation of the soil surface was ~~assumed to be $20.0\,\mathrm{m}$above sea level, corresponding roughly to the altitude of the study area (see Section ??)~~set to $0.0\,\mathrm{m}$. This value does not affect the simulation results, but it serves as a reference for the variation of the micro- and meso-scale topographies. For the *polygon* setup (Figure 2 b) we assumed that the rims were elevated by $e_R = 0.2\,\mathrm{m}$ relative to the polygon

355 centres, while the troughs had the same ~~altitude~~ initial elevation as the centres ($e_T = 0.0\,\mathrm{m}$). While this choice of parameters varies slightly from the values assumed in previous studies (Nitzbon et al., 2019, 2020), it allows for consistent comparability to the setups without micro-scale heterogeneity (see Table 3).

The meso-scale topography in the ~~homogeneous landscape~~*low-gradient slope* setup (Figure 2 c) was obtained by multiplying the meso-scale distances (D^m) with the slope of the terrain (S^m). ~~We set $D^m = 100\,\mathrm{m}$ and $S^m = 0.001$ for all *landscape* setups,~~

360 ~~yielding elevations of $0.1\,\mathrm{m}$ and $0.2\,\mathrm{m}$ relative to the outer tile for the intermediate and inner tiles, respectively.~~ The micro-scale topography of the *low-gradient* polygon ~~landscape~~*slope* setup (Figure 2 d) was obtained by ~~adding~~ summing up the relative topographic elevations of the meso- and micro-scales.

2.3.3 ~~Topology~~

Geometry: We made simplifying assumptions to determine the adjacency and geometrical relations such as distances and

365 contact lengths ~~between~~ among the tiles at the micro- and meso-scale. These ~~topological~~ geometrical characteristics determine the magnitude of lateral fluxes between the tiles, and only need to be specified if more than one tile is used to represent

the respective scale. For the ~~polygon setup at the~~ *polygon* setup with three micro-scale tiles, we assumed a geometry of a circle (~~C~~centre tile) surrounded by rings (~~R,T), following~~ rim and trough tiles), identical to the setup by Nitzbon et al. (2020). This geometry is fully defined by specifying the total area (A^μ) of a single polygonal structure ~~and~~ together with the areal fractions ($\gamma_{C,R,T}$) of the three tiles. Here, we chose values which constitute a compromise between observations from the study area and comparability to the setups without micro-scale heterogeneity (Table 3). For ~~this~~ the employed geometry, the micro-scale distances (D^μ) and contact lengths (L^μ) can be calculated ~~as~~ according to the formulas provided in the Supplementary Information to Nitzbon et al. (2020).

~~For the~~ For the *~~landscape~~low-gradient slope* setups with three meso-scale tiles, we assumed translational symmetry of the landscape in the direction perpendicular to the direction of the gradient. Furthermore, the three meso-scale tiles were assumed to be at equal distances of $D^{\mathrm{m}} = 100\,\mathrm{m}$ from each other. Hence, each meso-scale tile is representative ~~for~~ of the same areal fraction of the overall landscape. ~~For the translational symmetry, it is sufficient to specify D^{m} in order to calculate the lateral surface and subsurface water fluxes.~~

~~Parameter Symbol Unit C R T ∅ / Σ H Depth of excess ice layer d_x m 1.0 0.9 0.7 0.9 0.9 Ice content of excess ice layer θ_i - 0.65 0.75 0.95 0.75 0.75 Areal fraction γ - $\frac{1}{3}$ $\frac{1}{2}$ $\frac{1}{6}$ 1 1 Total area A^μ m² − − − 140 1 Initial elevation e m 0.0 0.2 0.0 0.1 0.0 Reservoir elevation poorly-drained $e_{\mathrm{res}}^{\mathrm{pd}}$ m − − 0.0 0.0 − 0.1 Reservoir elevation well-drained $e_{\mathrm{res}}^{\mathrm{wd}}$ m − − −10.0 −10.0 − −10.0 Overview of the model parameters for different representations of the micro-scale. Elevation values are given relative to the initial altitude of the center tile ($a_C = 20.0\,\mathrm{m}$). Note that on average the polygon setup (C,R,T) exhibits the same characteristics as the homogeneous setup (H). Note that setting the area of the simple tile to $A^\mu = 1\,\mathrm{m}^2$ is an arbitrary choice, as it cancels out during the calculation of the meso-scale fluxes due to the assumed symmetry.~~

2.3.3 ~~Forcing~~ Meteorological forcing data

We used the same meteorological forcing dataset which has been used in preceding studies based on CryoGrid 3 for the same study area (Westermann et al., 2016; Langer et al., 2016; Nitzbon et al., 2020). The dataset spans the period from 1901 until 2100 and is based on down-scaled CRU-NCEP v5.3 data for the period until 2014. For the period after 2014, climatic anomalies obtained from CCSM4 projections for the RCP8.5 scenarios were applied to a ~~repeatedly appended base climatological period~~fifteen-year climatological base period (2000-2014). A detailed description of how the forcing dataset was generated is provided by Westermann et al. (2016).

2.3.4 Simulations

~~To investigate the sensitivity to the micro-scale representation and to compare the *landscape* setup to the setups without meso-scale heterogeneity we conducted a total of six simulations . For each micro-scale representation (*homogeneous* versus polygon) we conducted three simulations under the RCP8.5 warming scenario: *well-drained, poorly-drained, landscape*. The well-drained and poorly-drained cases for the polygon setup correspond to the confining cases considered in Nitzbon et al. (2020), and reflect contrasting hydrological boundary conditions (Table 3). For~~ Table 4 provides an overview of all simulations which were conducted for the ~~well-drained case,~~ four different model setups introduced in section 2.2.1. For both the *single-tile* and the

13

400 *polygon* setups we conducted four model runs in which we varied the elevation of ~~external reservoir was set to $e_{\text{res}}^{\text{wd}} = -10.0\,\text{m}$, independent of the micro-scale representation~~the external water reservoir (e_{res}) in order to reflect a broad range of hydrological conditions. For the ~~poorly-drained case, the elevation of the external reservoir was set to $e_{\text{res}}^{\text{pd}} = -0.1\,\text{m}$ (*homogeneous*) and $e_{\text{res}}^{\text{pd}} = 0.0\,\text{m}$ (*polygon*), respectively. For the~~ *low-gradient slope* and the *low-gradient polygon slope* setups we conducted two model runs in which we varied the gradient of the slope (S^{m}) in order to reflect essentially flat ($S^{\text{m}} = 0.001$) as well as

405 gently-sloped terrain ($S^{\text{m}} = 0.01$). In all ~~landscape~~slope simulations, ~~only~~ one tile (Hᵒ and Tᵒ, respectively) was connected to an external reservoir (see Fig. 2 c,d; ~~$e_{\text{res}}^{\text{wd}} = -10.0\,\text{m}$), while the hydrological boundary fluxes of the intermediate and inner tiles resulted from adjacent tiles only.~~$e_{\text{res}} = -10.0\,\text{m}$).

The subsurface temperatures of each model run were initialized in ~~10/~~Oct 1999 with a typical temperature profile for that time of year which was based on long-term borehole measurements from the study area (Boike et al., 2019). Using multi-year

410 spin-up periods did not result in significant changes to the near-surface processes investigated in this study so that ~~uncertainty biases~~ related to the initial ~~condition~~subsurface temperature profile can be excluded. The analyzed simulation period was the twenty-first century from ~~01/~~Jan 2000 until ~~12/~~Dec 2099.

3 Results

3.1 ~~Landscape evolution~~

415 ### 3.0.1 ~~Simulations without micro-scale heterogeneity~~

~~Landscape evolution in the simulations with a homogeneous micro-scale representation under the RCP8.5 warming scenario. The well-drained and poorly-drained cases correspond to the model setup without micro- or meso-scale heterogeneity (Fig. 2 a) and the landscape case corresponds to the model setup with only meso-scale heterogeneity (Fig. 2 c).~~

~~The~~ The presentation of the results is structured according to the four different model setups described in Section 2.2.1

420 and visualized in Figure 2 a-d. Figures 3 to 6 provide an overview of the simulated landscape evolution in the four setups by displaying the landscape configuration in selected years during the simulation period. While these figures are intended to allow an intuitive overview of the qualitative behaviour of the model, Figures 7 and 8 provide a quantitative assessment of permafrost degradation by showing time series of the maximum thaw depths and accumulated ground subsidence for all simulations.

3.1 Single-tile

425 Figure 3 shows the landscape configuration for selected years throughout the twenty-first century under RCP8.5 for ~~all runs with a homogeneous micro-scale representation (setups presented in Fig. 2 a,c) is visualized in Figure ??.~~

~~Single-tile simulations:~~ ~~Until~~ the *single-tile* setup (see Figure 2 a) under four different hydrological boundary conditions. Until the middle of the simulation period (2050) no excess ice melt and associated ground subsidence occur~~in both the well-drained and the poorly-drained single-tile simulations~~, irrespective of the hydrological conditions (Fig. ~~??~~3 a–c, ~~first~~

430 ~~and fifth column).~~ all columns; Fig. 8 a). However, the maximum thaw depths are steadily increasing during that period (see

14

Figure 7 a), with negligible differences between the four runs under different hydrological conditions. Between 2050 and 2075 excess ice melt occurs in all *single-tile* simulations, leading to ground subsidence of about 0.2 m in the two well-drained cases (Figure 3 d, first and second column), about 0.1 m in the intermediate case (Figure 3 d, third column), and about 0.5 m in the poorly-drained case, where excess ice melt leads to the formation of a shallow surface water body (Figure 3 d, fourth column). By 2100 total ground subsidence amounts to about 0.8 m in the well-drained simulations (Fig. 4 e, first and second column), and about 1.0 m in the simulation with $e_{res} = -0.5$ m, where it is accompanied by the formation of a shallow surface water body (Fig. 4 e, third column). In the poorly-drained simulation ($e_{res} = -0.1$ m), excess ice melt proceeds fastest, causing the surface water body to deepen, and to reach a depth of about 2 m by 2100; a talik of about about 1.5 m thickness has formed underneath the water body by the end of the simulation period (Fig. 3 e, fifth column).

Overall, the simulation results indicate that permafrost degradation is strongest as soon as a limitation of water drainage results in the formation of a surface water body. The presence of surface water changes the energy transfer at the surface in different ways. First, it reduces the surface albedo (from 0.20 for barren ground to 0.07 for water), resulting in a higher portion of incoming shortwave radiation. Second, water bodies have a high heat capacity which slows down their freeze-back compared to soil. Third, the thawed saturated deposits beneath the surface water body have a higher thermal conductivity compared to unsaturated deposits, which allows heat to be transported more efficiently from the surface into deeper soil layers.

Interestingly, during the initial phase of excess ice melt which occurs between 2050 and 2075, our simulations suggest a non-monotonous dependence of permafrost degradation on the drainage conditions. This is indicated by the fact that the lowest degradation both in terms of maximum thaw depth and accumulated subsidence is simulated for the intermediate case with $e_{res} = -0.5$ m (see Figure 7 a and 8 a). This can likely be attributed to contrasting effects of the hydrological regime in the active layer on thaw depths. When the near-surface ground is unsaturated (as in the simulations with $e_{res} = -1.0$ m and $e_{res} = -10.0$ m), the highly-porous organic-rich surface layers (see Table 2) have an insulating effect on the ground below due their low thermal conductivity. At the same time, less heat is required to melt the ice contained in the mineral soil layers whose ice content corresponds to the field capacity than it would be needed if their pore space was saturated with ice. In the intermediate case with $e_{res} = -0.5$ m, the combination of dry, insulating near-surface layers and ice-saturated mineral layers beneath leads to the lowest thaw depths and hence the slowest initial permafrost degradation. However, as soon as a surface water body forms in that simulation (between 2075 and 2100), the positive feedback on thaw described above takes over, resulting in stronger degradation by 2100 compared to the well-drained settings ($e_{res} = -1.0$ m and $e_{res} = -10.0$ m) for which no surface water body forms during the simulation period.

In summary, the *single-tile* simulations illustrate the non-trivial relation between the ground hydrological regime and permafrost thaw, and demonstrate the positive feedback associated with surface water body formation resulting from excess ice melt.

3.2 Polygon

Figure 4 illustrates the landscape evolution throughout the twenty-first century under RCP8.5 for the simulations with the *polygon* setup, i.e., with a representation of micro-scale heterogeneity typical for ice-wedge polygonal tundra. In addition, it shows the geomorphological state of the polygon micro-topography, i.e., whether it is low-centered (LCP), intermediate-centered (ICP), high-centred with inundated troughs (HCPi), high-centred with drained troughs (HCPd), or covered by a surface water body (WB), according to Equations (??) to (??) in Appendix D. Initially, all simulations feature undegraded ice-wedge polygons with a low-centred micro-topography (Figure 4 a).

Between 2000 and 2025 a shallow surface water body of about $0.5\,\mathrm{m}$ depth forms in the poorly-drained simulation ($e_{\mathrm{res}} = 0.0\,\mathrm{m}$) as a result of excess ice melt in the center, rim, and trough tiles (Fig. 4 b, fourth column). The bottom of the water body has a high-centred topography. The landscape configuration does not change much until 2050 (Fig. 4 c, fourth column), and the maximum thaw depths and accumulated ground subsidence increase more slowly than in the initial two to three decades (Figures 7 b and 8 b, purple lines). We explain this interim stabilization with the subaqueous transport of sediment from the centres to the rims and from the rims to the troughs, where the additional sediment has an insulating effect on the ice wedge underneath. After 2050 excess ice melt proceeds faster, causing the surface water body to deepen, reaching a depth between about $1\,\mathrm{m}$ (centre tile) and more than $2\,\mathrm{m}$ (trough tile) by 2075 (Fig. 4 d, fourth column). We explain the acceleration of permafrost degradation at the beginning of the second half of the simulation period (Figures 7 b and 8 b, purple lines) by a combination of additional warming from the meteorological forcing, and positive feedbacks due to the surface water body (as explained for the *single-tile* simulation in Section 3.1). Until 2100 excess ice melt proceeds further, resulting in a water body depth of 2-4 m and the formation of an extended talik underneath (Fig. 4 e, fifth column). By the end of the simulation period, the lake is not entirely bottom-freezing in winter. This constitutes another positive feedback on the degradation rate, since the heat from the ground can be transported much more efficiently through bottom-freezing water bodies than through those which do not bottom-freeze, due to the higher thermal conductivity of ice compared to that of unfrozen water.

Landscape simulations: ~~The simulated evolution of the outer tile~~The remaining three simulations show a similar landscape evolution during the first half of the simulation period (2000-2050), with excess ice melt occurring only in the trough tiles, resulting in a transition from LCP to ICP micro-topography (Fig. 4 a–c, first to third column). In contrast to the *single-tile* setup, the *polygon* simulations show a monotonous relation between permafrost degradation and drainage conditions during this period. Higher elevations of the external water reservoir (i.e., poorer drainage) result in faster thaw-depth increase (Figures 7 b) and earlier onset of ground subsidence (Figure 8 b). Between 2050 and 2075, substantial excess ice melt occurs in the trough and rim tiles, involving a transition from the ICP to a pronounced HCP micro-topography (Fig. 4 d, first to third column). In addition to the positive feedback through surface water formation, the degradation rate in the *polygon* simulations is accelerated by a positive feedback through lateral snow redistribution. Snow is deposited preferentially in micro-topographic depressions such as initially subsided troughs where it improves the insulation and traps heat in the subsurface during winter, enabling faster and deeper thaw in the subsequent summer. Note that this positive feedback is not represented in the *single-tile* simulations.

By 2075 the influence of the drainage conditions on the surface water coverage is most pronounced. While a water body extending over all tiles has formed in the poorly-drained simulation ($e_{\mathrm{res}} = 0.0\,\mathrm{m}$), the polygon centres are (still) elevated above

the water table in the intermediate case with $e_{res} = -0.5\,\mathrm{m}$. For $e_{res} = -1.0\,\mathrm{m}$, surface water is found only in the trough tile, while all surface water is drained in the simulation with $e_{res} = -10.0\,\mathrm{m}$. Irrespective of the hydrological boundary conditions, permafrost degradation continues in the final decades until 2100. While the high-centred polygon in the well-drained simulation ($e_{res} = -10.0\,\mathrm{m}$) remains free of surface water (Fig. 4 e, first column), surface inundation increases in the runs with intermediate hydrological conditions (Fig. 4 e, second and third column), resulting in the formation of a water body of 1-3 m depth underlain by a talik in the simulation with $e_{res} = -0.5\,\mathrm{m}$. However, the water body is (still) bottom-freezing in ~~the landscape simulation~~ 2100, in contrast to the water body with floating ice in the simulation with $e_{res} = 0.0\,\mathrm{m}$.

Overall, the *polygon* simulations reveal a marked dependence of the pathways of landscape evolution and associated permafrost degradation on the hydrological conditions, consistent with previous results under recent climatic conditions (Nitzbon et al., 2019).

3.3 Low-gradient slope

While the *single-tile* and *polygon* simulations illustrated general feedbacks due to excess ice melt and micro-scale lateral fluxes, they cannot reflect heterogeneous landscape dynamics at the meso-scale. The simulations with the *low-gradient slope* setup illustrate how meso-scale lateral water fluxes in gently-sloped terrain give rise to diverse pathways of landscape evolution and how these depend on the slope gradient (S^{m}).

Figure 5 shows the landscape evolution throughout the twenty-first century for the simulations with the *low-gradient slope* setup, i.e., with a meso-scale representation according to a slope but without micro-scale heterogeneities. Irrespective of the slope gradient, the simulated evolution of the outer tiles is very similar to that of the well-drained ~~single-tile throughout the~~ *single-tile* simulations ($e_{res} = -10.0\,\mathrm{m}$ and $e_{res} = -1.0\,\mathrm{m}$) throughout the entire simulation period (~~Fig. ??~~ compare Figure 3 first and second columns with Figure 5 first and fourth column). ~~In the intermediate and inner tiles of the landscape simulation~~ The outer tiles are stable until about the half of the simulation period. During the second half, excess ice melt sets in and the ground subsides at an increasing rate, reaching an accumulated subsidence of about $0.8\,\mathrm{m}$ by 2100. The similarity to the well-drained *single-tile* simulations can be explained by the fact that the outer tile is very efficiently drained ($e_{res} = -10.0$), such that the lateral water input from the intermediate tile is directly routed further into the external reservoir. Hence, the "upstream" influence on the outer tile becomes negligible.

For both slope gradients, the evolution of the intermediate tile is similar to that of the inner tile. However, the evolution of the two tiles is different among the two simulations for different slope gradients. For the lower slope gradient ($S^{m} = 0.001$), which reflects an essentially flat landscape, melting of excess ice and associated ground subsidence occur during the first half of the simulation period, and ~~there is~~ a shallow layer of surface water (about $0.2\,\mathrm{m}$) forms in these tiles (Fig. ~~??~~ 5 a–c, ~~third and fourth~~ second and third column). By 2050, the soil surface in the intermediate and inner tiles has subsided below the surface elevation of the outer tile such that the initial slope is dissipated. After 2050 excess ice melt proceeds faster and the surface water body in the intermediate and inner tiles reaches a depth of almost $1\,\mathrm{m}$ by 2075 (Fig. ~~?? d, third and fourth~~ 5 d, second and third column). The permafrost table in these tiles lowered by about $2\,\mathrm{m}$ relative to its initial position. Between 2075 and

2100 a talik ~~of about 2 m thickness~~ forms beneath the water body in the two inland tiles (Fig. ~~?? e, third and fourth column) .~~ ~~By~~ 5 e, second and third column) which by 2100 ~~the water body has~~ reaches a depth of about ~~1.5 m in both tiles.~~

2.0 m. The ground subsidence in the outer tile during the second half of the simulation enables surface and subsurface water transport from the intermediate tile into the external reservoir, and thus leads to a lowering of the water level of the ~~surface~~ water body in the intermediate and inner tiles (Fig. ~~??~~ 5 d–e). ~~As a result, the surface~~ By 2100 the water body depth ~~by 2100~~ ~~is about 1.5 m in the landscape simulation, while it is~~ is about $1.2 - 1.5$ m, which is significantly lower than the water body of about 2.0 m depth which forms in the poorly-drained ~~single-tile simulation~~ *single-tile* simulations (Fig. ~~?? e, third to fifth~~ 3 e, fourth column). This difference in water body depths is ~~observed~~ despite excess ice melt and surface water formation ~~in the landscape simulation~~ set on several decades earlier in the *low-gradient slope* simulation than in the poorly-drained ~~single-tile simulation.~~

3.3.1 ~~Simulations with micro-scale heterogeneity reflecting ice-wedge polygons~~

~~Landscape evolution in the simulations with a polygon micro-scale representation under the RCP8.5 warming scenario. The well-drained and poorly-drained cases correspond to the model setup with only micro-scale heterogeneity (Fig. 2 b) and the landscape case corresponds to the model setup with both micro- and meso-scale heterogeneity (Fig. 2 d). Note that the horizontal width of the tiles does not match with the vertical scale. Based on the relative soil surface elevations of the polygons, these were classified in to low-centered (LCP), intermediate-centered (ICP), high-centered (HCP), and water body (WB), following the definitions in Nitzbon et al. (2020). The same legend as in Fig. ?? applies.~~

~~In analogy to Figure ??, Figure 4 illustrates the landscape evolution throughout the twenty-first century under RCP8.5 for the simulations with the micro-scale heterogeneity reflecting ice-wedge polygons. In addition, it shows the geomorphological state of the polygon micro-topography, i.e., whether it is low-centered (LCP), intermediate-centered (ICP), or high-centered (HCP), or turned into a water body (WB), according to the definitions in Nitzbon et al. (2020). Initially, all simulations feature undegraded ice-wedge polygons with an LCP micro-topography (Fig. 4 a).~~ *single-tile* simulation. These different pathways of water body and talik formation illustrate that there is no linear relationship between the water body depth and talik extent, since lateral interactions at the meso-scale can give rise to different transient dynamics.

Single-polygon simulations: ~~Between 2000 and 2050, initial ice-wedge degradation~~ For the higher slope gradient ($S^{\mathrm{m}} = 0.01$), which reflects moderately-sloped terrain, initial excess ice melt occurs in the ~~well-drained single-polygon simulation, indicated by subsiding troughs and a transition from the LCP to the ICP micro-topography~~ intermediate and inner tiles between 2000 and 2025, and by 2050 these have subsided by about 0.2 m (Fig. 4 ~~a–c, first column). Between 2050 and~~ 5, fifth and sixth column), similar to the simulation with $S^{\mathrm{m}} = 0.001$. By 2075, ~~substantial~~ ground subsidence has reached about 0.5 m in the intermediate and inner tiles. The overall shape of the slope does not change much because excess ice melt occurs ~~in the trough and rim tile , leading to a transition to a pronounced HCP micro-topography for the well-drained polygons (Fig. 4 d, first column). The degradation continues until~~ also in the outer tile during that time. By 2100, ~~when the trough tile has~~ the intermediate and inner tile have subsided by about ~~2 m, the rim~~ 1.2 m, and the outer tile by about ~~1 m, and the center tile by more than 0.2 m.~~ ~~As a consequence of the connection to a low-lying external reservoir (see Table 3) the well-drained polygon does not show~~

18

~~any surface water formation~~ 0.8 m, resulting in a slightly concave slope. The presence of a thin layer of surface water in the intermediate and inner tiles in the years 2025, 2075, and 2100 indicates a wetter hydrological regime compared to the outer tile. However, as the moderate slope is sustained throughout the simulation~~period.~~

~~In contrast, a shallow~~ , it facilitates drainage of surface water and precludes the formation of a surface water body ~~of about 0.5 m depth forms between 2000 and 2025 in the poorly-drained single-polygon simulation , as a result of~~ as it is the case in the simulation with the flatter topography ($S^\mathrm{m} = 0.001$). We suspect, however that if the simulations would be prolonged beyond 2100, the excess ice melt in the ~~center, rim, and trough tiles (Fig. 4 b, fifth column). The bottom of the water body has a high-centered topography. Little excess ice melt occurs in this polygon between 2025 and 2050 (Fig. 4 c, fifth column). After 2050 excess ice melt proceeds faster, causing the water body to deepen, reaching a depth between 1 m (center tile) and more than 2 m (trough tile) by 2075 (Fig. 4 d,fifth column). Until~~ intermediate and inner tiles would likely continue at a faster rate than in the outer tile and this would result in the reversal of the initial slope and promote the formation of an inland surface water body.

While the overall dynamics of the three-tile slope simulations could also be reflected using a two-tile setup, we would like to point to the small but significant differences between the evolution of the intermediate tile and the inner tile. For both slope gradients, the intermediate tile shows a slightly stronger degradation rate than the inner tile. This can be explained due to the additional water input from the inner tile which sustains saturated conditions in the near-surface soil layers during the thawing season. The inner tile in turn lacks this lateral water input and is thus more likely to develop dry, thermally insulating conditions in the near-surface soil.

Overall, the slope gradient (S^m) has a similar influence on permafrost degradation in the *low-gradient slope* setup, as the elevation of the external reservoir (e_res) has in the *single-tile* simulations (see Figures 7 a,c and 8 a,c). This can be attributed to the direct influence of the slope gradient on drainage efficiency. Due to the positive feedbacks related to the formation of a surface water body, the overall permafrost degradation in the setting with $S^\mathrm{m} = 0.001$ is almost twice as much as in the setting with $S^\mathrm{m} = 0.01$ for which no water body forms. We note that the maximum thawed ground and the accumulated ground subsidence by 2100 ~~excess ice melt proceeds further, resulting in a water body depth of 2 − 4 m and the formation of an extended talik underneath (Fig. 4 e, fifth column). By the end of the simulation period,~~ in both *low-gradient slope* simulations are within those simulated for the two extreme settings in the *single-tile* simulations.

3.4 Low-gradient polygon slope

Finally, we consider the most complex setup which reflects gently-sloped polygonal tundra via nine tiles, incorporating heterogeneities on both the micro- and the meso-scale. Figure 6 shows different stages of the simulated landscape evolution in the ~~lake is not entirely bottom-freezing in winter~~*low-gradient polygon slope* setup throughout the twenty-first century for two different slope gradients S^m.

~~Polygon landscape simulation:~~ ~~The outer polygon in the landscape simulation shows a very similar evolution to~~ Like the outer tiles in the *low-gradient slope* setup, the outer polygons show an evolution which is very similar to that of the well-drained ~~single-polygon throughout the entire simulation period (Fig. 4, first and second column). The~~ (single) *polygon* simulation with

$e_{\mathrm{res}} = -10.0\,\mathrm{m}$, irrespective of the slope gradient (compare Fig. 6 first and fourth column with Fig. 4 first column): until 2050 initial excess ice melt occurs in the trough tiles, entailing a transition from LCP to ICP topography; during the second half of the simulation period, permafrost degradation proceeds at an increasing rate and brings about a transition to a pronounced HCP topography with the troughs having subsided by about $2\,\mathrm{m}$. Again, the similarity between the outer polygon evolution and the well-drained single polygon evolution can be explained by the efficient drainage of the outer polygon troughs which leads to a negligible "upstream" influence.

For the lower slope gradient ($S^{\mathrm{m}} = 0.001$), the intermediate and inner polygons show an evolution which is similar to each other, but different from ~~both single-polygon simulations~~ (each of the single *polygon* simulations (compare Fig. 4 ~~, third and fourth~~ with Fig. 6 second and third column). Between 2000 and 2025 excess ice melt in the rim and trough tiles ~~cause the~~ leads to ponding of surface water in the intermediate and inner polygons (Fig. ~~4 b, third and fourth~~ 6 b, second and third column) with the soil surface of the ~~center~~ polygon centre being close to or elevated above the water table. Besides a lowering of the water table, the configuration of these ~~high-centered~~ polygons does not change much until 2050 (Fig. ~~4 c, third and fourth column)~~ 6 c, second and third column) when both have developed an HCPi topography, i.e., inundated rims and troughs which subsided below the level of the centres. Between 2050 and 2075, excess ice melt continues, leading to a pronounced high-centered topography (Fig. ~~4 d, third and fourth~~ 6 d, second and third column). Meanwhile, the surface water disappears from the rim and trough tiles, as a consequence of marked ~~ice-wedge degradation~~ excess ice melt in the outer ~~polygon~~ polygons rim and troughs tiles during that period (Fig. ~~4 d, second~~ 6 d, first column). The ~~elevation in~~ soil surface elevation of the trough tiles increases ~~toward the inland tiles, allowing an~~ from the outer towards the inner polygon, allowing for efficient drainage of the entire landscape. ~~After~~ Between 2075 ~~all polygons of the landscape simulation~~ and 2100 all three polygons show a similar evolution, resulting in pronounced high-centered topographies with troughs about $2\,\mathrm{m}$ deep and rims that subsided by about $1\,\mathrm{m}$ ~~by 2100.~~ in total. Note that between 2075 and 2100 the troughs of the intermediate and inner polygons subsided more than that of the outer polygon, ~~so that the drainage efficiencyis decreased and~~ resulting in an decreased drainage efficiency. Hence, surface water starts to pond again in the intermediate and inner troughs (Fig. ~~4 e, third and fourth~~ 6 e, second and third column).

3.5 ~~Permafrost thaw and ground subsidence~~

~~The changes in the landscape configuration described in the previous section are linked to the degradation of ice-rich rich permafrost, which causes ground subsidence and alters lateral hydrological fluxes in the multi-tile settings. The projected quantitative changes in terms of maximum thawed ground depth and accumulated ground subsidence are displayed in more detail in Figure 7. Note that the sum of thaw-depth increase (i.e., active-layer-deepening) and accumulated ground subsidence correspond to the absolute lowering of~~ Overall, the ~~permafrost table.~~

~~11-year running mean of maximum annual thawed ground extent (a,b) and the accumulated ground subsidence (c,d) for different micro-scale representations (homogeneous and polygon).~~

3.4.1 ~~Simulations without micro-scale heterogeneity~~

low-gradient polygon slope simulation with $S^{\mathrm{m}} = 0.001$ shows a transient phase in which the formation of a water body is initiated, but its growth is impeded due to the formation of efficient drainage pathways through the subsiding troughs in the outer ("downstream") polygon.

635 *~~Maximum thawed ground:~~* ~~In all simulations without micro-scale heterogeneity, the maximum thawed ground extent increases steadily from less than 0.5 m in the year 2000 until it roughly has doubled around the years 2070 (Fig. 7 a) . Throughout this period, thawed ground is slightly higher in the landscape simulation than in the single-tile simulations. The thawed ground extents in the single-tile simulations diverge during the last three decades~~ The simulated landscape evolution for the moderate slope gradient ($S^{\mathrm{m}} = 0.01$) differs from that for the lower slope gradient during the first half of the simula-

640 tion ~~, with the increase being about two to three times faster in the poorly-drained (about 2.6 m in 2100) than in~~ period. Until 2025, excess ice melt is restricted to the ~~well-drained simulation (about 1.1 m in 2100). Thawed ground extent in the landscape simulation also accelerates in the last three decades, to an intermediate increase rate~~ trough tiles, leading to a transition from LCP to ICP topography in all three polygons (Fig. 6 b, fifth and sixth column). In the intermediate and inner polygons, permafrost degradation proceeds faster than in the outer polygon, such that ~~by 2100 it is about 2.4 m and thus lies within the~~

645 ~~range spanned by the two single-tile simulations under contrasting hydrological conditions, but closer to the poorly-drained simulation.~~

~~Ground subsidence:~~ ~~While ground subsidence starts already after about two decades in the landscape simulation, no subsidence occurs until about 2060 in both single-tile simulations~~ these develop a HCPd topography by 2050. The faster degradation can be explained by the overall wetter hydrological regime compared to the very efficiently drained outer polygon.

650 However, the meso-scale slope still allows for sufficient drainage of surface water, such that (in contrast to the simulation with $S^{\mathrm{m}} = 0.001$) the ponding of surface water is mostly precluded (Fig. ~~7 c). The accumulated mean ground subsidence in the landscape simulation reaches about 0.3 m in 2060, and accelerates afterwards, reaching about 1.8 m in 2100. Ground subsidence in the single-tile simulations sets on abruptly around the year 2070 and is about three times faster in the poorly-drained than in the well-drained simulation. By 2100, it reaches about 2.0 m in~~ 6 c, fifth and sixth column). During the second

655 half of the simulation period, the ~~poorly-drained case,~~ evolution of the polygons is very similar for both slope gradients. Ice-wedge degradation proceeds at an increasing pace between 2050 and ~~about 0.7 m in the well-drained, such that the landscape simulation is within the range spanned by the single-tile simulations, but closer to the poorly-drained simulation~~ 2100, resulting in polygons with pronounced HCP topography. While the troughs of the outer polygons are efficiently drained (HCPd, Fig. 6 e, first and fourth column), some surface water pools in the troughs of the intermediate and inner polygons (HCPi, Fig.

660 6 second, third, fifth and sixth column).

3.4.1 ~~Simulations with micro-scale heterogeneity reflecting ice-wedge polygons~~

The overall similarity among the two *~~Maximum thawed ground: All simulations with polygons as the micro-scale representation, had a similar maximum thawed ground extent of about 0.5 m in 2000~~* *low-gradient polygon slope* simulations for different

slope gradients is also reflected in the time series of maximum thaw depths (Fig. 7 ~~b) . This amount increased steadily until about 2060, but at different rates among the three simulations. The permafrost thaw rate is fastest for the poorly-drained single-polygon where the maximum thawed ground reaches about 1.2 m in 2060, and it is slowest for the well-drained single-polygon for which it reaches about 0.7 m by the same time. After 2060 the increase in the simulated thawed ground extents becomes faster in~~ d) and accumulated ground subsidence (Fig. 8 d). During a transient phase spanning roughly from 2010 until 2070, the ~~single-tile simulations. By 2100 it reaches about 1.2 m in the well-drained simulation , and more than 4 m in the poorly-drained simulation. The mean thawed ground in the polygon landscape simulation lies~~ permafrost degradation in the simulation with $S^m = 0.001$ is slightly higher than in the simulation with $S^m = 0.01$. Before and after this transient period, the maximum thaw depths and the accumulated ground subsidence are almost identical for the two settings. This is a qualitative difference to the *low-gradient slope* simulations without micro-scale heterogeneity, where the simulation with $S^m = 0.001$ resulted in almost twice the amount of permafrost degradation compared to the simulation with $S^m = 0.01$ (Fig. 7 c,d and Fig. 8 c,d). The projected permafrost degradation in both *low-gradient polygon slope* simulations is confined within the range spanned by the ~~two single-polygon simulations throughout the 21st century. However, during the last three to four decades, the increase does not accelerate such that it aligns more with the well-drained simulation, reaching a value of about 1.3 m by 2100. As a general pattern, thaw depths are consistently larger in the single-polygon simulations than in the single-tile simulations with homogeneous micro-scale representation. In contrast,~~ projections for the *polygon* setup (see Fig. 7 b, d and Fig. 8 b, d). However, by 2100 the projected maximum thaw depths and the ~~thaw depths in the polygon landscape simulation are consistently lower than in the homogeneous landscape simulation, particularly during the last three decades.~~

~~*Ground subsidence:* Excess ice melt and associated ground subsidence occur within the first decade in the poorly-drained single-polygon simulation and in the polygon landscape simulation, while the ground does not subside before 2050 in the poorly-drained polygon simulation (Fig. 7 d). As for the thawed ground discussed above, mean ground subsidence in the polygon landscape simulation is constrained by the two single-polygon simulations. By 2060, mean ground subsidence in the polygon landscape reaches about 0.4 m. During the last four decades, ground subsidence sets in and proceeds in the~~ accumulated ground subsidence are very close to the single *polygon* simulation under well-drained ~~single-polygon simulation, reaching a value of about 1.0 m by 2100. In the poorly-drained single-polygon simulation, subsidence rates are about three times faster, reaching more than 3 m by 2100. In the polygon landscape simulation, subsidence rates do not accelerate markedly during the last decades and~~ conditions ($e_{res} = -10.0$ m).

While the *low-gradient polygon slope* setup provides the most complex representation of landscape heterogeneities – and hence potentially captures most feedback processes – the projected pathways of landscape evolution and permafrost degradation showed little sensitivity to the initial gradient of the ~~mean total subsidence is close to that of the well-drained polygon by 2100. A similar general pattern as for~~ meso-scale slope, and, overall, the ~~thaw depths is found for the accumulated subsidence. Simulated ground subsidence in the single-polygon simulations consistently exceeds the respective projections of the homogeneous single-tile simulations, while the mean ground subsidence by 2100 is substantially larger in the homogeneous landscape than in the polygon landscape~~ projected landscape response was more gradual than in the other setups which feature abrupt initiation or acceleration of permafrost degradation (Figures 7 and 8). We also note that the *low-gradient polygon slope*

setup is the only one, for which the formation of a talik was not projected for any of the tiles and for any of the parameter
700 settings (Fig. 6 a–e).

4   Discussion

4.1   Simulating permafrost landscape degradation pathways under consideration of micro- and meso-scale heterogeneityheterogeneities

The multi-scale tiling approach employed introduced in this study (see Section 2.2.1) facilitates the simulation of degradation
705 pathways of ice-rich permafrost landscapes in response to a warming climate, under consideration of feedback processes
feedbacks emerging from heterogeneities and lateral fluxes on subgrid-scales. The following qualitative assessment based
on observed landscape changes across the Arctic demonstrates that the model is able to realistically represent the dominant
pathways of landscape evolution and important feedback processes induced by permafrost thaw and excess ice melt.
The most idealized cases considered were one-tile single-tile simulations without heterogeneities on the micro- or meso-
710 scale(Fig. 2 a ; Fig. ?? first and fifth column). Depending on the hydrological boundary conditions, these simulations reflect
different real-world cases.Under , corresponding to previous simulations with models that incorporate a representation of
excess ice melt and ground subsidence (Lee et al., 2014; Westermann et al., 2016). The simulations with this setup reflect the
fundamental modes of landscape change due to excess ice melt (i.e., thermokarst) (Kokelj and Jorgenson, 2013). These changes
are ranging from the gradual subsidence of a well-drained conditions, the simulation reflects an "upland" setting for which
715 steady ground subsidence was projected under RCP8.5 during the second half of the twenty-first century and no surface
water can form. If drainage was precludedto the formation of thaw lakes in a water-logged "lowland" setting. The marked
sensitivity of the simulations to the prescribed hydrological conditions underlines that landscape evolution and permafrost
degradation crucially depend on whether water from melted excess ice drains or ponds at the surface. On the one hand,
the simulations projected the formation of a thaw lake to occur during the second half of the twenty-first century. While
720 these model configurations correspond to the two cases considered by Westermann et al. (2016), the response of the presented
simulations in this study differs both qualitatively and quantitatively. Overall, the projected permafrost degradation in this study
is considerably lower than in the projections of Westermann et al. (2016) who assumed similar excess ice contents and used
the same meteorological forcing data. This can most likely be attributed to the inclusion of a water balance into CryoGrid
3 (Nitzbon et al., 2019; Martin et al., 2019). reveal a positive feedback on permafrost degradation through ponding of water
725 from melted excess ice at the surface. The presence of surface water alters the energy exchange with the atmosphere and
increases the heat input into the ground (albedo, thermal properties), which in turn allows for additional excess ice melt.
This positive feedback is in agreement with previous observations (Connon et al., 2018; O'Neill et al., 2020) and modelling
results (Rowland et al., 2011; Langer et al., 2016; Westermann et al., 2016). On the other hand, simulations under well-drained
conditions favoured stabilization due to the improved insulation by dry organic surface layers which is also in agreement with
730 observations (Göckede et al., 2017, 2019) and modelling results (Martin et al., 2019; Nitzbon et al., 2019).

~~These simple cases, however, do not reflect a lot of processes observed in real-word landscapes, such as dynamically changing hydrological conditions due to lateral water fluxes.These have been taken into account in the homogeneous landscape setting (Fig.2 c, ?? second to fourth column). Compared to the single-tile cases, the landscape evolution is affected by lateral interactions between different parts of the simulated landscape . Surface water formation~~ In the *polygon* setup, micro-scale heterogeneities associated with ice-wedge polygons and represented lateral fluxes of heat, water, snow, and sediment were considered. The simulated landscape evolution pathways under a warming climate correspond to those simulated and discussed by Nitzbon et al. (2020) (for the "Holocene Deposits" stratigraphy). They range from the rapid formation of a deep surface water body to the development of high-centred polygons with a pronounced relief. While observations of initial ice-wedge degradation and the development of high-centred polygons are reported across the Arctic (Farquharson et al., 2019; Liljedahl et al., 2016), the likelihood of thaw lake formation in ice-wedge terrain is debated and likely depends on the overall wedge-ice content (Kanevskiy et al., 2017). Despite the same ground ice distribution in terms of excess ice content (θ_x) and depth (d_x) on average (see Table 3), the simulated permafrost degradation in the *polygon* settings exceeds that in the respective *single-tile* simulations, suggesting that positive feedbacks (e.g., preferential accumulation of snow and water in troughs) exceed the influence of stabilizing feedbacks (e.g., slumping of sediment from rims into troughs). Hence, the simulations suggest that the presence of micro-scale heterogeneities can crucially affect the timing and the rate of permafrost degradation in ice-rich lowlands. Ultimately, both the *single-tile* and the *polygon* setups are limited by the prescription of static hydrological boundary conditions which do not allow transient changes between different pathways but rather prescribe the possible landscape evolution a priori.

In the *low-gradient slope* setup, the hydrological conditions in the inland ~~parts is projected to occur earlier than in poorly-drained single-tile case, which can be attributed to very poor drainage along the low-gradient slope. Furthermore, the subsiding outer part causes a gradual drainage of~~ part of the model domain can develop dynamically and the water level in a given part of the landscape adapts to topographic changes in adjacent parts due to the representation of meso-scale lateral water fluxes. From an almost flat initial topography ($S^m = 0.001$, Fig. 5 left), the formation of a thaw lake in the ~~inner part, such that it is substantially more shallow by the end of the simulation than in the poorly-drained single-tile case. Shallow water bodies favor bottom-freezing, such that the gradual lake drainage would constitute a stabilizing feedback on the ground thermal regime in the simulations. However, real world thaw lakes are also known to drain "catastrophically", for example, upon the incision of a thermo-erosional gully as a result of either gully growth or lake expansion (Jones et al., 2011; Kessler et al., 2012). Both are a consequence of lateral erosion which is not represented in our model at the meso-scale. Besides feedbacks through meso-scale water fluxes, previous modeling studies~~ inland has been simulated, succeeded by the gradual drainage of the lake in response to ground subsidence in the outer part. This setup thus captures in a stylized way the competing mechanisms of thaw lake formation and growth on the one hand, and (gradual) lake drainage on the other hand. Gradual or partial drainage of mature thaw lakes has been observed (Morgenstern et al., 2013) and simulated (Kessler et al., 2012), and we note that also the thermokarst lakes in the southeastern and southwestern part of Samoylov Island are indicative of gradual drainage (Figure A1 a). This gradual lake drainage constitutes a potential negative feedback on permafrost degradation, since shallower water bodies are more likely to bottom-freeze, allowing more efficient cooling of the ground during wintertime (Boike et al., 2015; Langer et al., 2016; O'Ne

Previous modelling studies have also demonstrated that the stability and the thermal regime of permafrost in the vicinity of thaw lakes is affected by meso-scale lateral heat fluxes from taliks forming underneath the lakes (Rowland et al., 2011; Langer et al., 2016). These effects have not been considered in this study, but constitute another feedback due to lateral fluxes at the meso-scale.

As suggested by several studies (Nitzbon et al., 2019; Abolt et al., 2020), the degradation pathways of ice-rich permafrost become more involved, if the micro-scale heterogeneity associated with ice-wedge polygons is taken into account, for example due to the lateral rerouting of surface and subsurface water according to the micro-scale topography. Here, we took into account micro-scale lateral fluxes of heat, water, snow, and sediment (see Fig. 2 b). The single-polygon simulations in this study correspond to the simulations for "Holocence Deposits" presented in Nitzbon et al. (2020) in terms of the ground ice distribution and the meteorological forcing data. Consequently, qualitatively identical landscape evolution pathways have been simulated (Fig. 4 first and fifth column). Under well-drained conditions the Finally, the most complex pathways of landscape evolution are revealed, when both micro- and meso-scale heterogeneities are taken into account. The simulation of a *low-gradient polygon slope* reflects the transition from low-centred polygons evolve into polygonal tundra with inundated centres and troughs towards efficiently drained terrain with a high-centred polygons with a pronounced relief, while a deep thaw lake underlain by a talik has been simulated to from, under poorly-drained conditions. These two cases span a wide range of uncertainty in terms of projected permafrost degradation.

The simulation of the polygon landscape that takes into account polygon relief. This transient landscape evolution which resembles well the schematic evolution of polygonal tundra depicted by (Liljedahl et al., 2016) has not been simulated in a numerical model before, as it involves an interaction between micro-scale (i.e., ice-wedge degradation) and meso-scale water fluxes (Fig.2 d, Fig.4 second to fourth column) has been conducted to provide a more realistic representation of heterogeneity in (i.e., drainage along slope) processes. Due to the inclusion of a wide range of feedback processes on multiple scales, we consider the simulations conducted with the *low-gradient polygon slope* setup to most realistically mirror the real-world dynamics of ice-rich terrain, and it revealed a subtle transient landscape evolution in response to climate warming. In that simulation surface water ponds early in the inland parts of the landscape, associated with initial ice-wedge degradation. The degradation is slowed down, however, by lateral transport of sediment (slumping) from the rims into the troughs (see Fig. 4 b–c, fourth column), such that the high-centred polygons are stabilized temporarily. During the second half of the twenty-first century, rapid ice-wedge degradation occurs in the outer part of the landscape , and the entire landscape drains as a consequence. Overall, permafrost lowlands. Interestingly, the simulation reflects a transition from a low-gradient landscape of undegraded low-centered polygons to well-drained high-centered polygons within less than a century. This transient simulation thus corresponds to the schematic landscape evolution depicted by Liljedahl et al. (2016). This constitutes a significant improvement over the previous versions of the model (Nitzbon et al., 2019, 2020), for which it was not possible to simulate this type of landscape dynamics. It should further projected thaw-depth increase and ground subsidence showed little sensitivity to the meso-scale slope graident (Fig. 7 d and 8 d), suggesting a higher robustness of these projections against parameter variations compared to the more simple setups.

800　Despite the capacity of reflecting a wide range landscape evolution pathways, certain forms of landscape change that have been observed in ice-rich permafrost landscapes are not possible to reflect using the presented model framework due to a lack of necessary process parametrizations. For instance, real-world thaw lakes are known to drain "catastrophically" instead of gradually upon the incision of a lake basin by a thermo-erosional gully. This can happen as a result of either gully growth or lake expansion (Jones et al., 2011; Kessler et al., 2012), both of which are a consequence of lateral erosion. This process is,

805　however, not represented in our model at the meso-scale. Similarly, the dynamic development of retrogressive thaw slumps and their interactions with other landforms would require additional parametrizations of mass-wasting processes as well as slope- and aspect-dependent modifications of incoming radiation (Lewkowicz, 1986). Beyond this, it should be noted that ~~the simulated shifts in the subsurface hydrological regime have important consequences for whether the decomposition of soil organic carbon occurs under aerobic or anaerobic conditions (Lara et al., 2015; Schuur et al., 2015; Schädel et al., 2016; Knoblauch et al., 2~~

810

4.2 ~~Constraining the response of ice-rich permafrost to a warming climate~~

further potential feedbacks mechanisms are not represented in our model, such as lateral heat and sediment transport at the meso-scale, or ecological processes such as vegetation succession, all of which potentially alter the ground thermal and hydrological regimes (Shur and Jorgenson, 2007; Kokelj and Jorgenson, 2013; Kanevskiy et al., 2017) and affect permafrost

815　thaw.
~~Depending on the inclusion of landscape heterogeneities at different scales, the presented simulations reveal very different permafrost degradation trajectories (Fig. 7). Irrespective of the representation of micro-scale heterogeneity, the simulations under well-drained and poorly-drained conditions provide outer boundaries in terms of thaw and subsidence for the landscape simulations. The landscape-scale mean of the three-tile simulation without representation of micro-scale heterogeneity, revealed~~

820　~~permafrost degradation trajectories which proceed slower than the poorly-drained case, but align closer to it than to the well-drained case. However, when the micro-scale was represented as ice-wedge polygons, the resulting degradation trajectories aligned closer to~~

4.2 Implications for simulating high-latitude land surface processes using macro-scale models

The presence of permafrost in high-latitude landscapes crucially affects hydrological and biogeochemical processes and makes

825　their realistic representation within macro-scale LSM frameworks challenging (Chadburn et al., 2017; Andresen et al., 2020; Burke et al., 2 Beyond the requirement to accurately simulate freeze-thaw processes near the surface, the ~~well-drained case, as a consequence of the drainage network formation described in the previous section. The simulations thus indicate that the overall (landscape-mean) permafrost degradation, is crucially affected by small-scale heterogeneities, and that model projections have to be considered with care in light of these complexities. Hence, our simulations do not allow a final judgment with respect to whether the~~

830　~~formation of new thaw lakes and taliks, or the formation of new drainage systems will dominate the evolution of real-world permafrost lowlands under a warming climate. For a more realistic assessment of~~ presence of excess ice in the subsurface is an additional source of complexity. Indeed, its melting involves rapid changes in the topography which affect hydrological,

ecological, and biogeochemical processes, and these in turn feed back on the thermal dynamics of the subsurface. Here, our results support previous findings which have suggested that micro- (Abolt et al., 2018, 2020; Nitzbon et al., 2019) and

835 meso-scale (Langer et al., 2016; Jafarov et al., 2018) heterogeneities and lateral fluxes exert important controls on the simulated thermal, hydrological, and biogeochemical state of the ~~most likely response of~~ subsurface in ice-rich ~~permafrost~~ terrain. Beyond the importance of subgrid-scale heterogeneity, our simulations suggest that interactions *across* scales can introduce further complexities and feedbacks in the land surface evolution in response to climate warming, ~~additional configurations than the two exemplary cases presented here would need to be considered, for example by incorporating also different~~

840 ~~meso-scale topologies which could correspond to different catchment geometries. This could also help to test the hypotheses on thaw lake abundance which underlie other models' projections of greenhouse gas emissions from thermokarst terrain (Schneider von Deimling et al., 2015; Walter Anthony et al., 2018).~~

~~Our simulations further suggest, that abrupt degradation of ice-rich permafrost across entire landscapes is less likely than spatially distributed and gradual degradation dynamics. When either~~ which are not represented in LSMs. For example, the rapid

845 subsidence of inter-polygon troughs due to melting of ice wedges can entail landscape-wide regime shifts of the soil moisture state and runoff generation. Similarly, the setups which reflect micro- ~~and~~/or meso-scale ~~heterogeneities (or both) are taken into account in~~ heterogeneity enable to simulate pathways of landscape evolution in which some parts of the landscape are inundated (e.g., deepening troughs), while other parts are subject to drained conditions. The spatial variability of the ~~simulations, the projected degradation trajectories are more gradual and steady than in the overly simplistic one-tile simulations (Fig.7). The~~

850 ~~one-tile simulations show a relatively abrupt onset of subsidence and thaw-depth increase, and similar abrupt changes in~~ ground thermal and hydrological regimes ~~have been found using similarly simplistic model setup (Teufel and Sushama, 2019). We interpret our findings to suggest that abrupt responses of permafrost terrain to climate warming may occur locally, but are not likely at regional or even global scales~~ directly affects other ecosystem processes such as the decomposition of soil organic carbon (Lara et al., 2015). In fact, several studies have suggested that small water bodies could constitute "hotspots" for carbon

855 decomposition and greenhouse gas emissions (Laurion et al., 2010; Abnizova et al., 2012; Langer et al., 2015; Elder et al., 2020), which would be missed in projections of macro-scale models used to constrain the global permafrost carbon-climate feedback (Schuur et al., 2015).

The modelling approach of multi-scale landscape tiling pursued in our study constitutes a promising way to represent subgrid-scale heterogeneities of permafrost landscapes without the need to increase the spatial resolution of a macro-scale

860 model. Our modelling suggests that key feedback processes acting at and across the micro- and meso-scales of ice-rich terrain could be represented in a nine-tile setup, corresponding to an increase in computational demand by about an order of magnitude. Despite mathematical and technical challenges that would need to be addressed before multi-scale tiling schemes could be incorporated within established LSMs (Fisher and Koven, 2020), we consider the concept of multi-scale tiling to bear considerable potential for a computationally affordable representation of subgrid-heterogeneity and lateral interactions in

865 high-latitude ecosystems within LSM frameworks.

4.3 ~~Simulating~~ Towards simulating the cyclic evolution of ice wedges and thaw lakes in thermokarst terrain

27

Beyond the discussed implications for simulating permafrost degradation in response to the expected climate warming within the course of the twenty-first century, our modelling work reveals novel potentials for investigating the geomorphological evolution of thermokarst terrain under both past and future climatic conditions. It has been suggested that thermokarst terrain ~~evolves~~ is evolving in a cyclic manner on centennial-to-millennial timescales. For example, ~~the~~ cycles of degradation and stabilization have been suggested to describe the evolution of ice wedges (Jorgenson et al., 2006, 2015; Kanevskiy et al., 2017) on these time scales. Similarly, but at a larger spatial scale, the cyclic evolution of thaw lakes has been hypothesized (Billings and Peterson, 1980) (see Grosse et al. (2013) for a review of the hypothesis). While we do not want to discuss here to which extent ice-rich permafrost landscapes have been evolving or are evolving according to these models, we would like to ~~point out~~ mention that the model framework presented in this study ~~, is in principle~~ is able to capture a wide range of the processes involved in these cycles. Figure 9 provides a schematic of the cyclic evolution of thermokarst terrain ~~based~~ and highlights the capacities of our model to simulate different pathways of (cyclic) landscape evolution.

~~Schematic depiction of pathways of ice-rich permafrost landscape evolution as simulated within the presented model framework. The "inner" cycle reflects the cyclic evolution of ice wedges as described by Kanevskiy et al. (2017). The outer cycle involving the thaw lake stage reflects the thaw lake cylce as hypothesized by Billings and Peterson (1980). Formation of excess ice is lacking in the model such that the full cycles cannot be simulated. Adapted from Jorgenson et al. (2015) and Nitzbon et al. (2019).~~

The initial and advanced degradation of ice wedges and the associated transition from low-centered to high-centered polygons was captured by the model setup by Nitzbon et al. (2019). Nitzbon et al. (2020) complemented this by the ~~stabilizing~~ stabilization of ice wedges due to sediment accumulation in the troughs, and also showed that it is possible to simulate ice-wedge collapse and thaw lake formation in response to climate warming scenarios. The simulations with representation of landscape heterogeneity and lateral water fluxes at the meso-scale, which are presented in this study, allow to capture further feedbacks. First, the formation of efficient drainage pathways through degrading ice-wedge networks, as depicted by Liljedahl et al. (2016), was qualitatively captured by the simulation using the ~~polygon landscape~~ *low-gradient polygon slope* setup (Fig. 2 d and 6). While ~~this~~ the simulated landscape drainage did not completely interrupt the ice-wedge degradation (as indicated in Fig. 9), it did lead to a significantly slower degradation compared to the simulations without meso-scale heterogeneity (Fig. 7 b,~~e~~d). Second, representing meso-scale lateral water fluxes (Fig. 2 c,d) enables our model in principle to simulate the drainage of thaw lakes, which would result in the exposure of unfrozen ground (talik) to the atmosphere. While it is not possible to simulate the catastrophic drainage of lakes as discussed above, ~~gradual~~ subsidence of the terrain surrounding the thaw lake, can lead to its gradual drainage on longer timescales than considered here. It is further likely that using a model setup with a more complex meso-scale landscape topology, could result in more rapid drainage of water bodies.

As indicated in Fig. 9, several processes are not represented in our model, such that it cannot capture the full cycles of ice-rich permafrost evolution. In order to represent the initial stabilization of ice wedges more realistically, further ecological processes like vegetation succession and organic matter formation would need to be represented ~~Jorgenson et al. (2015); Kanevskiy et al. (2017)~~(Jorge However, lateral sediment transport into the troughs captures this initial stabilization stage to a certain extent. The advanced stabilization of ice wedges ~~,~~ involves the formation of ice-rich layers consisting of segregation ice above the massive ice

wedge. The process of ice-segregation would require a more sophisticated subsurface hydrology scheme, representing the migration of liquid pore water towards the freezing front, as well as vertical displacement of sediment resulting from frost heave ~~(O'Neill et al., 2019). Finally ,~~ (Ballantyne, 2018). Finally – and probably most importantly ~~,~~ – the formation of wedge ice is

905 not yet represented in the model, which is ~~, however, necessary to from~~ necessary to form the initial stage of undegraded ice wedges from various other evolutionary stages (Fig. 9). In contrast to the formation of segregation ice, wedge-ice formation involves both vertical and horizontal processes, which presupposes the formation of frost cracks due to mechanical stress, which in turn is controlled by climatic conditions at the ground surface and at the top of permafrost~~(Lachenbruch, 1962)~~, and mechanical properties of the soil (Lachenbruch, 1962; Matsuoka et al., 2018). Despite the lack of parametrizations for these

910 processes, our numerical model developments provide important progress towards an improved understanding of the long-term geomorphological evolution of periglacial landscapes under both, past and future, climatic conditions.

5 Conclusions

In the present study, we employed a multi-scale ~~hierarchical~~ tiling approach in the CryoGrid 3 numerical permafrost model to assess the response of ice-rich permafrost ~~landscapes in northeast Siberia~~ lowlands to a warming climate. Specifically, we

915 explored the sensitivity of the ~~model simulations~~ simulated pathways of landscape evolution and permafrost degradation to different representations of micro- and meso-scale heterogeneities~~and lateral fluxes~~. From the results of this study, we draw the following conclusions:

1. Representing micro- and meso-scale ~~heterogeneity and lateral fluxes allows to represent a wider range of permafrost degradation pathways under a warming climate, including, e.g., the large-scale drainage initiated by ice-wedge degradation~~

920   ~~or~~ heterogeneities facilitates the simulation of manifold pathways of permafrost landscape evolution such as the dynamic formation and drainage of thaw lakes, the transition from low-centred to high-centred ice-wedge polygons, and the formation of meso-scale drainage systems in polygonal tundra. These degradation pathways are currently observed across the Arctic but cannot be simulated with models that do not represent spatial heterogeneities and lateral fluxes on subgrid-scales.

925 2. ~~Representing micro-scale heterogeneity and lateral fluxes associated with ice-wedge polygons affects the timing and the rate of permafrost thaw, as well as the hydrological~~ Excess ice melt, and micro- and meso-scale lateral fluxes give rise to both positive and negative feedbacks on permafrost degradation. These feedback processes and their interaction across scales control the pace of permafrost degradation in response to climate warming. ~~In particular, the drainage network that evolves when ice wedges melt, favors large-scale drainage of the landscape and can impede new thaw lake formation~~

930 3. Projections of permafrost degradation in ice-rich lowlands are highly sensitive to the prevailing drainage conditions. Ponding of surface water entails deeper thaw and faster permafrost degradation while efficient drainage leads to shallower thaw depths and slower degradation in response to warming.

4. ~~Incorporating subgrid-scale heterogneities and lateral fluxes using a multi-scale tiling approach allows to constrain uncertainties in the~~ Multi-scale tiling models which represent topographic changes due to thermokarst activity and lateral water fluxes can explicitly simulate transient changes in the drainage conditions and hence bear the potential to more robustly project the response of ice-rich permafrost landscapes to a warming climate ~~. The response of permafrost is more gradual in simulations representing subgrid-scale processes compared to abrupt changes projected by simple~~ than simplistic one-dimensional ~~representations. Micro-scale lateral sediment transport is an example for a stabilizing process in ice-wedge terrain, which moderates rapid thaw processes.~~

5. ~~Irrespective of uncertainties associated with future climate forcing, robust projections of the response of permafrost to climate change require solid knowledge on the distribution of (excess) ground ice on different scales, as well as information on topographic conditions (i.e. , slope, connectivity, topology of drainage systems, etc.) which govern the meso-scale hydrology.~~ models.

~~In summary, our work provides further constraints on projections of future permafrost degradation and landscape evolution in ice-rich lowland tundra of northeast Siberia, and contributes to the development of realistic and computationally efficient representations of the permafrost region in land surface schemes of ESMs.~~

6 ~~Outlook~~

~~The presented modeling framework allows to reflect a multitude of transient degradation pathways and feedback processes in ice-rich permafrost landscapes and can thus contribute to an improved understanding of permafrost evolution in response to changing climatic conditions. In order to evaluate and validate the process representations in the model further, anext step would be to apply the model to different sites across the permafrost region, provided the necessary field data to set up and evaluate the simulations. Depending on site-specific or regional circumstances, the model would need to be extended by further parameterizations. For example, Zweigel et al. (2020) introduced an improved snow scheme into the CryoGrid model, in order to capture more complex snow dynamics at a high-Arctic permafrost site on Svalbard. Such case studies employing field data for validation will contribute to build confidence in permafrost models' projections in general, and in the CryoGrid framework in particular.~~

~~Besides such site-specific case studies, our model provides the opportunity to assess the response of (ice-rich)permafrost on regional to pan-Arctic scales. Given the sensitivity of permafrost thaw dynamics to subgrid-scale heterogeneity and lateral fluxes, we suggest that a combination of tiling concepts as presented in this study, and statistical methods such as model ensembles could provide more robust and realistic projections. Facilitating further abstraction of real-world landscapes in numerical models, methods from graph theory (i.e., network theory) could be explored as a potential technique to represent lateral processes such water transport across spatial scales (e.g. , Zuecco et al. (2019)) . The tiling setups depicted in Fig. 2 correspond to simple graph topologies.~~

~~Finally, remotely-sensed data thatprovide information on topographic and hydrological characteristics, such as the distance to a downstream drainage point, the upstream catchment area, or the slope, are an opportunity to inform and improve numerical~~

model assessments.In addition, such data can be used to evaluate model performance under recent climatic conditions. For example, various recent studies addressed the mapping of ice-wedge polygon geomorphology based on high-resolution DEMs (e.g., Kartoziia (2019)), and machine-learning techniques are being developed to map ice-wedge polygons in increasingly large areas of hundreds of square kilometers (Abolt et al., 2019; Zhang et al., 2018; Abolt and Young, 2020; Zhang et al., 2020). In the future, time series of such high-resolution elevation data of ice-rich terrain, would allow better evaluation and improvement of numerical models like CryoGrid 3 that simulated elevation changes due to melting of excess ice(e. g. , Wagner et al. (2018)) . It is thus desirable, that high-resolution elevation models would become a key observable of long-term permafrost monitoring efforts, similar to the systematic monitoring of ground temperatures and active layer depths.

Appendix A: Details on the study area

Samoylov Island ($72.36972\,°$N, $126.47500\,°$E) is located in the central southern part of the Lena River delta within the lowland tundra vegetation zone and features cold continuous permafrost (mean annual ground temperature of about $-9\,°$C (Boike et al., 2019)), which has been warming rapidly in recent years (about $0.9\,°$C per decade (Biskaborn et al., 2019)). The island belongs to the first terrace of the Lena River delta which formed during the Holocene (Schwamborn et al., 2002). The fluvial deposits contain substantial amounts of excess ice, mainly in form of ice wedges up to $10\,$m deep, which can be of epigenetic and syngenetic type. The surface of the island is characterized by ice-wedge polygons and water bodies of different sizes, ranging from ponds in polygon troughs and centres to thaw lakes several hundred meters in diameter (Figure A1 a). Ice-wedge polygons show different features across different parts of the island, including mostly low-centered polygons with water-covered centres, but also water-filled troughs indicative of ice-wedge degradation, and some high-centred polygons with drained troughs. Polygons of different geomorphological type tend to occur as grouped "clusters" in the same areas of the island (see mapping by Kartoziia (2019)), and the pre-dominant types differ along gently-sloped (about 0.1%) transects across the island (Fig. A1 b).

Appendix B: Derivation of the relation between ground ice content and ground subsidence

Excess ice is defined as "the volume of ice in the ground which exceeds the total pore volume that the ground would have under natural unfrozen conditions" (NSIDC, 2020). Hence, the total volumetric ice content (θ_i) of a given frozen soil layer can be separated into a pore ice content (θ_p) and an excess ice content (θ_x). Assuming an air fraction of zero, these volumetric ice contents and the soil matrix contents (mineral and organic) add up to one:

$$\theta_m + \theta_o + \theta_i = \theta_m + \theta_o + \theta_x + \theta_p = 1 \ . \tag{B1}$$

The excess ice scheme of CryoGrid 3 assumes, that, once a grid cell containing excess ice thaws, the entire excess ice melts and the ground volume it occupied is filled with saturated soil of the natural porosity (ϕ_{nat}) from above-lying soil layers Westermann et al. (2016). Thus, the ground surface subsides by exactly the amount of excess ice which was contained in that cell before it thawed. Figure B1 illustrates how the content of a frozen grid cell of thickness Δd can be partitioned into an excess ice part (Δx) and a part which reflects the soil under unfrozen conditions (Δu), i.e. with the natural porosity, such that:

$$\Delta d = \Delta s + \Delta u. \tag{B2}$$

The following relation for Δu can be derived geometrically from Figure B1:

$$\Delta u = \Delta d \frac{\theta_m + \theta_o}{1 - \phi_{nat}} \tag{B3}$$

$$= \Delta d \underbrace{\frac{1 - \theta_i}{1 - \phi_{nat}}}_{\theta_p / \phi_{nat}} \tag{B4}$$

where Eq. (B1) was used to obtain the second expression. Note that $\Delta u = \Delta d$ for $\theta_i = \phi_{nat}$, i.e., if the cell contains only pore ice and no excess ice. Solving Eq. (B2) for Δs and inserting Eq. (B4) for Δu yields:

$$\Delta s = \Delta d - \Delta u \tag{B5}$$

$$= \Delta d - \Delta d \frac{1 - \theta_i}{1 - \phi_{nat}} \tag{B6}$$

$$= \Delta d \underbrace{\frac{\theta_i - \phi_{nat}}{1 - \phi_{nat}}}_{\theta_x}. \tag{B7}$$

Note that $\Delta s = 0$ if the cell contains only pore ice ($\theta_i = \phi_{nat}$), and that $\Delta s = \Delta d$ for $\theta_i = 1$, i.e. if the cell contains only excess ice and no soil matrix.

Appendix C: Calculation of lateral surface and subsurface water fluxes

Lateral water fluxes (q_α [$\mathrm{m\,s^{-1}}$]) to a tile α from hydrologically connected tiles $\beta \in \mathcal{N}(\alpha)$ were calculated as the sum of surface and subsurface contributions:

$$q_\alpha = q_\alpha^{surf} + q_\alpha^{subs} \tag{C1}$$

Following Darcy's law, both surface and subsurface fluxes were assumed to be proportional to a gradient in the hydraulic heads (h), but assuming different saturated hydraulic conductivities ($K^{\text{surf/subs}}$) and contact heights ($H^{\text{surf/subs}}$):

$$q_\alpha^{\text{surf}} = \frac{1}{A_\alpha} \sum_{\beta \in \mathcal{N}(\alpha)} K_{\alpha\beta}^{\text{surf}} \frac{h_\beta - h_\alpha}{D_{\alpha\beta}} H_{\alpha\beta}^{\text{surf}} L_{\alpha\beta} \tag{C2}$$

$$q_\alpha^{\text{subs}} = \frac{1}{A_\alpha} \sum_{\beta \in \mathcal{N}(\alpha)} K_{\alpha\beta}^{\text{subs}} \frac{h_\beta - h_\alpha}{D_{\alpha\beta}} H_{\alpha\beta}^{\text{subs}} L_{\alpha\beta} \tag{C3}$$

where D is the distance between the tiles and L the contact length which have been introduced in Section ??2.3.2. The hydraulic head of each tile was identified with the water table elevation (w), or the frost table elevation (f) if no water table was present ($h = \max(w, f)$). The contact heights H for the surface and subsurface fluxes were obtained as follows:

$$H_{\alpha\beta}^{\text{surf}} = \max\left(0, h^{\text{max}} - \max\left(s^{\text{max}}, f^{\text{max}}\right)\right) \tag{C4}$$

$$H_{\alpha\beta}^{\text{subs}} = \max\left(0, \min\left(h^{\text{max}} - f^{\text{max}}, s^{\text{max}} - f^{\text{max}}\right)\right) \tag{C5}$$

where $h^{\text{max}} = \max(h_\alpha, h_\beta)$ is the maximum hydraulic head, $s^{\text{max}} = \max(s_\alpha, s_\beta)$ is the maximum soil surface elevation, and $f^{\text{max}} = \max(f_\alpha, f_\beta)$ is the maximum frost table elevation of the two involved tiles. As described in Nitzbon et al. (2019), lateral Lateral water fluxes were only applied, when both tiles were snow-free and the uppermost soil grid cell unfrozen.

Appendix D: Definitions of the micro-topographic state in the *polygon* simulations

We largely followed the definitions of Nitzbon et al. (2019) and Nitzbon et al. (2020) to define the micro-topographic state of a three-tile polygon via the relative soil surface altitudes ($a_{\text{C/R/T}}$) and water table altitudes ($w_{\text{C/R/T}}$) of the center, rim, and trough tiles. We distinguished between low-centred polygons (LCP), intermediate-centred polygons (ICP), high-centred polygons with inundated troughs (HCPi), high-centred polygons with drained troughs (HCPd), and water bodies (WB):

References

Aas, K. S., Martin, L., Nitzbon, J., Langer, M., Boike, J., Lee, H., Berntsen, T. K., and Westermann, S.: Thaw processes in ice-rich permafrost landscapes represented with laterally coupled tiles in a land surface model, The Cryosphere, 13, 591–609, https://doi.org/10.5194/tc-13-591-2019, 2019.

Abnizova, A., Siemens, J., Langer, M., and Boike, J.: Small ponds with major impact: The relevance of ponds and lakes in permafrost landscapes to carbon dioxide emissions, Global Biogeochemical Cycles, 26, https://doi.org/10.1029/2011GB004237, 2012.

Abolt, C. J. and Young, M. H.: High-resolution mapping of spatial heterogeneity in ice wedge polygon geomorphology near Prudhoe Bay, Alaska, Scientific Data, 7, 87, https://doi.org/10.1038/s41597-020-0423-9, 2020.

Abolt, C. J., Young, M. H., Atchley, A. L., and Harp, D. R.: Microtopographic control on the ground thermal regime in ice wedge polygons, The Cryosphere, 12, 1957–1968, https://doi.org/10.5194/tc-12-1957-2018, 2018.

Abolt, C. J., Young, M. H., Atchley, A. L., and Wilson, C. J.: Brief communication: Rapid machine-learning-based extraction and measurement of ice wedge polygons in high-resolution digital elevation models, The Cryosphere, 13, 237–245, https://doi.org/10.5194/tc-13-237-2019, 2019.

Abolt, C. J., Young, M. H., Atchley, A. L., Harp, D. R., and Coon, E. T.: Feedbacks Between Surface Deformation and Permafrost Degradation in Ice Wedge Polygons, Arctic Coastal Plain, Alaska, Journal of Geophysical Research: Earth Surface, 125, e2019JF005 349, https://doi.org/10.1029/2019JF005349, 2020.

AMAP: Snow, Water, Ice and Permafrost in the Arctic (SWIPA) 2017, Arctic Monitoring and Assessment Programme, Oslo, Norway, oCLC: 1038467657, 2017.

Andresen, C. G., Lawrence, D. M., Wilson, C. J., McGuire, A. D., Koven, C., Schaefer, K., Jafarov, E., Peng, S., Chen, X., Gouttevin, I., Burke, E., Chadburn, S., Ji, D., Chen, G., Hayes, D., and Zhang, W.: Soil moisture and hydrology projections of the permafrost region – a model intercomparison, The Cryosphere, 14, 445–459, https://doi.org/10.5194/tc-14-445-2020, 2020.

Ballantyne, C. K.: Periglacial geomorphology, John Wiley & Sons, Hoboken, NJ, 2018.

Billings, W. D. and Peterson, K. M.: Vegetational Change and Ice-Wedge Polygons through the Thaw-Lake Cycle in Arctic Alaska, Arctic and Alpine Research, 12, 413–432, https://doi.org/10.1080/00040851.1980.12004204, 1980.

Biskaborn, B. K., Smith, S. L., Noetzli, J., Matthes, H., Vieira, G., Streletskiy, D. A., Schoeneich, P., Romanovsky, V. E., Lewkowicz, A. G., Abramov, A., Allard, M., Boike, J., Cable, W. L., Christiansen, H. H., Delaloye, R., Diekmann, B., Drozdov, D., Etzelmüller, B., Grosse, G., Guglielmin, M., Ingeman-Nielsen, T., Isaksen, K., Ishikawa, M., Johansson, M., Johannsson, H., Joo, A., Kaverin, D., Kholodov, A., Konstantinov, P., Kröger, T., Lambiel, C., Lanckman, J.-P., Luo, D., Malkova, G., Meiklejohn, I., Moskalenko, N., Oliva, M., Phillips, M., Ramos, M., Sannel, A. B. K., Sergeev, D., Seybold, C., Skryabin, P., Vasiliev, A., Wu, Q., Yoshikawa, K., Zheleznyak, M., and Lantuit, H.: Permafrost is warming at a global scale, Nature Communications, 10, 264, https://doi.org/10.1038/s41467-018-08240-4, 2019.

Boike, J., Wille, C., and Abnizova, A.: Climatology and summer energy and water balance of polygonal tundra in the Lena River Delta, Siberia, Journal of Geophysical Research, 113, G03 025, https://doi.org/10.1029/2007JG000540, 2008.

Boike, J., Kattenstroth, B., Abramova, K., Bornemann, N., Chetverova, A., Fedorova, I., Fröb, K., Grigoriev, M., Grüber, M., Kutzbach, L., Langer, M., Minke, M., Muster, S., Piel, K., Pfeiffer, E.-M., Stoof, G., Westermann, S., Wischnewski, K., Wille, C., and Hubberten, H.-W.: Baseline characteristics of climate, permafrost and land cover from a new permafrost observatory in the Lena River Delta, Siberia (1998–2011), Biogeosciences, 10, 2105–2128, https://doi.org/10.5194/bg-10-2105-2013, 2013.

Boike, J., Georgi, C., Kirilin, G., Muster, S., Abramova, K., Fedorova, I., Chetverova, A., Grigoriev, M., Bornemann, N., and Langer, M.: Thermal processes of thermokarst lakes in the continuous permafrost zone of northern Siberia – observations and modeling (Lena River Delta, Siberia), Biogeosciences, 12, 5941–5965, https://doi.org/https://doi.org/10.5194/bg-12-5941-2015, 2015.

Boike, J., Nitzbon, J., Anders, K., Grigoriev, M., Bolshiyanov, D., Langer, M., Lange, S., Bornemann, N., Morgenstern, A., Schreiber, P., Wille, C., Chadburn, S., Gouttevin, I., Burke, E., and Kutzbach, L.: A 16-year record (2002–2017) of permafrost, active-layer, and meteorological conditions at the Samoylov Island Arctic permafrost research site, Lena River delta, northern Siberia: an opportunity to validate remote-sensing data and land surface, snow, and permafrost models, Earth System Science Data, 11, 261–299, https://doi.org/10.5194/essd-11-261-2019, 2019.

Burke, E. J., Ekici, A., Huang, Y., Chadburn, S. E., Huntingford, C., Ciais, P., Friedlingstein, P., Peng, S., and Krinner, G.: Quantifying uncertainties of permafrost carbon–climate feedbacks, Biogeosciences, 14, 3051–3066, https://doi.org/https://doi.org/10.5194/bg-14-3051-2017, 2017.

Burke, E. J., Zhang, Y., and Krinner, G.: Evaluating permafrost physics in the Coupled Model Intercomparison Project 6 (CMIP6) models and their sensitivity to climate change, The Cryosphere, 14, 3155–3174, https://doi.org/https://doi.org/10.5194/tc-14-3155-2020, 2020.

Chadburn, S. E., Krinner, G., Porada, P., Bartsch, A., Beer, C., Belelli Marchesini, L., Boike, J., Ekici, A., Elberling, B., Friborg, T., Hugelius, G., Johansson, M., Kuhry, P., Kutzbach, L., Langer, M., Lund, M., Parmentier, F.-J. W., Peng, S., Van Huissteden, K., Wang, T., Westermann, S., Zhu, D., and Burke, E. J.: Carbon stocks and fluxes in the high latitudes: using site-level data to evaluate Earth system models, Biogeosciences, 14, 5143–5169, https://doi.org/10.5194/bg-14-5143-2017, 2017.

Connon, R., Devoie, E., Hayashi, M., Veness, T., and Quinton, W.: The Influence of Shallow Taliks on Permafrost Thaw and Active Layer Dynamics in Subarctic Canada, Journal of Geophysical Research: Earth Surface, 123, 281–297, https://doi.org/10.1002/2017JF004469, 2018.

Connon, R. F., Quinton, W. L., Craig, J. R., Hanisch, J., and Sonnentag, O.: The hydrology of interconnected bog complexes in discontinuous permafrost terrains, Hydrological Processes, 29, 3831–3847, https://doi.org/10.1002/hyp.10604, 2015.

Elder, C. D., Thompson, D. R., Thorpe, A. K., Hanke, P., Anthony, K. M. W., and Miller, C. E.: Airborne Mapping Reveals Emergent Power Law of Arctic Methane Emissions, Geophysical Research Letters, 47, e2019GL085 707, https://doi.org/10.1029/2019GL085707, 2020.

Farquharson, L. M., Romanovsky, V. E., Cable, W. L., Walker, D. A., Kokelj, S. V., and Nicolsky, D.: Climate Change Drives Widespread and Rapid Thermokarst Development in Very Cold Permafrost in the Canadian High Arctic, Geophysical Research Letters, 46, 6681–6689, https://doi.org/10.1029/2019GL082187, 2019.

Fisher, R. A. and Koven, C. D.: Perspectives on the Future of Land Surface Models and the Challenges of Representing Complex Terrestrial Systems, Journal of Advances in Modeling Earth Systems, 12, e2018MS001 453, https://doi.org/10.1029/2018MS001453, 2020.

Fortier, D., Allard, M., and Shur, Y.: Observation of rapid drainage system development by thermal erosion of ice wedges on Bylot Island, Canadian Arctic Archipelago, Permafrost and Periglacial Processes, 18, 229–243, https://doi.org/10.1002/ppp.595, 2007.

Godin, E., Fortier, D., and Coulombe, S.: Effects of thermo-erosion gullying on hydrologic flow networks, discharge and soil loss, Environmental Research Letters, 9, 105 010, https://doi.org/10.1088/1748-9326/9/10/105010, 2014.

Gouttevin, I., Langer, M., Löwe, H., Boike, J., Proksch, M., and Schneebeli, M.: Observation and modelling of snow at a polygonal tundra permafrost site: spatial variability and thermal implications, The Cryosphere, 12, 3693–3717, https://doi.org/10.5194/tc-12-3693-2018, 2018.

Grosse, G., Jones, B., and Arp, C.: 8.21 Thermokarst Lakes, Drainage, and Drained Basins, in: Treatise on Geomorphology, edited by Shroder, J. F., pp. 325–353, Academic Press, San Diego, https://doi.org/10.1016/B978-0-12-374739-6.00216-5, 2013.

Göckede, M., Kittler, F., Kwon, M. J., Burjack, I., Heimann, M., Kolle, O., Zimov, N., and Zimov, S.: Shifted energy fluxes, increased Bowen ratios, and reduced thaw depths linked with drainage-induced changes in permafrost ecosystem structure, The Cryosphere, 11, 2975–2996, https://doi.org/10.5194/tc-11-2975-2017, 2017.

Göckede, M., Kwon, M. J., Kittler, F., Heimann, M., Zimov, N., and Zimov, S.: Negative feedback processes following drainage slow down permafrost degradation, Global Change Biology, 25, 3254–3266, https://doi.org/10.1111/gcb.14744, 2019.

Hjort, J., Karjalainen, O., Aalto, J., Westermann, S., Romanovsky, V. E., Nelson, F. E., Etzelmüller, B., and Luoto, M.: Degrading permafrost puts Arctic infrastructure at risk by mid-century, Nature Communications, 9, 5147, https://doi.org/10.1038/s41467-018-07557-4, 2018.

Jafarov, E. E., Coon, E. T., Harp, D. R., Wilson, C. J., Painter, S. L., Atchley, A. L., and Romanovsky, V. E.: Modeling the role of preferential snow accumulation in through talik development and hillslope groundwater flow in a transitional permafrost landscape, Environmental Research Letters, 13, 105 006, https://doi.org/10.1088/1748-9326/aadd30, 2018.

Jones, B. M., Grosse, G., Arp, C. D., Jones, M. C., Anthony, K. M. W., and Romanovsky, V. E.: Modern thermokarst lake dynamics in the continuous permafrost zone, northern Seward Peninsula, Alaska, Journal of Geophysical Research: Biogeosciences, 116, https://doi.org/10.1029/2011JG001666, 2011.

Jorgenson, M. T., Shur, Y. L., and Pullman, E. R.: Abrupt increase in permafrost degradation in Arctic Alaska, Geophysical Research Letters, 33, L02 503, https://doi.org/10.1029/2005GL024960, 2006.

Jorgenson, M. T., Kanevskiy, M., Shur, Y., Moskalenko, N., Brown, D. R. N., Wickland, K., Striegl, R., and Koch, J.: Role of ground ice dynamics and ecological feedbacks in recent ice wedge degradation and stabilization, Journal of Geophysical Research: Earth Surface, 120, 2280–2297, https://doi.org/10.1002/2015JF003602, 2015.

Kanevskiy, M., Shur, Y., Jorgenson, T., Brown, D. R., Moskalenko, N., Brown, J., Walker, D. A., Raynolds, M. K., and Buchhorn, M.: Degradation and stabilization of ice wedges: Implications for assessing risk of thermokarst in northern Alaska, Geomorphology, 297, 20–42, https://doi.org/10.1016/j.geomorph.2017.09.001, 2017.

Kartoziia, A.: Assessment of the Ice Wedge Polygon Current State by Means of UAV Imagery Analysis (Samoylov Island, the Lena Delta), Remote Sensing, 11, 1627, https://doi.org/10.3390/rs11131627, 2019.

Kessler, M. A., Plug, L. J., and Anthony, K. M. W.: Simulating the decadal- to millennial-scale dynamics of morphology and sequestered carbon mobilization of two thermokarst lakes in NW Alaska, Journal of Geophysical Research: Biogeosciences, 117, G00M06, https://doi.org/10.1029/2011JG001796, 2012.

Kleinen, T. and Brovkin, V.: Pathway-dependent fate of permafrost region carbon, Environmental Research Letters, 13, 094 001, https://doi.org/10.1088/1748-9326/aad824, 2018.

Knoblauch, C., Beer, C., Liebner, S., Grigoriev, M. N., and Pfeiffer, E.-M.: Methane production as key to the greenhouse gas budget of thawing permafrost, Nature Climate Change, 8, 309–312, https://doi.org/10.1038/s41558-018-0095-z, 2018.

Kokelj, S. V. and Jorgenson, M. T.: Advances in Thermokarst Research, Permafrost and Periglacial Processes, 24, 108–119, https://doi.org/10.1002/ppp.1779, 2013.

Lachenbruch, A. H.: Mechanics of Thermal Contraction Cracks and Ice-Wedge Polygons in Permafrost, in: Geological Society of America Special Papers, vol. 70, pp. 1–66, Geological Society of America, https://doi.org/10.1130/SPE70-p1, 1962.

Langer, M., Westermann, S., Muster, S., Piel, K., and Boike, J.: The surface energy balance of a polygonal tundra site in northern Siberia - Part 2: Winter, The Cryosphere, 5, 509–524, https://doi.org/10.5194/tc-5-509-2011, 2011a.

Langer, M., Westermann, S., Muster, S., Piel, K., and Boike, J.: The surface energy balance of a polygonal tundra site in northern Siberia - Part 1: Spring to fall, The Cryosphere, 5, 151–171, https://doi.org/10.5194/tc-5-151-2011, 2011b.

Langer, M., Westermann, S., Walter Anthony, K., Wischnewski, K., and Boike, J.: Frozen ponds: production and storage of methane during the Arctic winter in a lowland tundra landscape in northern Siberia, Lena River delta, Biogeosciences, 12, 977–990, https://doi.org/https://doi.org/10.5194/bg-12-977-2015, 2015.

1155 Langer, M., Westermann, S., Boike, J., Kirillin, G., Grosse, G., Peng, S., and Krinner, G.: Rapid degradation of permafrost underneath waterbodies in tundra landscapes—Toward a representation of thermokarst in land surface models, Journal of Geophysical Research: Earth Surface, 121, 2446–2470, https://doi.org/10.1002/2016JF003956, 2016.

Lara, M. J., McGuire, A. D., Euskirchen, E. S., Tweedie, C. E., Hinkel, K. M., Skurikhin, A. N., Romanovsky, V. E., Grosse, G., Bolton, W. R., and Genet, H.: Polygonal tundra geomorphological change in response to warming alters future CO2 and CH4 flux on the Barrow

1160 Peninsula, Global Change Biology, 21, 1634–1651, https://doi.org/10.1111/gcb.12757, 2015.

Laurion, I., Vincent, W. F., MacIntyre, S., Retamal, L., Dupont, C., Francus, P., and Pienitz, R.: Variability in greenhouse gas emissions from permafrost thaw ponds, Limnology and Oceanography, 55, 115–133, https://doi.org/10.4319/lo.2010.55.1.0115, 2010.

Lawrence, D. M., Slater, A. G., and Swenson, S. C.: Simulation of Present-Day and Future Permafrost and Seasonally Frozen Ground Conditions in CCSM4, Journal of Climate, 25, 2207–2225, https://doi.org/10.1175/JCLI-D-11-00334.1, 2012.

1165 Lee, H., Swenson, S. C., Slater, A. G., and Lawrence, D. M.: Effects of excess ground ice on projections of permafrost in a warming climate, Environmental Research Letters, 9, 124 006, https://doi.org/10.1088/1748-9326/9/12/124006, 2014.

Lewkowicz, A. G.: Rate of Short-Term ablation of Exposed Ground Ice, Banks Island, Northwest Territories, Canada, Journal of Glaciology, 32, 511–519, https://doi.org/10.3189/S0022143000012223, 1986.

Liljedahl, A. K., Boike, J., Daanen, R. P., Fedorov, A. N., Frost, G. V., Grosse, G., Hinzman, L. D., Iijma, Y., Jorgenson, J. C., Matveyeva,

1170 N., Necsoiu, M., Raynolds, M. K., Romanovsky, V. E., Schulla, J., Tape, K. D., Walker, D. A., Wilson, C. J., Yabuki, H., and Zona, D.: Pan-Arctic ice-wedge degradation in warming permafrost and its influence on tundra hydrology, Nature Geoscience, 9, 312–318, https://doi.org/10.1038/ngeo2674, 2016.

Martin, L. C. P., Nitzbon, J., Aas, K. S., Etzelmüller, B., Kristiansen, H., and Westermann, S.: Stability Conditions of Peat Plateaus and Palsas in Northern Norway, Journal of Geophysical Research: Earth Surface, 124, 705– 719, https://doi.org/10.1029/2018JF004945, 2019.

1175 Matsuoka, N., Christiansen, H. H., and Watanabe, T.: Ice-wedge polygon dynamics in Svalbard: Lessons from a decade of automated multi-sensor monitoring, Permafrost and Periglacial Processes, 29, 210–227, https://doi.org/10.1002/ppp.1985, 2018.

Morgenstern, A., Grosse, G., Günther, F., Fedorova, I., and Schirrmeister, L.: Spatial analyses of thermokarst lakes and basins in Yedoma landscapes of the Lena Delta, The Cryosphere, 5, 849–867, https://doi.org/10.5194/tc-5-849-2011, 2011.

Morgenstern, A., Ulrich, M., Günther, F., Roessler, S., Fedorova, I., Rudaya, N., Wetterich, S., Boike, J., and Schirrmeis-

1180 ter, L.: Evolution of thermokarst in East Siberian ice-rich permafrost: A case study, Geomorphology, 201, 363–379, https://doi.org/10.1016/j.geomorph.2013.07.011, 2013.

Muster, S., Langer, M., Heim, B., Westermann, S., and Boike, J.: Subpixel heterogeneity of ice-wedge polygonal tundra: a multi-scale analysis of land cover and evapotranspiration in the Lena River Delta, Siberia, Tellus B: Chemical and Physical Meteorology, 64, 17 301, https://doi.org/10.3402/tellusb.v64i0.17301, 2012.

1185 Nitzbon, J., Langer, M., Westermann, S., Martin, L., Aas, K. S., and Boike, J.: Pathways of ice-wedge degradation in polygonal tundra under different hydrological conditions, The Cryosphere, 13, 1089–1123, https://doi.org/10.5194/tc-13-1089-2019, 2019.

Nitzbon, J., Westermann, S., Langer, M., Martin, L. C. P., Strauss, J., Laboor, S., and Boike, J.: Fast response of cold ice-rich permafrost in northeast Siberia to a warming climate, Nature Communications, 11, 2201, https://doi.org/10.1038/s41467-020-15725-8, 2020.

Nitze, I., Grosse, G., Jones, B. M., Romanovsky, V. E., and Boike, J.: Remote sensing quantifies widespread abundance of permafrost region disturbances across the Arctic and Subarctic, Nature Communications, 9, 5423, https://doi.org/10.1038/s41467-018-07663-3, 2018.

Nitze, I., Cooley, S., Duguay, C., Jones, B. M., and Grosse, G.: The catastrophic thermokarst lake drainage events of 2018 in northwestern Alaska: Fast-forward into the future, The Cryosphere Discussions, pp. 1–33, https://doi.org/https://doi.org/10.5194/tc-2020-106, 2020.

NSIDC: Cryosphere Glossary, frozen ground or permafrost, https://nsidc.org/cryosphere/glossary-terms/frozen-ground-or-permafrost, 2020.

Olefeldt, D., Goswami, S., Grosse, G., Hayes, D., Hugelius, G., Kuhry, P., McGuire, A. D., Romanovsky, V. E., Sannel, A. B. K., Schuur, E. a. G., and Turetsky, M. R.: Circumpolar distribution and carbon storage of thermokarst landscapes, Nature Communications, 7, 13 043, https://doi.org/10.1038/ncomms13043, 2016.

O'Neill, H. B., Wolfe, S. A., and Duchesne, C.: New ground ice maps for Canada using a paleogeographic modelling approach, The Cryosphere, 13, 753–773, https://doi.org/10.5194/tc-13-753-2019, 2019.

O'Neill, H. B., Roy-Leveillee, P., Lebedeva, L., and Ling, F.: Recent advances (2010–2019) in the study of taliks, Permafrost and Periglacial Processes, 31, 346–357, https://doi.org/10.1002/ppp.2050, 2020.

Painter, S. L., Coon, E. T., Atchley, A. L., Berndt, M., Garimella, R., Moulton, J. D., Svyatskiy, D., and Wilson, C. J.: Integrated surface/subsurface permafrost thermal hydrology: Model formulation and proof-of-concept simulations, Water Resources Research, 52, 6062–6077, https://doi.org/10.1002/2015WR018427, 2016.

Porter, C., Morin, P., Howat, I., Noh, M.-J., Bates, B., Peterman, K., Keesey, S., Schlenk, M., Gardiner, J., Tomko, K., Willis, M., Kelleher, C., Cloutier, M., Husby, E., Foga, S., Nakamura, H., Platson, M., Wethington, M., Williamson, C., Bauer, G., Enos, J., Arnold, G., Kramer, W., Becker, P., Doshi, A., D'Souza, C., Cummens, P., Laurier, F., and Bojesen, M.: ArcticDEM, Harvard Dataverse, https://doi.org/10.7910/DVN/OHHUKH, type: Dataset, 2018.

Rowland, J. C., Jones, C. E., Altmann, G., Bryan, R., Crosby, B. T., Hinzman, L. D., Kane, D. L., Lawrence, D. M., Mancino, A., Marsh, P., McNamara, J. P., Romanvosky, V. E., Toniolo, H., Travis, B. J., Trochim, E., Wilson, C. J., and Geernaert, G. L.: Arctic Landscapes in Transition: Responses to Thawing Permafrost, Eos, Transactions American Geophysical Union, 91, 229–230, https://doi.org/10.1029/2010EO260001, 2010.

Rowland, J. C., Travis, B. J., and Wilson, C. J.: The role of advective heat transport in talik development beneath lakes and ponds in discontinuous permafrost, Geophysical Research Letters, 38, https://doi.org/10.1029/2011GL048497, 2011.

Schneider von Deimling, T., Grosse, G., Strauss, J., Schirrmeister, L., Morgenstern, A., Schaphoff, S., Meinshausen, M., and Boike, J.: Observation-based modelling of permafrost carbon fluxes with accounting for deep carbon deposits and thermokarst activity, Biogeosciences, 12, 3469–3488, https://doi.org/10.5194/bg-12-3469-2015, 2015.

Schneider von Deimling, T., Lee, H., Ingeman-Nielsen, T., Westermann, S., Romanovsky, V., Lamoureux, S., Walker, D. A., Chadburn, S., Cai, L., Trochim, E., Nitzbon, J., Jacobi, S., and Langer, M.: Consequences of permafrost degradation for Arctic infrastructure – bridging the model gap between regional and engineering scales, The Cryosphere Discussions, pp. 1–31, https://doi.org/https://doi.org/10.5194/tc-2020-192, 2020.

Schuur, E. A. G. and Mack, M. C.: Ecological Response to Permafrost Thaw and Consequences for Local and Global Ecosystem Services, Annual Review of Ecology, Evolution, and Systematics, 49, 279–301, https://doi.org/10.1146/annurev-ecolsys-121415-032349, 2018.

Schuur, E. A. G., McGuire, A. D., Schädel, C., Grosse, G., Harden, J. W., Hayes, D. J., Hugelius, G., Koven, C. D., Kuhry, P., Lawrence, D. M., Natali, S. M., Olefeldt, D., Romanovsky, V. E., Schaefer, K., Turetsky, M. R., Treat, C. C., and Vonk, J. E.: Climate change and the permafrost carbon feedback, Nature, 520, 171–179, https://doi.org/10.1038/nature14338, 2015.

Schwamborn, G., Rachold, V., and Grigoriev, M. N.: Late Quaternary sedimentation history of the Lena Delta, Quaternary International, 89, 119–134, https://doi.org/10.1016/S1040-6182(01)00084-2, 2002.

Schädel, C., Bader, M. K.-F., Schuur, E. A. G., Biasi, C., Bracho, R., Čapek, P., De Baets, S., Diáková, K., Ernakovich, J., Estop-Aragones, C., Graham, D. E., Hartley, I. P., Iversen, C. M., Kane, E., Knoblauch, C., Lupascu, M., Martikainen, P. J., Natali, S. M., Norby, R. J., O'Donnell, J. A., Chowdhury, T. R., Šantrůčková, H., Shaver, G., Sloan, V. L., Treat, C. C., Turetsky, M. R., Waldrop, M. P., and Wickland, K. P.: Potential carbon emissions dominated by carbon dioxide from thawed permafrost soils, Nature Climate Change, 6, 950–953, https://doi.org/10.1038/nclimate3054, 2016.

Shur, Y. L. and Jorgenson, M. T.: Patterns of permafrost formation and degradation in relation to climate and ecosystems, Permafrost and Periglacial Processes, 18, 7–19, https://doi.org/10.1002/ppp.582, 2007.

Slater, A. G. and Lawrence, D. M.: Diagnosing Present and Future Permafrost from Climate Models, Journal of Climate, 26, 5608–5623, https://doi.org/10.1175/JCLI-D-12-00341.1, 2013.

Teufel, B. and Sushama, L.: Abrupt changes across the Arctic permafrost region endanger northern development, Nature Climate Change, 9, 858–862, https://doi.org/10.1038/s41558-019-0614-6, 2019.

Turetsky, M. R., Abbott, B. W., Jones, M. C., Walter Anthony, K., Olefeldt, D., Schuur, E. A. G., Koven, C., McGuire, A. D., Grosse, G., Kuhry, P., Hugelius, G., Lawrence, D. M., Gibson, C., and Sannel, A. B. K.: Permafrost collapse is accelerating carbon release, Nature, 569, 32–34, https://doi.org/10.1038/d41586-019-01313-4, 2019.

Turetsky, M. R., Abbott, B. W., Jones, M. C., Anthony, K. W., Olefeldt, D., Schuur, E. A. G., Grosse, G., Kuhry, P., Hugelius, G., Koven, C., Lawrence, D. M., Gibson, C., Sannel, A. B. K., and McGuire, A. D.: Carbon release through abrupt permafrost thaw, Nature Geoscience, 13, 138–143, https://doi.org/10.1038/s41561-019-0526-0, 2020.

Vincent, W. F., Lemay, M., and Allard, M.: Arctic permafrost landscapes in transition: towards an integrated Earth system approach, Arctic Science, 3, 39–64, https://doi.org/10.1139/as-2016-0027, 2017.

Wagner, A. M., Lindsey, N. J., Dou, S., Gelvin, A., Saari, S., Williams, C., Ekblaw, I., Ulrich, C., Borglin, S., Morales, A., and Ajo-Franklin, J.: Permafrost Degradation and Subsidence Observations during a Controlled Warming Experiment, Scientific Reports, 8, 1–9, https://doi.org/10.1038/s41598-018-29292-y, 2018.

Walter Anthony, K., Deimling, T. S. v., Nitze, I., Frolking, S., Emond, A., Daanen, R., Anthony, P., Lindgren, P., Jones, B., and Grosse, G.: 21st-century modeled permafrost carbon emissions accelerated by abrupt thaw beneath lakes, Nature Communications, 9, 3262, https://doi.org/10.1038/s41467-018-05738-9, 2018.

Westermann, S., Langer, M., Boike, J., Heikenfeld, M., Peter, M., Etzelmüller, B., and Krinner, G.: Simulating the thermal regime and thaw processes of ice-rich permafrost ground with the land-surface model CryoGrid 3, Geosci. Model Dev., 9, 523–546, https://doi.org/10.5194/gmd-9-523-2016, 2016.

Zhang, W., Witharana, C., Liljedahl, A., Kanevskiy, M., Zhang, W., Witharana, C., Liljedahl, A. K., and Kanevskiy, M.: Deep Convolutional Neural Networks for Automated Characterization of Arctic Ice-Wedge Polygons in Very High Spatial Resolution Aerial Imagery, Remote Sensing, 10, 1487, https://doi.org/10.3390/rs10091487, 2018.

Zhang, W., Liljedahl, A. K., Kanevskiy, M., Epstein, H. E., Jones, B. M., Jorgenson, M. T., and Kent, K.: Transferability of the Deep Learning Mask R-CNN Model for Automated Mapping of Ice-Wedge Polygons in High-Resolution Satellite and UAV Images, Remote Sensing, 12, 1085, https://doi.org/10.3390/rs12071085, 2020.

Zuecco, G., Rinderer, M., Penna, D., Borga, M., and van Meerveld, H. J.: Quantification of subsurface hydrologic connectivity in four headwater catchments using graph theory, Science of The Total Environment, 646, 1265–1280, https://doi.org/10.1016/j.scitotenv.2018.07.269, 2019.

Zweigel, R., Westermann, S., Nitzbon, J., Langer, M., Boike, J., Etzelmüller, B., and Vikhamar Schuler, T.: Simulating snow redistribution and its effect on the ground thermal regime at a high-Arctic site on Svalbard, Journal of Geophysical Research: Earth Surface, in review, 2020.

1265
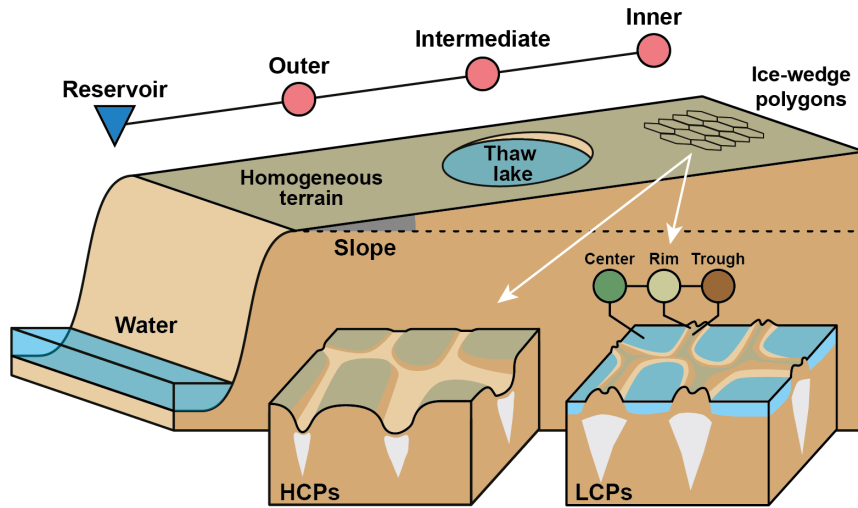
Figure 1. Schematic illustration of ice-rich permafrost lowlands featuring spatial heterogeneity on different scales. At the meso-scale, the terrain is gently-sloped and features larger landforms like thaw lakes. At the micro-scale, ice-wedge polygons entail a periodic patterning of the terrain which can have a low-centred (LCPs) or high-centred (HCPs) topography, depending on the grade of degradation. In this study, a tile-based modelling approach is pursued to represent these heterogeneities and investigate their effect on projections of landscape evolution and permafrost degradation.
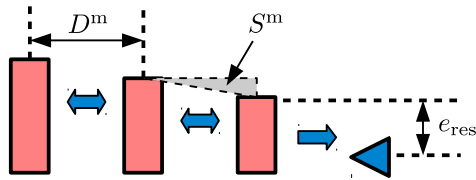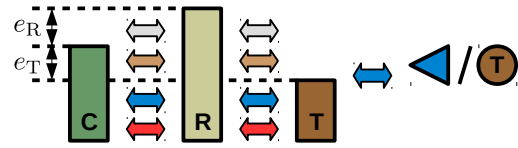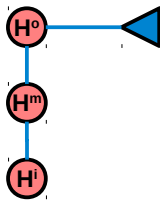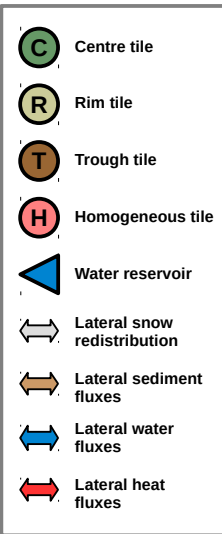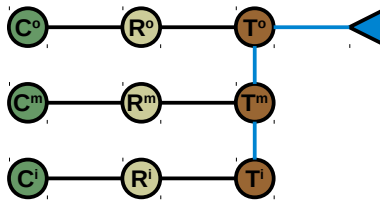
Figure 2. Overview of the the different tile-based model setups used to represent heterogeneity at micro- and meso-scales. An external reservoir (blue triangle) at a fixed elevation (e_{res}) prescribes the hydrological boundary conditions. a: The *single-tile* setup used only one tile (H) and does not reflect any subgrid-scale heterogeneity. b: The *polygon* setup reflects micro-scale heterogeneity of topography and ground ice distribution associated with ice-wedge polygons via three tiles: polygon centres (C), polygon rims (R) and inter-polygonal troughs (T). The parameters e_R and e_T indicate the (initial) elevation of rims and troughs relative to the center. The micro-scale tiles are interacting through lateral fluxes of heat, water, snow, and sediment. c: The *low-gradient slope* reflects meso-scale heterogeneity of an ice-rich lowland via three tiles ($H^{o,m,i}$) of which the outer one (H^o) is connected to a draining reservoir. The intermediate (H^m) and inner tiles (H^i) are located at distances D^m along a low-gradient slope S^m. The meso-scale tiles are interacting through lateral surface and subsurface water fluxes. d: The *low-gradient polygon slope* incorporates heterogeneities at both micro- and meso-scales via a total of nine tiles.
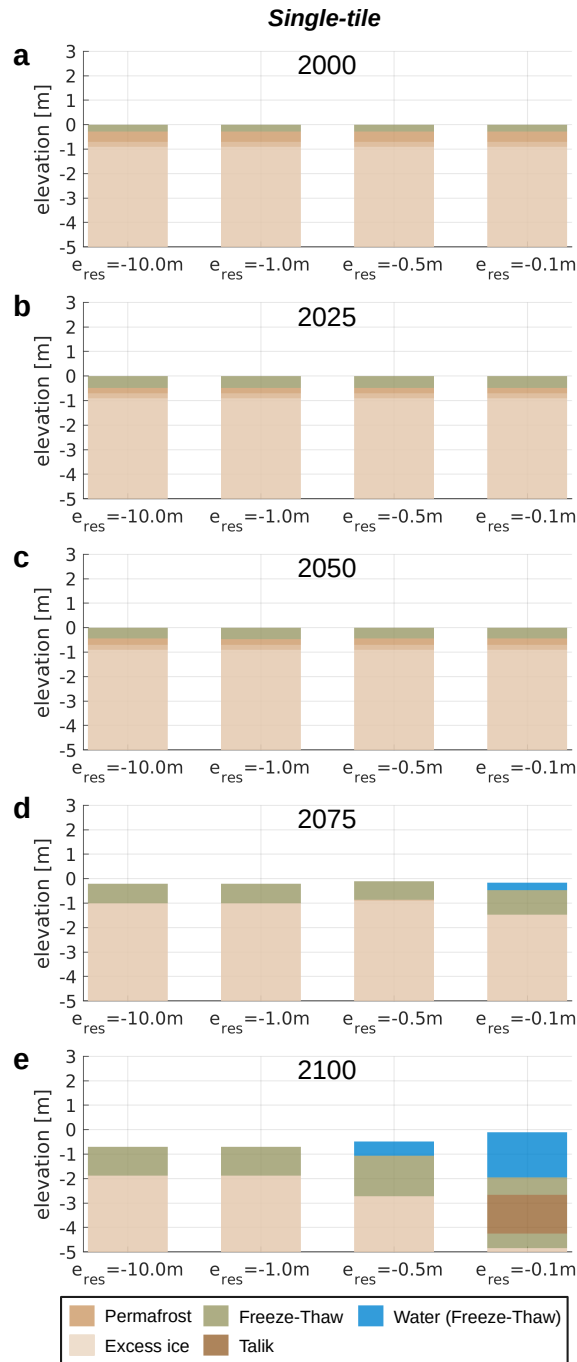
42

Figure 3. Landscape configurations in selected years (a-e) simulated with the *single-tile* setup (see Fig. 2 a) under four different hydrological boundary conditions (left to right). e_{res} denotes the elevation of the external water reservoir, so that lower values correspond to better drainage.
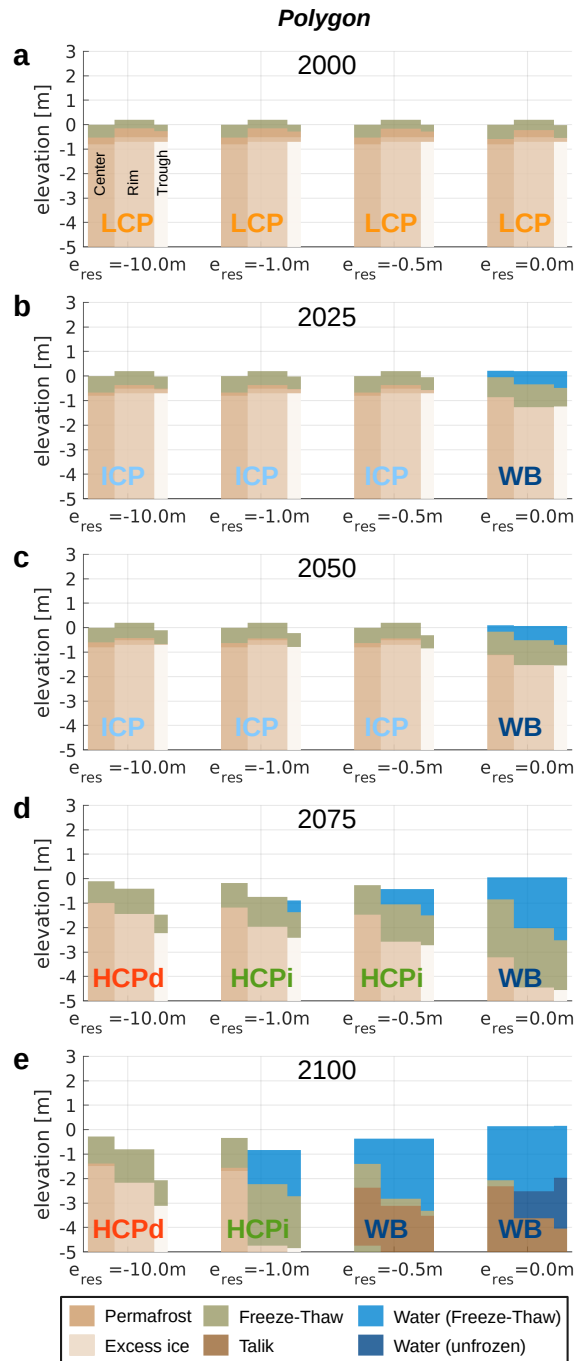
Figure 4. Landscape configurations in selected years (a-e) simulated with the *polygon* setup (see Fig. 2 b) under four different hydrological boundary conditions (left to right). e_{res} denotes the elevation of the external water reservoir, so that lower values correspond to better drainage. The width of the three tiles corresponds to their areal fractions. Brighter colours reflect higher excess ice contents of the permafrost (see Table 3). Labels indicate the state of the micro-topography according to Eqn. (**??**) to (**??**).
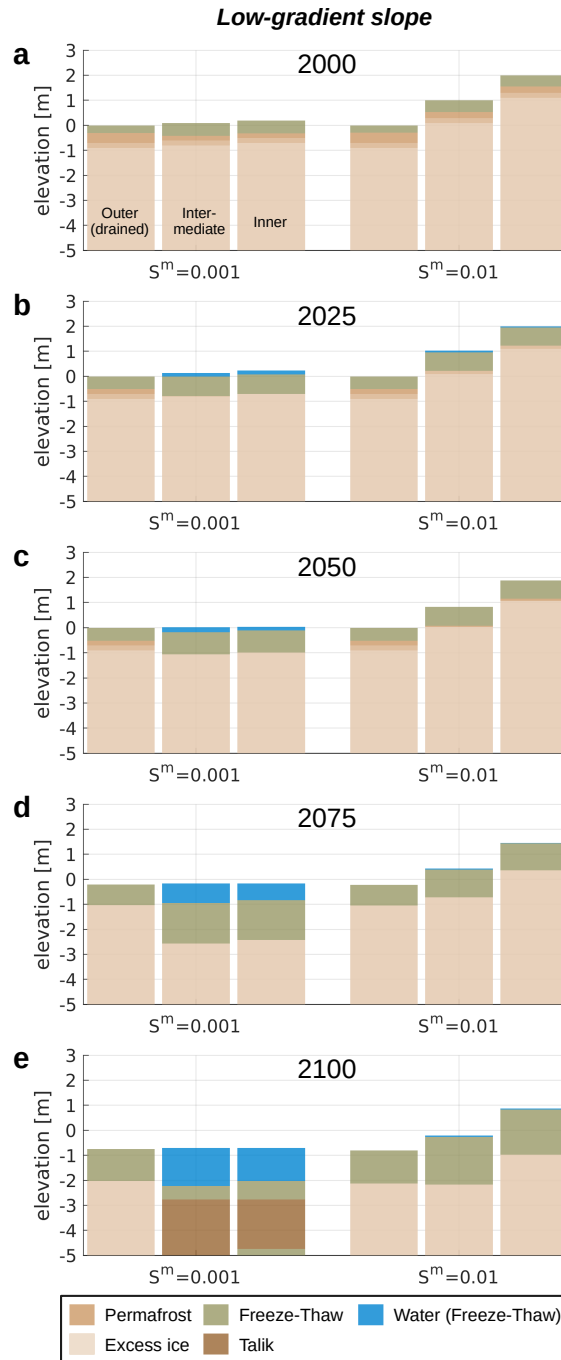
Figure 5. Landscape configurations in selected years (a-e) simulated with the *low-gradient slope* setup (see Fig. 2 c) for two different slope gradients (S^m). The "outer" tile is connected to an external reservoir ($e_{res} = -10.0$ m) which allows for efficient drainage, while the "intermediate" and "inner" tiles can drain only to adjacent tiles.
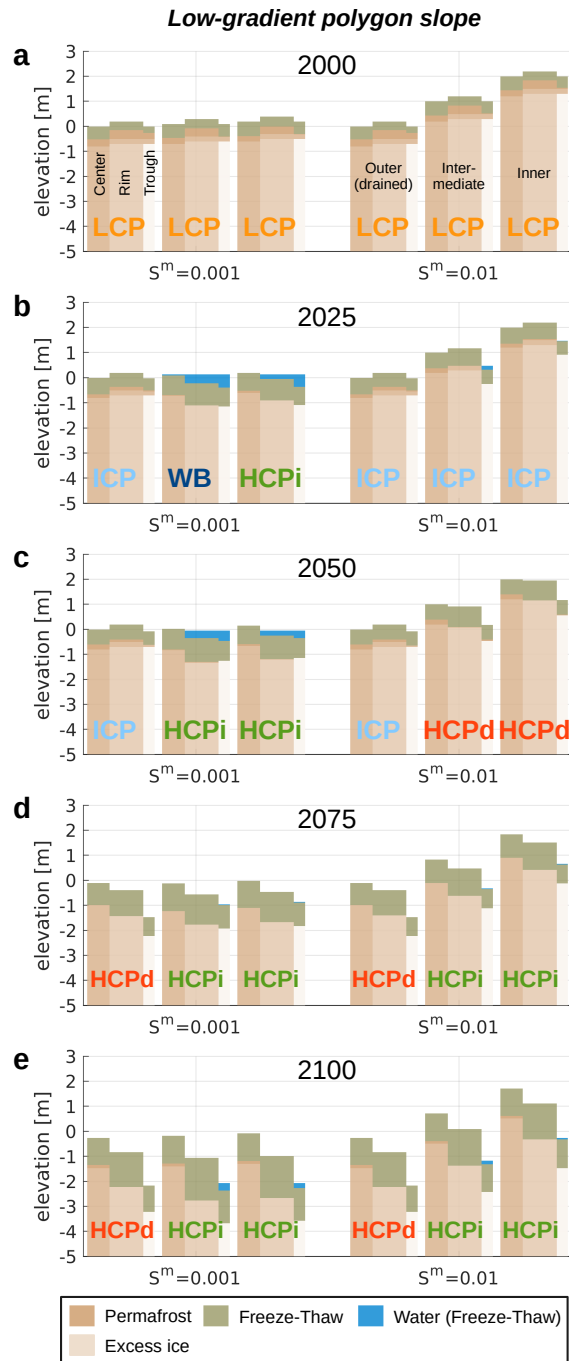
45

Figure 6. Landscape configurations in selected years (a-e) simulated with the *low-gradient polygon slope* setup (see Fig. 2 d) for two different slope gradients (S^m). The trough tile of the "outer" polygon is connected to an external reservoir ($e_{res} = -10.0$ m) which allows for efficient drainage. The trough tiles of adjacent polygons are connected to each other and constitute the drainage channels for the entire model domain. Brighter colours reflect higher excess ice contents of the permafrost (see Table 3). Labels indicate the state of the micro-topography according to Eqn. (??) to (??).
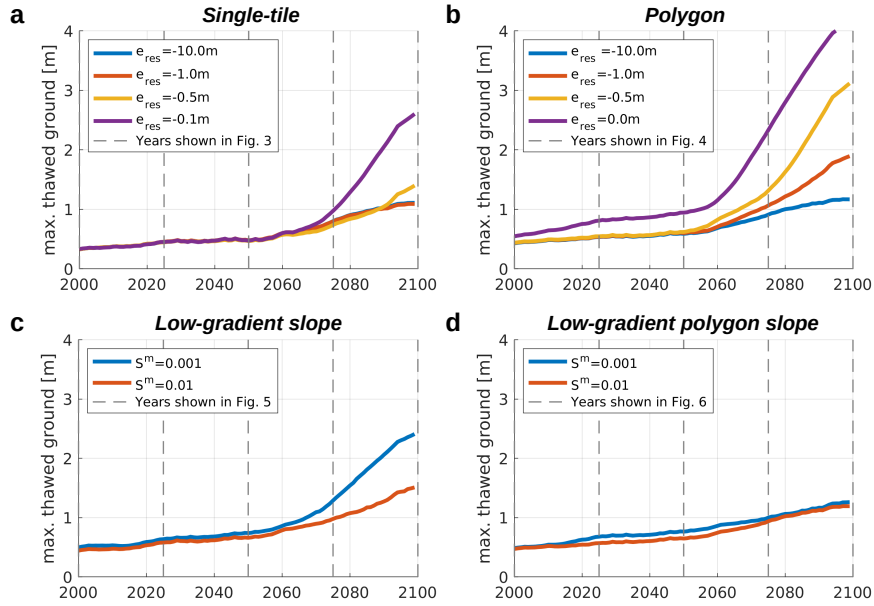
Figure 7. Time series of the maximum thawed ground thickness throughout the simulation period for all model setups (a to d) and parameter settings. e_{res} denotes the elevation of the external water reservoir, so that lower values correspond to better drainage. S^m denotes the gradient of the meso-scale slope. To derive the maximum thawed ground thickness, we first took the maximum annual thaw depth of each tile, and then averaged these, weighted according to the areal fractions of the different tiles. We then took the 11-year running mean to obtain a smoothed time series. Dashed gray lines indicate the selected years for which the landscape configuration is explicitly shown in Figures 3 to 6.
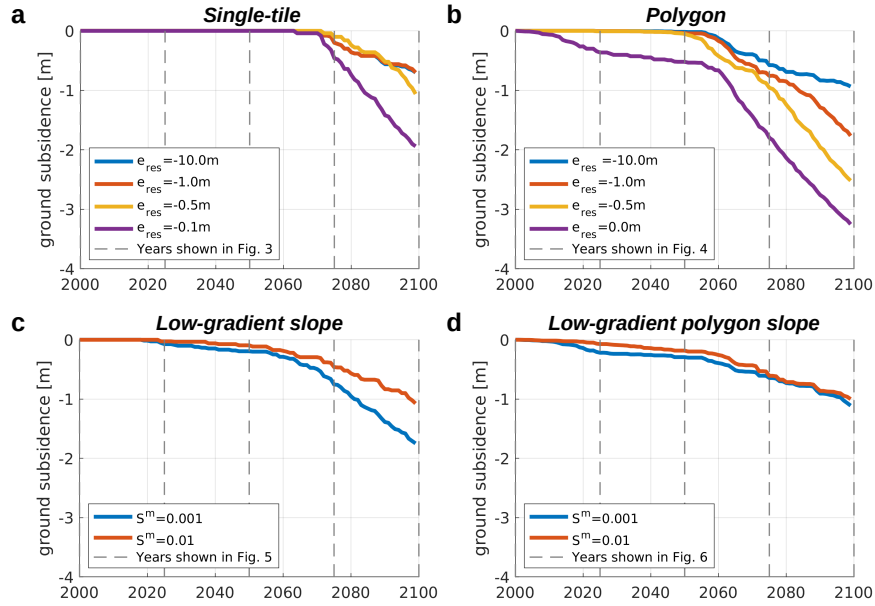
Figure 8. Time series of the accumulated ground subsidence throughout the simulation period for all model setups (a to d) and parameter settings. e_{res} denotes the elevation of the external water reservoir, so that lower values correspond to better drainage. S^m denotes the gradient of the meso-scale slope. To obtain the accumulated ground subsidence, we first took the difference between the soil surface elevation in each year and the soil surface elevation at the start of the simulation period. We then averaged these differences, weighted according to the areal fractions of the different tiles. Dashed gray lines indicate the selected years for which the landscape configuration is explicitly shown in Figures 3 to 6.
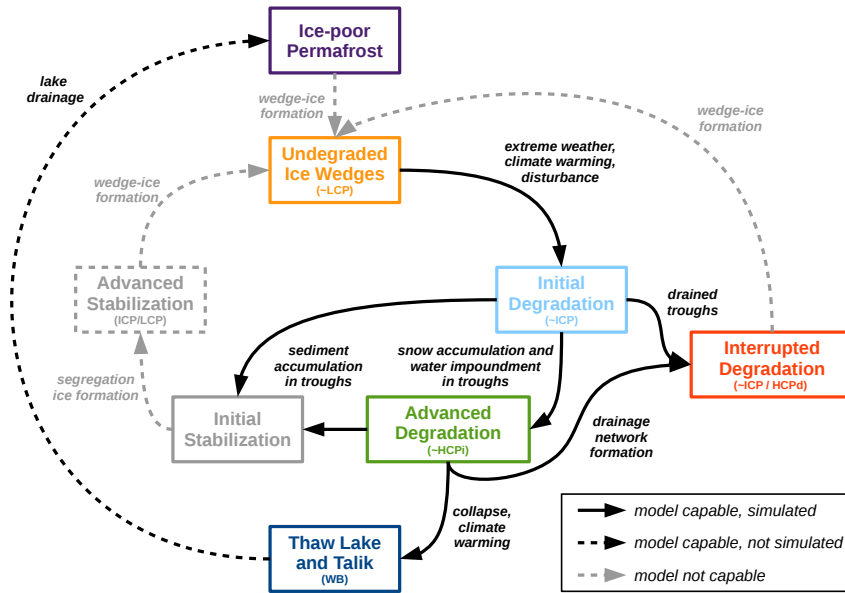
Figure 9. Schematic depiction of pathways of ice-rich permafrost landscape evolution as simulated within the presented model framework. The "inner" cycle reflects the cyclic evolution of ice-wedge polygons as described by Kanevskiy et al. (2017). The outer cycle involving the thaw lake stage reflects the thaw lake cylce as hypothesized by Billings and Peterson (1980). Formation of excess ice is lacking in the model such that the full cycles cannot be simulated. The expressions in brackets correspond to the simulated landscape configurations: low-centred polygons (LCP), intermediate-centred polygons (ICP), high-centred polygons with inundated troughs (HCPi), high-centred polygons with drained troughs (HCPd), and water bodies (WB). Figure adapted from Jorgenson et al. (2015) and Nitzbon et al. (2019).
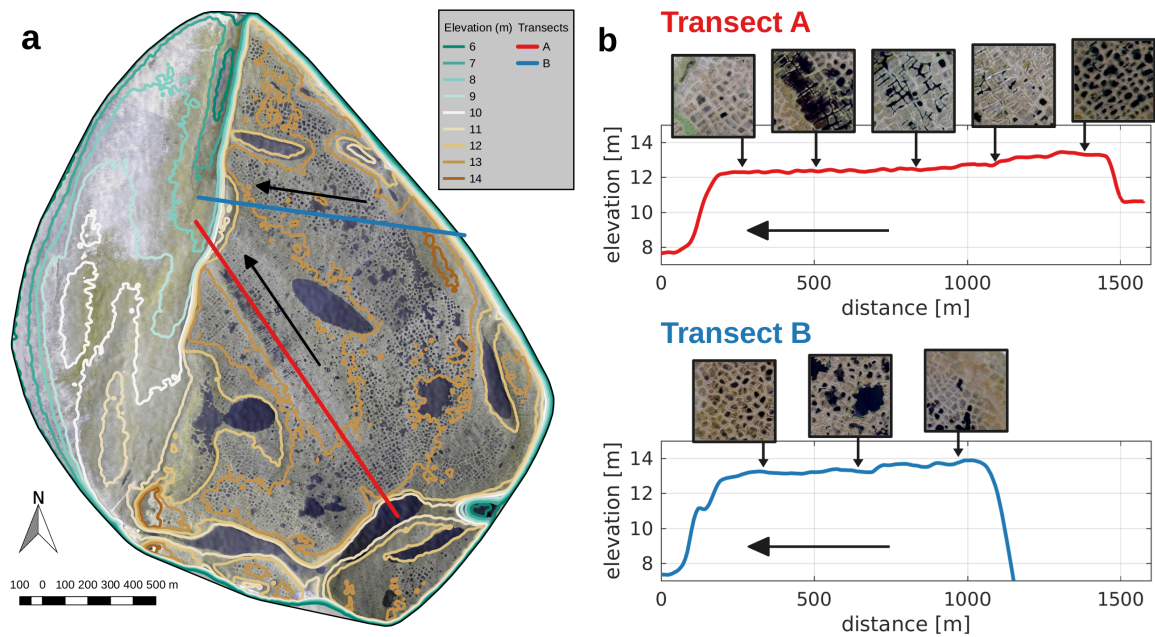
Figure A1. a: Aerial photography of Samoylov Island with elevation contour lines based on the ArcticDEM (Porter et al., 2018). The study area is covered with water bodies of different sizes and ice-wedge polygons of different geomorphological stages. b: Two (arbitrary) examples of transects across the island, reflecting the low-gradient sloped terrain with steep cliffs at the margins. The inlets are details (about 100 m in diameter) of the aerial photography, reflecting polygon clusters of similar type along the transects. Horizontal arrows point in the main drainage direction. Note that ice-wedge polygons show little signs of degradation in the highest-elevated parts and close to the margins of the island (first and last inlet of both Transects). Along Transect A, the abundance of thermokarst troughs increases in the downstream direction of the slope. Small water bodies are visible in the central part of Transect B.
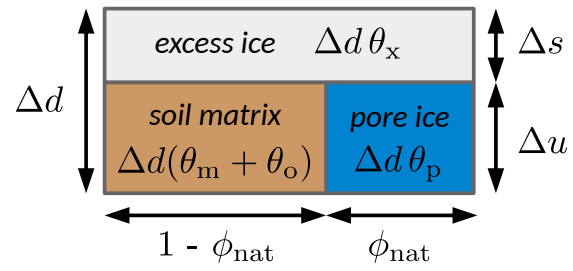
Figure B1. Schematic illustration of an ice-rich soil layer of thickness Δd which is composed of excess ice (θ_x), pore ice (θ_p), and a soil matrix ($\theta_\text{m} + \theta_\text{o}$).

Table 1. Overview of the terminology used in this manuscript to refer to the spatial scale of permafrost landscape features and processes.

Terminology	Superscript	Length scale	Examples
subgrid	–	$\lesssim 10^5\,\mathrm{m}$	all mentioned below
micro	μ	$\simeq 10^0\text{–}10^1\,\mathrm{m}$	Ice-wedge polygons, Hummocks
meso	m	$\simeq 10^2\text{–}10^3\,\mathrm{m}$	Thermo-erosion catchments, Thaw lakes
macro	–	$\simeq 10^4\text{–}10^5\,\mathrm{m}$	River delta, LSM grid cell

Table 2. Generic soil stratigraphy used to represent the subsurface composition of all tiles. An ice-rich layer of variable ice content (θ_i) is located at variable depth (d_x) from the surface. Note that the effective excess ice content (θ_x) is linked to the total ice content (θ_i) and the natural porosity (ϕ_{nat}) via the relation given in Equation (2). The soil texture is used to parametrize the freezing-characteristic curve of the respective layer (see Westermann et al. (2016) for details).

Depth from [m]	Depth to [m]	Mineral θ_m	Organic θ_o	Nat. por. ϕ_{nat}	Soil texture	Water/ice θ_w^0	Comment
0	0.1	0	0.15	0.85	sand	0.85	Vegetation layer
0.1	0.2	0.10	0.15	0.75	sand	0.75	Organic layer
0.2	$d_x - 0.2$	0.25	0.10	0.65	silt	0.65	Mineral layer
$d_x - 0.2$	d_x	0.20	0.15	0.55	sand	0.65	Intermediate layer
d_x	10	$\frac{1.05 - \theta_i}{2}$	$\frac{0.95 - \theta_i}{2}$	0.55	sand	θ_i	Variable excess ice layer
10	30	0.50	0.05	0.45	sand	0.45	Ice-poor layer (Taberit)
30	1000	0.90	0	0.10	sand	0.10	Bedrock

Table 3. Overview of the model parameters for different representations of the micro-scale. Note that on average the *polygon* tiles (C,R,T) feature the same excess ice content and depth as the *homogeneous* tile (H). Setting the area of the homogeneous tile to $A^\mu = 1\,\mathrm{m}^2$ is an arbitrary choice, as it does not affect the magnitude of the lateral fluxes due to the assumption of translational symmetry.

Parameter	Symbol	Unit	C	R	T	area-weighted mean	sum	H
Stratigraphy								
Depth of excess ice layer	d_x	[m]	1.0	0.9	0.7	0.9	–	0.9
Ice content of excess ice layer	θ_i	[-]	0.65	0.75	0.95	0.75	–	0.75
Topography								
Areal fraction	γ	[-]	$\frac{1}{3}$	$\frac{1}{2}$	$\frac{1}{6}$	–	1	1
Total area	A^μ	[m^2]	46.7	70	23.3	–	140	1
Initial elevation	e	[m]	0.0	0.2	0.0	0.1	–	0.0

Table 4. Overview of the parameter variations in the simulations which were conducted for the four different model setups (see Figure 2). Note that the last value for e_{res} in the *single-tile* and *polygon* setups – which reflects poorly-drained conditions – was chosen to be $0.1\,\text{m}$ less than the mean initial elevation of the respective setting (see Table 3).

Setup name	Number of tiles (N)	Parameter varied	Parameter values	Figures
Single-tile	1	e_{res}	$-10.0\,\text{m}; -1.0\,\text{m}; -0.5\,\text{m}; -0.1\,\text{m}$	3, 7a, 8a
Polygon	3	e_{res}	$-10.0\,\text{m}; -1.0\,\text{m}; -0.5\,\text{m}; 0.0\,\text{m}$	4, 7b, 8b
Low-gradient slope	3	S^{m}	$0.001; 0.01$	5, 7c, 8c
Low-gradient polygon slope	9	S^{m}	$0.001; 0.01$	6, 7d, 8d